COMMUNICATION FREQUENCY RESPONSE OF HIGH VOLTAGE POWER LINES

by

JOSE LUIS A. NAREDO V.

B. OF ELEC. ENG., UNIVERSIDAD ANAHUAC, MEXICO D. F., 1984

A THESIS SUBMITTED IN PARTIAL FULFILMENT OF

THE REQUIREMENTS FOR THE DEGREE OF

MASTER OF APPLIED SCIENCE

in

THE FACULTY OF GRADUATE STUDIES

DEPARTMENT OF ELECTRICAL ENGINEERING

We accept this thesis as conforming

to the required standard

THE UNIVERSITY OF BRITISH COLUMBIA

APRIL 1987

32

DEPARTMENT OF ELECTRICAL ENGINEERING

The University of British Columbia
2075 Wesbrook Place
Vancouver, Canada
V6T 1W5

Date: APRIL 1987

ABSTRACT

Several methods for calculating the electrical phase and modal parameters of overhead transmission lines are described in this thesis; then, a graphical method for evaluating communication frequency response of delta transmission lines -based on the guidelines given by W. H. Senn [12,13,14]- is developed. The graphical method, combined with the parameters calculation methods, obviates the need of large mainframe computers for the analysis of power line carrier (PLC) systems.

A new technique for assessing coupling alternatives, based on Senn's method, is developed. The technique is applied to generate coupling recommendations; it is found that many of the current recommendations given elsewhere [21] are not reliable.

Finally, future work to be done in this field is proposed.

TABLE OF CONTENTS

LIST OF FIGURES.

LIST OF TABLES

ACKNOWLEDGEMENTS

To my parents Antonio Naredo and Caritina Villagran for their encouragement and their support that far exceed the mere parental duty.

To Professor Wedepohl (whose name is not Professor but Martin) for his endless patience at sharing his knowledge and his teachings that trascend the field of Engineering.

To Professor Dommel for his readiness to help as well as to share his vast experience.

To my former colleagues: Leonardo Guardado, Felipe Gutierrez, Pablo Moreno, Ricardo Romero and Jose Luis Silva; from whom I have received the benefits of our common professional interests.

To the National Research Council of Mexico (CONACYT) for the provision of a research studentship.

To the Instituto de Investigaciones Electricas de Mexico (IIE) for the granting of a leave of absence along with the provision of supplementary financial aid through the Bank of Mexico.

CHAPTER 1. INTRODUCTION.

The use of power lines as a medium for conveying communication signals goes as far back as the early 1920s. This technique known as "power line carrier" (**PLC**), when properly designed, is highly reliable; probably the most reliable communication system on a single link basis, because of the ruggedness of the power lines.

The lack of understanding of the propagation phenomenon in multiconductor lines, on the other hand, previously precluded the better use of **PLC** systems. In the early days of power line communications, the conventional analytical tools of the power engineer were of no help in dealing with its analysis. Neither was the classical line theory, used by communication engineers, for it only considers unidimensional lines. In 1963, Wedepohl set the basis for dealing with multiconductor lines [1]; this led him and his coauthors [2,3,4,5] to developing a new multiconductor line theory.

The multiconductor or modal line theory is able to explain the phenomenon of high frequency electromagnetic waves propagating in power lines; however, its practical application to **PLC** design is still not very generalized. One reason might be that the theory is fairly new and it is still spread over several dozens of papers. Another reason might be that the theory makes use of matrix calculus that may be intimidating for the uninitiated. As a consequence, several misconceptions, prior to the development of the theory, have persisted until this day; some of them, when pertinent, will be refuted in this thesis. Another source

of misunderstandings is the oversimplification of the modal theory; this has also led to fallacies.

In this thesis, a series of results using multiconductor line theory are presented, with the intention of improving the understanding of the propagation phenomena in power lines and, at the same time, to providing a simpler way of analyzing power line carrier systems. Additionally, a new technique for assessing **PLC** couplings is proposed and -by means of it- new results are obtained.

In chapter 2 recent advances in the calculation of electrical parameters of aerial lines [6,7,8,9,10] are presented. Then, in chapter 3, after a summary of the modal theory, some practical aspects concerning the calculation of the propagation modes of the line and their propagation constants are presented. Special emphasis is given to a set of formulae for calculating modal parameters of delta lines; they were first published in Wedepohl's 1963 paper [1] and, since then, they have been largely overlooked. The simplicity of these formulae, together with the procedures of chapter 2 for calculating electrical line parameters, suggests the possibility of performing line analysis by means of programmable calculators.

It should be mentioned at this point, that the developements -either in modal theory or in electrical parameters calculation- are relevant to several other areas of power system analysis, such as:

- Transient behaviour of transmission systems [9,11].
- Corona noise performance of power lines.
- Fault detection and location in transmission lines.

After chapter 3, the attention is focused on three-phase lines in delta configuration. There are two reasons for this. The first one is that this type of lines is, if not the most common, among the most commonly found in practice. The second reason is that the delta lines and specially the horizontal one, which is a particular case of the delta, are the ones that present the worst propagation problem -the so called modal cancellation effect [13].

A simplified, but powerful method, is the one proposed by Walter H. Senn [12,13,14]. The method presented in chapter 4 may be considered Senn's method, since there is a coincidence between the results derived from it and those published by Senn. Whereas the line analysis based on the general modal theory requires lengthy computer programs hosted on a mainframe, Senn's technique is graphical; therefore, it is more suitable for field engineering work. It will become apparent, further on in the thesis, that both methods are necesary.

Senn's method is used as the basis for a technique, which is proposed in chapter 5, for comparing **PLC** coupling alternatives. The technique is applied there to make coupling recommendations for common line transposition schemes, as well as to analyze the performance of non-conventional couplings.

Finally, the conclusion of the work is given in chapter 6. Suggestions concerning future work to be done in this field are also included there.

CHAPTER 2. ELECTRICAL CHARACTERISTICS OF OVERHEAD TRANSMISSION LINES.

The propagation of electromagnetic waves on overhead transmission lines is accurately described by means of the following differential equations:

$$\frac{d\mathbf{V}}{dx} = -\mathbf{Z}\,\mathbf{I} \qquad \text{.....(2.1)}$$

and

$$\frac{d\mathbf{I}}{dx} = -\mathbf{Y}\,\mathbf{V} \qquad \text{.....(2.2)}$$

known as the Telegrapher's Equations.

The propagation phenomenon in power lines involves usually several conductors as well as the earth plane; thus, equations 2.1 and 2.2 are multidimensional relationships [1,2]. **Z** and **Y** are respectively the matrices of series impedance and of shunt admittance; both are given in per unit of length. **V** and **I** are vectors † composed of the voltages with the ground plane as reference and of the currents on each conductor of the line respectively.

Before attempting to solve equations 2.1 and 2.2, the electrical parameter matrices of the line, **Z** and **Y**, must be obtained.

† NOTE: The terms vector and column matrix are used here indistinctively.

2.1. ELECTRICAL PARAMETERS OF TRANSMISSION LINES.

The series impedance per unit of length of a transmission line can be considered as composed by four terms as follows [8,9]:

$$\mathbb{Z} = \mathbb{Z}_G + \mathbb{Z}_E + \mathbb{Z}_C + \mathbb{Z}_{GW} \qquad \text{.....(2.3)}$$

$\mathbf{Z}_g$ depends only on the line geometry; it is therefore called geometrical impedance and it is related to the Maxwell's potential coefficients matrix **"P"** in the following way [2]:

$$\mathbb{Z}_0 = j\frac{\omega\mu}{2\pi}\mathbb{P} \; ; \qquad \text{.....(2.4)}$$

$\mathbf{Z}_e$ is the additional impedance due to the finite conductivity of the earth; $\mathbf{Z}_c$ is the impedance due to the conductors; and $\mathbf{Z}_{gw}$ is a term due to the presence of grounded ground wires.

The shunt admittance per unit of length of an aerial line depends practically only on the capacitance between the conductors and the ground plane. It is also related to the Maxwell potential coefficients matrix in the following way [2]:

$$\mathbb{Y} = j\omega\, 2\pi\epsilon\, \mathbb{P}^{-1} \qquad \text{.....(2.5)}$$

or, if the line has grounded ground wires:

$$\mathbb{Y} = j\omega\, 2\pi\epsilon\, (\mathbb{P} + \mathbb{P}_{GW})^{-1} \qquad \text{.....(2.6)}$$

The calculation of the electrical parameters of aerial lines is carried out in general as indicated in reference 2; however, some changes have been suggested recently; two of them will be presented here. One deals with the earth impedance calculation [6,7,16]; the other one consists in expressing the ground wires impedance explicitly, as in equation 2.3 [8,9,10].

2.2. EARTH IMPEDANCE CALCULATION.

The self and mutual impedance terms of two conductors above a perfectly conducting ground (see figure 2.1) are given respectively by the following expressions:

$$Z_{ii} = \frac{j\omega\mu}{2\pi} \ln\left(\frac{2h}{r}\right) \qquad \text{.....(2.7)}$$

$$Z_{ij} = \frac{j\omega\mu}{2\pi} \ln\left(\frac{D_{ij}}{d_{ij}}\right)$$

$$= \frac{j\omega\mu}{2\pi} \ln\left[\frac{\sqrt{(x_i-x_j)^2+(h_i+h_j)^2}}{\sqrt{(x_i-x_j)^2+(h_i-h_j)^2}}\right] \qquad \text{.....(2.8)}$$

These terms are readily obtained by means of the well known method of the images, which is illustrated by figure 2.1; they correspond to the elements of the

geometrical impedance matrix.

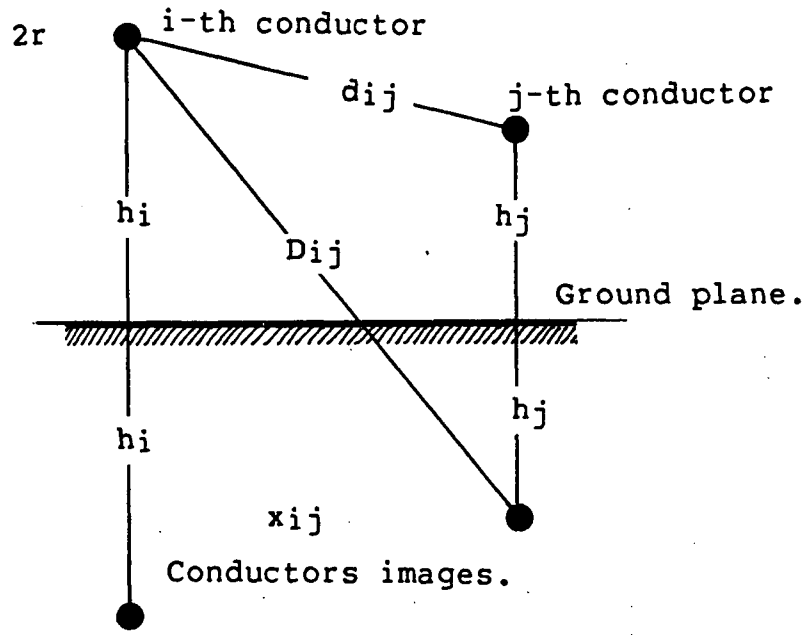

FIGURE 2.1) Conductors above a perfect conducting ground.

If the ground is not a perfect conductor, the above expressions have to be modified. Carson demonstrated [15] that the impedance could be expressed as the geometrical terms 2.1 and 2.2 plus correction terms; furthermore, he also found that -after several simplifying assumptions- the correction terms would be given, for the self impedance by the following integral:

$$Ze_{ii} = \frac{j\omega\mu}{\pi} \int_0^{\infty} \frac{e^{-2h_i\alpha}}{\alpha + \sqrt{\alpha^2 + j\omega\mu\sigma}} \, d\alpha \, , \qquad \text{.....(2.9)}$$

and, for the mutual impedance:

$$Z_{e_{ij}} = \frac{j\omega\mu}{2\pi} \int_0^\infty \frac{e^{-(h_i+h_j)\alpha} \cos\left[\alpha(x_i - x_j)\right]}{\alpha + \sqrt{\alpha^2 + j\omega\mu\sigma}} \, d\alpha \qquad \text{.....(2.10)}$$

where "σ" is the earth conductivity in Siemens/m and "α" is an integrating parameter.

Carson integrals cannot be solved analytically. Tables as well as series expansions have been used in the past to handle them; more recently, they have been dealt with by means of numerical integration. A remarkably good approximation to the Carson integral, which is also very simple to evaluate, was proposed by Dubanton in 1969 [6]. As the term

$$p = \frac{1}{\sqrt{j\omega\mu\sigma}} \quad ,$$

that appears very often at skin effect studies, plays the role of a mean penetration depth for fields and for currents, it seemed logical to place the plane of symmetry of the images at a complex distance "p" underneath the earth plane in order to account for the effects of the finite ground conductivity; this is illustrated in figure 2.2.

For the self impedance, the following expression is obtained:

$$Z_{ii} = \frac{j\omega\mu}{2\pi} \ln\left[\frac{2(h+p)}{r}\right]$$

$$Z_{ii} = j\frac{\omega\mu}{2\pi}\ln\left(\frac{2h}{r}\right) + j\frac{\omega\mu}{2\pi}\ln\left(\frac{h+p}{h}\right) \qquad \text{.....(2.11)}$$

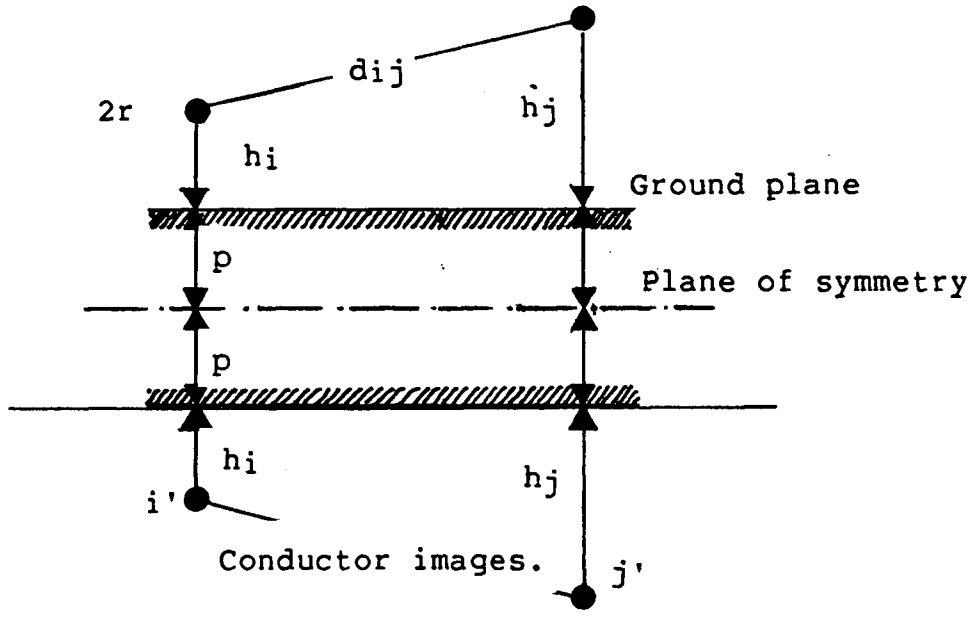

FIGURE 2.2) Complex depth of penetration.

Since the first term corresponds to the geometrical impedance (expression 2.7), the second term must account for the earth correction factor. Dubanton used this method only for the self impedance calculation. In 1976 C. Gary extended it to the calculation of the mutual impedances [7]:

$$Z_{eij} = j\frac{\omega\mu}{2\pi}\ln\left[\frac{\sqrt{(x_i-x_j)^2 + (h_i+h_j+2p)^2}}{d_{ij}}\right]$$

$$= j\frac{\omega\mu}{2\pi}\ln\left(\frac{D_{ij}}{d_{ij}}\right) + j\frac{\omega\mu}{2\pi}\ln\left[\frac{\sqrt{(x_i-x_j)^2+(h_i+h_j+2p)^2}}{D_{ij}}\right] \qquad \text{.....(2.12)}$$

Gary made also comparisons between the above correction formulae and the

numerical calculation of the Carson integrals. The results from both methods were so similar that he suggested that the complex depth formulae could be the exact solution of the Carson integrals [6].

In 1981 Deri and Semlyen derived the above formulae as approximated solutions of the Carson integrals [16]. They evaluated also the figures of error, finding that the errors are negligible at most frequencies, except for a narrow band where they become more noticeable. Inside that band, however, in most practical cases the error will be below 3%, and in the worst case it will not exceed 9%.

The error of the Dubanton-Gary formulae can be dismissed in most practical studies as, in general, it is smaller than the one introduced by the limited knowledge of the physical parameters of the transmission lines -specially the earth resistivity along a line.

2.3. IMPEDANCE CORRECTION DUE TO GROUNDED GROUND WIRES.

For a transmission line with "**m**" phase conductors and "**n**" ground wires, the matrix equations 2.1 and 2.2 can be partitioned as follows:

$$\begin{bmatrix} \frac{dV_m}{dx} \\ \hline \frac{dV_n}{dx} \end{bmatrix} = - \left[\begin{array}{c|c} Z_{mm} & Z_{mn} \\ \hline Z_{nm} & Z_{nn} \end{array}\right] \begin{bmatrix} I_m \\ \hline I_n \end{bmatrix} \qquad \text{.....(2.13)}$$

and

$$\begin{bmatrix} \frac{d\mathbb{I}_m}{dx} \\ \hline \frac{d\mathbb{I}_n}{dx} \end{bmatrix} = \left[\begin{array}{c|c} \mathbb{Y}_{mm} & \mathbb{Y}_{mn} \\ \hline \mathbb{Y}_{nm} & \mathbb{Y}_{nn} \end{array}\right] \begin{bmatrix} \mathbb{V}_m \\ \hline \mathbb{V}_n \end{bmatrix} \qquad \text{.....(2.14)}$$

Usually, the ground wires are not directly involved in the transmission of either communication signals or of electric power; thus, the explicit knowledge of their voltages or currents may not be required; however, their influence must be taken into account.

The ground wires are usually grounded at each tower. In most studies, it may be assumed that their voltage profile all along the line is zero (i. e., $\mathbf{V}_n$ and $d\mathbf{V}_n/dx = 0$). Only when the separation between towers is close to an even multiple of half a wavelength, the assumption of zero voltage is not valid and a more complex solution due to Wedepohl and Wasley has to be used [17]. With the former approach the ground wire terms are easily eliminated from equation 2.14 by erasing the last n columns, as they are multiplied by zero, as well as the last n rows, since they are not required:

$$\frac{d\mathbb{I}_m}{dx} = \mathbb{Y}_{mm}\,\mathbb{V}_m \qquad \text{.....(2.15)}$$

The reduction of equation 2.13 requires some extra work. Under the assumption that $d\mathbf{V}_n/dx = 0$, the following expressions are obtained from 2.13:

$$\frac{d\mathbb{V}_m}{dx} = -\left(\mathbb{Z}_{mm}\mathbb{I}_m + \mathbb{Z}_{mn}\mathbb{I}_n\right) \qquad \text{.....(2.16)}$$

$$0 = \mathbb{Z}_{nm}\mathbb{I}_m + \mathbb{Z}_{nm}\mathbb{I}_n \qquad \text{.....(2.17)}$$

Expression 2.17 can be used to eliminate $\mathbf{I}_n$ from equation 2.16

$$\frac{d\mathbb{V}_m}{dx} = -\left(\mathbb{Z}_{mm} - \mathbb{Z}_{mn}\mathbb{Z}_{nn}^{-1}\mathbb{Z}_{nm}\right)\mathbb{I}_m \qquad \text{.....(2.18)}$$

The term "$\mathbf{Z}_{gw}$" of expression 2.3 is thus:

$$\mathbb{Z}_{GW} = -\mathbb{Z}_{mn}\mathbb{Z}_{nn}^{-1}\mathbb{Z}_{nm} \qquad \text{.....(2.19)}$$

It can be shown in a similar way that the term "$\mathbf{P}_{gw}$ of expression 2.6 is given by:

$$\mathbb{P}_{GW} = -\mathbb{P}_{mn}\mathbb{P}_{nn}^{-1}\mathbb{P}_{nm}$$

Another method for reducing the **Z** matrix consists in inverting it; then as the following relationship holds:

$$\begin{bmatrix} \mathbb{I}_m \\ \hline \mathbb{I}_n \end{bmatrix} = -\left[\mathbb{Z}_{(m+n,m+n)}\right]^{-1} \begin{bmatrix} \frac{d\mathbb{V}_m}{dx} \\ \hline 0 \end{bmatrix}, \qquad \text{.....(2.20)}$$

the last n columns and rows can be eliminated in the same way as it was done

for the admittance matrix; the inversion of the reduced matrix will yield the impedance matrix with the ground wires term implicitly incorporated. This method is the traditional one [2]. In the next chapter it will become apparent that the explicit method has more advantages.

2.4. EXAMPLE OF ELECTRICAL PARAMETERS CALCULATION.

As an example the electrical parameters corresponding to the line depicted in figure 2.3 are provided next.

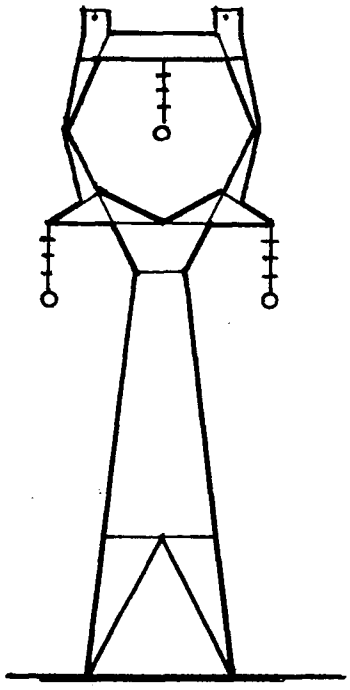

Phase conductors.	
Outer conductor medium height.	15.24 m
Central conductor medium height.	23.62 m
Horizontal distance between conductors.	6.248 m
Conductors.	2x1152-ACSR
Bundle diameter.	0.45 m
Ground wires.	
Medium height.	36.17 m
Horizontal distance	7.874 m
Radius.	0.489 cm
Material	Alumoweld
Ground resistivity.	100.0 ohm-m
Frequency.	500.0 kHz.

FIGURE 2.3) Example of a 500 kV delta line.

Geometrical Impedance. (Ohm/km)

$$\begin{bmatrix} 3571.89 & 833.05 & 609.02 & 561.47 & 509.96 \\ 833.05 & 3847.20 & 833.05 & 952.75 & 952.75 \\ 609.02 & 833.05 & 3571.89 & 509.96 & 561.47 \\ 561.47 & 952.75 & 509.96 & 6033.09 & 1397.19 \\ 509.96 & 952.75 & 561.47 & 1397.19 & 6033.09 \end{bmatrix} \quad J$$

Earth Return Impedance. (Ohm/km)

$$\begin{bmatrix} 117.556 & 94.818 & 106.420 & 75.922 & 73.854 \\ 94.818 & 81.807 & 94.818 & 66.365 & 66.365 \\ 106.420 & 94.818 & 117.556 & 73.854 & 75.922 \\ 75.922 & 66.365 & 73.854 & 56.134 & 55.595 \\ 73.854 & 66.365 & 75.922 & 55.595 & 56.134 \end{bmatrix} \quad +$$

$$\begin{bmatrix} 142.927 & 110.457 & 124.047 & 85.918 & 82.969 \\ 110.457 & 93.522 & 110.457 & 73.896 & 76.896 \\ 124.047 & 110.457 & 142.927 & 82.969 & 85.918 \\ 85.918 & 73.896 & 82.969 & 61.476 & 60.774 \\ 82.969 & 76.896 & 85.918 & 60.774 & 61.476 \end{bmatrix} \quad J$$

Conductors Impedance. (Ohm/km)

$$\begin{bmatrix} 1.330 & 0.0 & 0.0 & 0.0 & 0.0 \\ 0.0 & 1.330 & 0.0 & 0.0 & 0.0 \\ 0.0 & 0.0 & 1.330 & 0.0 & 0.0 \\ 0.0 & 0.0 & 0.0 & 12.756 & 0.0 \\ 0.0 & 0.0 & 0.0 & 0.0 & 12.756 \end{bmatrix} +$$

$$\begin{bmatrix} 1.330 & 0.0 & 0.0 & 0.0 & 0.0 \\ 0.0 & 1.330 & 0.0 & 0.0 & 0.0 \\ 0.0 & 0.0 & 1.330 & 0.0 & 0.0 \\ 0.0 & 0.0 & 0.0 & 12.756 & 0.0 \\ 0.0 & 0.0 & 0.0 & 0.0 & 12.756 \end{bmatrix} J$$

Ground Wires Impedance. (Ohm/km)

$$\begin{bmatrix} 22.924 & 28.450 & 22.877 \\ 28.450 & 31.450 & 28.450 \\ 22.877 & 28.450 & 22.924 \end{bmatrix} +$$

$$\begin{bmatrix} 100.886 & 167.471 & 100.249 \\ 167.471 & 277.995 & 167.471 \\ 100.249 & 167.471 & 100.886 \end{bmatrix} J$$

Reduced Admittance. (milli-mhos/km)

$$\begin{bmatrix} 33.101 & -5.635 & -3.918 \\ -5.635 & 32.613 & -5.635 \\ -3.918 & -5.635 & 33.101 \end{bmatrix}$$

CHAPTER 3. MODAL ANALYSIS OF MULTICONDUCTOR TRANSMISSION LINES.

The propagation equations 2.1 and 2.2 can be transformed as follows:

$$\frac{d^2\mathbb{V}}{dx^2} = \mathbb{Z}\mathbb{Y}\mathbb{V} \qquad \text{.....(3.1)}$$

$$\frac{d^2\mathbb{I}}{dx^2} = \mathbb{Y}\mathbb{Z}\mathbb{I} \qquad \text{.....(3.2)}$$

Each expression represents a system of n differential equations, where each equation involves all the n variables of voltage or of current.

The modal approach for solving either 3.1 or 3.2 consists in transforming the systen of n coupled equations to an n unidimensional or uncoupled system whose solution is straightforward. This approach, apart of being convenient from the mathematical standpoint, provides a valuable physical interpretation of the propagation phenomenon.

In the first section of this chapter the results of the modal theory, that are relevant to the thesis, will be summarized; for detailed explanations, as well as for the proofs of these results, references 1, 2, 3, 4, 5, 18 and 19 should be consulted. In section 3.2, practical aspects concerning the calculation of modal parameters are presented. Section 3.3 is devoted to the special case of modal parameters of delta lines, which is central to the thesis.

3.1. MODAL SOLUTION OF THE PROPAGATION EQUATIONS.

3.1.1. Equation for voltage.

Expression 3.1 is transformed into a decoupled system of equations by means of the matrix **M**, which diagonalizes the **ZY** matrix product as follows:

$$\mathbb{M}^{-1}\mathbb{Z}\mathbb{Y}\mathbb{M} = \Lambda \qquad \text{.....(3.3)}$$

where Λ is a diagonal matrix, whose elements are the eigenvalues of **ZY** and the columns of **M** are its eigenvectors - also known as modal vectors.

Any vector **V** of phase voltages may be regarded as an assemblage of the eigenvectors. Let $\mathbf{M}_i$ the i-th column of **M**, then:

$$\mathbb{V} = \mathbb{M}_1 v_{m1} + \mathbb{M}_2 v_{m2} + \dots + \mathbb{M}_n v_{mn}$$

where v_{mi} is the contribution of the i-th mode to **V**. It follows then that the transformation :

$$\mathbb{V}_m = \mathbb{M}^{-1}\mathbb{V} \qquad \text{.....(3.4)}$$

converts any vector **V** from the phase domain to the modal domain.

By applying 3.3 and 3.4 to 3.1:

$$\frac{d^2}{dx^2}\mathbb{V}_m = \Lambda \mathbb{V}_m \qquad \text{.....(3.5)}$$

As Λ is diagonal, it is clear that expression 3.5 is already the desired system of n decoupled equations. Its solution may be written as follows:

$$\mathbb{V}_m(x) = \exp(-\Gamma x)\mathbb{V}_{mF} + \exp(+\Gamma x)\mathbb{V}_{mB} \qquad \text{.....(3.6)}$$

where exp(+/-Γx) is shorthand for:

$$\begin{bmatrix} e^{\pm\gamma_1 x} & & & 0 \\ & e^{\pm\gamma_2 x} & & \\ & & \ddots & \\ 0 & & & e^{\pm\gamma_n x} \end{bmatrix}$$

and

$$\gamma_i \triangleq \sqrt{\lambda_i}$$

$$\gamma_i = \alpha_i + j\,\beta_i$$

V_{mF} and V_{mB} are integration constant vectors, which can be determined by knowing the value of $V_m(x)$ at two different points.

γ_i plays the role of the propagation constant of the i-th mode; its real part "α_i" represents the attenuation, and its imaginary part β_i represents its change of phase, which is related to the mode velocity. The presence of the positive exponential term in solution 3.6 is physically interpreted as a reflected wave traveling backwards.

Expression 3.6 may be transformed to the phase domain by applying the inverse

of relation 3.4 to it

$$\mathbb{V}_m(x) = \mathbb{M}\exp(-\Gamma x)\mathbb{M}^{-1}\mathbb{V}_F + \mathbb{M}\exp(\Gamma x)\mathbb{M}^{-1}\mathbb{V}_B \qquad \text{.....(3.7)}$$

If the following definition is introduced:

$$\Psi \triangleq \mathbb{M}\,\Gamma\,\mathbb{M}^{-1}, \qquad \text{.....(3.8)}$$

it may be shown that expression 3.7 becomes:

$$\mathbb{V}(x) = \exp(-\Psi x)\mathbb{V}_F + \exp(\Psi x)\mathbb{V}_B \qquad \text{.....(3.9)}$$

which is the solution to equation 3.1. Expressions 3.6 and 3.9 make use of matrix functions and of matrix calculus concepts; details about them may be found in references 18 and 19.

In the same way as in expression 3.6, the negative exponential term of 3.9 represents a wave traveling forwards, and the positive one a reflected wave traveling backwards. Here also, the integration constant vectors may be determined from the knowledge of V(x) at two different points along the line. At the beginning of the line (x = 0) 3.9 becomes:

$$\mathbb{V}(0) = \mathbb{V}_F + \mathbb{V}_B$$

At x = ℓ

$$\mathbb{V}(\ell) = \exp(-\Psi\ell)\mathbb{V}_F + \exp(\Psi\ell)\mathbb{V}_B \qquad \text{.....(3.10)}$$

solving for $\mathbf{V}_B$

$$\mathbb{V}_B = \exp(-\psi \ell)\,\mathbb{V}(\ell) - \exp(-2\psi \ell)\,\mathbb{V}_F$$

Now, for a semi-infinite line, taking the limit as $\ell \to \infty$:

$$\mathbb{V}_B = 0$$

replacing this result in 3.10:

$$\mathbb{V}_F = \mathbb{V}(0)$$

Thus for the semi-infinite line, expression 3.9 becomes:

$$\mathbb{V}(x) = \exp(-\psi x)\,\mathbb{V}(0) \qquad \text{.....(3.11)}$$

This result is consistent with the physics of the propagation phenomenon, in the sense that an infinite line does not produce reflected waves.

3.1.2. Equation for the current.

The equation of currents 3.2 may be solved either directly, as the voltage equation, or from the voltage solution. Both approaches are complementary.

The first approach helps to establish the relationship between voltage modes and current modes. Let **N** be the matrix that diagonalizes **YZ** as follows:

$$\mathbb{N}^{-1}\mathbb{Y}\mathbb{Z}\mathbb{N} = \Lambda$$

In the same way as with the voltage equation, **N** is the matrix of modes of current, and $\boldsymbol{\Lambda}'$ is the diagonal matrix of eigenvallues. It may be proved [19] that:

$$\boldsymbol{\Lambda}' = \boldsymbol{\Lambda} \quad \text{and} \quad \mathbb{N}^{-1} = \mathbb{N}^{T}$$

The second approach leads to the concept of multidimensional characteristic admittance. Rewriting 2.1 as follows:

$$\mathbb{I}(x) = -\mathbb{Z}^{-1} \frac{d\mathbb{V}(x)}{dx}$$

and from the value of **V**(x) obtained in 3.9:

$$\mathbb{I}(x) = \mathbb{Z}^{-1}\psi \left[\exp(-\psi x)\, \mathbb{V}_F - \exp(\psi x)\, \mathbb{V}_B \right]$$

Here, the term $\mathbf{Z}^{-1}\psi$ plays the same role as the characteristic admittance in the unidimensional case; therefore it is refered to as "characteristic admittance" and it is denoted by $\mathbf{Y}_c$. Its inverse, the characteristic impedance, by $\mathbf{Z}_c$.

3.1.3. Nonhomogeneous transmission systems representation.

The solutions of the voltage propagation equation 3.1 and of the current equation 3.2 lead to the two port representation of a homogeneous line section; for example, the chain matrix form:

$$\begin{bmatrix} \mathbb{V}_\ell \\ \mathbb{I}_\ell \end{bmatrix} \begin{bmatrix} \cosh(\psi\ell) & -\sinh(\psi\ell)\mathbb{Z}_c \\ -\mathbb{Y}_c\sinh(\psi\ell) & \cosh(\psi\ell) \end{bmatrix} \begin{bmatrix} \mathbb{V}_o \\ \mathbb{I}_o \end{bmatrix} \qquad \text{.....(3.12)}$$

or, the nodal form:

$$\begin{bmatrix} \mathbb{I}_o \\ \mathbb{I}_\ell \end{bmatrix} = \begin{bmatrix} \mathbb{Y}_c\coth(\psi\ell) & -\mathbb{Y}_c\,\mathrm{cosech}(\psi\ell) \\ -\mathbb{Y}_c\,\mathrm{cosech}(\psi\ell) & \mathbb{Y}_c\coth(\psi\ell) \end{bmatrix} \begin{bmatrix} \mathbb{V}_o \\ \mathbb{V}_\ell \end{bmatrix} \qquad \text{.....(3.13)}$$

Non-homogeneous transmission systems may be broken into homogeneous sections and inhomogeneities (such as, transpositions, faults, lumped elements, etc.), each part is represented as a two port network, and the two port sections are combined according to the system layout.

It seems, at first glance, that the modeling of transmission systems composed mostly of cascaded sections is more conveniently done by means of the chain matrix representation; however, because of its poor numerical stability, the nodal form 3.13 is preferred [18].

3.2. NUMERICAL COMPUTATION OF POWER LINE EIGENVALUES AND EIGENVECTORS.

For a transmission line without ground wires, the **ZY** product can be expressed, from relation 2.3, as follows [2]:

$$\mathbb{Z}\mathbb{Y} = \mathbb{Z}_G\mathbb{Y} + (\mathbb{Z}_E + \mathbb{Z}_C)\mathbb{Y} \qquad \text{.....(3.14)}$$

but from 2.4 and 2.5:

$$\mathbb{Z}_G\mathbb{Y} = -\omega^2\mu\epsilon\,\mathbb{U}$$

where **U** denotes the unit matrix. If instead of **ZY**, only the second term of expression 3.14 is diagonalized:

$$(\mathbb{Z}_E + \mathbb{Z}_C)\mathbb{Y} = \mathbb{M}''\Lambda''(\mathbb{M}'')^{-1}, \qquad \text{.....(3.15)}$$

it may be shown that the eigenvectors do not change [2]:

$$\mathbb{M}'' = \mathbb{M}$$

and that the new eigenvalues Λ'' are related to the **ZY** matrix eigenvalues as follows:

$$\Lambda = \Lambda'' - \omega^2\mu\epsilon\,\mathbb{U}$$

There are some numerical advantages on dealing with expression 3.15 rather than with **ZY**. As the elements of $\mathbf{Z}_g$ are much larger than those of $\mathbf{Z}_e$ and $\mathbf{Z}_c$- it is not recommendable to form the **Z** matrix, for the information conveyed by $\mathbf{Z}_e$ and $\mathbf{Z}_c$ may be lost by numerical truncation. The eigenvalues of **ZY** are all numerically close to $-\omega^2\mu\epsilon$. The removal of $\mathbf{Z}_g$ thus solves the numerical truncation problem as well as accelerating the convergence.

A lossless line has repeated eigenvalues

$$\lambda = -\omega^2 \mu \epsilon$$

and propagation constants:

$$\gamma = j\omega\sqrt{\mu\epsilon} = \frac{j\omega}{c}$$

where c is the speed of light. It follows then that, in addition to the attenuation, the losses reduce the wave velocity slightly.

Where ground wires are concerned, the expression analogous to 3.14 takes a somewhat more complicated form [8,9]:

$$\mathbb{Z}\mathbb{Y} = -\omega^2 \mu \epsilon \left[\mathbb{U} + (\mathbb{Z}_E + \mathbb{Z}_c + \mathbb{Z}_{GW} - \mathbb{P}_{GW}\right] \mathbb{Y} \quad \text{.....(3.16)}$$

3.3. MODAL PARAMETERS OF DELTA TRANSMISSION LINE CONFIGURATION.

One of the most common line configurations is the delta (see figure 2.3). The **ZY** product of this type of line is of the form:

$$\mathbb{Z}\mathbb{Y} = \begin{bmatrix} a & b & c \\ d & e & d \\ c & b & a \end{bmatrix} \quad \text{.....(3.17)}$$

This form is valid also when the line has one ground wire at the center, or two of them located symmetrically with respect to the vertical axis of symmetry

of the line. The horizontal configuration is a particular case where all conductors have the same height above ground.

The delta configuration is a special case of "odd" symmetry as described in reference [1]; where the derivation of analytical formulae for the eigenvalues and eigenvectors of 3.17 are also given. It may be shown that:

$$\mathbb{M} = \begin{bmatrix} 1 & 1 & 1 \\ p & 0 & q \\ 1 & -1 & 1 \end{bmatrix} \qquad \text{.....(3.18)}$$

and corresponding:

$$\Lambda = \begin{bmatrix} \lambda_1 & 0 & 0 \\ 0 & \lambda_2 & 0 \\ 0 & 0 & \lambda_3 \end{bmatrix}$$

with

$$p = \frac{e-a-c-\sqrt{(a+c-e)^2+8bd}}{2b} \qquad \text{.....(3.19)}$$

$$q = \frac{e-a-c+\sqrt{(a+c-e)^2+8bd}}{2b} \qquad \text{.....(3.20)}$$

$$\lambda_1 = a+c+bp \qquad \text{.....(3.21)}$$

$$\lambda_2 = a - c \qquad \text{.....(3.22)}$$

$$\lambda_3 = a + c + bq \qquad \text{.....(3.23)}$$

In the event that the line is completely symmetrical, with e = a and b = c = d:

$$\lambda_1 = \lambda_2 = \mathbf{a} - \mathbf{c},\ p = -2 \text{ and } q = 1,$$

M becomes then a true Clarke matrix.

3.3.1. Example of eigenvalue/eigenvector calculation in a delta line.

Consider the line depicted in figure 2.3. From the impedance and admittance matrices derived in section 2.4, the corresponding modal parameters are derived next by means of formulae 3.18 to 3.23.

Matrix of eigenvectors of voltage.

$$\begin{bmatrix} 1.0 + 0.0 & 1.0+0.0j & 1.0 + 0.0j \\ -3.559-0.062j & 0.0+0.0j & 0.812-0.006j \\ 1.0 + 0.0 & -1.0+0.0j & 1.0 + 0.0j \end{bmatrix}$$

Matrix of eigenvectors of current.

$$\begin{bmatrix} 0.0928+0.0005j & 0.5+0.0j & 0.4069+0.0123j \\ -0.2287-0.0029j & 0.0+0.0j & -0.2287-0.0029j \\ 0.0928+0.0005j & -0.5+0.0j & 0.4069+0.0123j \end{bmatrix}$$

Modal propagation constants.

	attenuation (dB/km)	velocity (km/s)
Mode 1	0.1954	299,172.
Mode 2	0.1904	298,984.
Mode 3	2.1877	291,192.

3.4. REMARKS.

Whereas section 3.1 provides the concepts of modal analysis that are required further on in the thesis, section 3.2 focuses on practical aspects of modal parameters calculation.

Delta lines occur very frequently in practice; from a practical point of view, the formulae for calculating modal parameters of delta lines given in section 3.3 are very valuable. In power line communications, the delta lines -and, specially the horizontal ones- are the most likely to present propagation problems; therefore, they require special consideration. In the field of frequency domain transient analysis, the modal parameters of lines have to be evaluated for different frequencies, typically from 128 to 1024 times; thus, when formulae 3.19 to 3.23

are applicable, substantial savings of computation time are possible [11].

CHAPTER 4. GRAPHICAL METHOD FOR PREDICTING FREQUENCY RESPONSE OF DELTA LINES.

It was shown in the previous chapter that any vector of voltages or currents in a transmission line could be regarded as a linear combination of the line natural modes. Since the modal velocities generally differ, the relative phase angles between modes change as they propagate. These phase shifts cause fluctuations of the signal amplitude along the line.

Sometimes the components of two modes, which were in phase on the coupled conductors at the sending end, arrive at the receiving end with phase reversal. In the worst case, the phase reversal occurs when the modulii of the components are equal and the signal is lost entirely. This phenomenon is refered to as "modal cancellation", and the frequencies where the signal is totally lost are known as "cancellation poles".

When a coupling arrangement is selected, it is desirable to ensure that there are no poles in the PLC frequency band; this, however, may not be easy to achieve. Pole location is very sensitive to physical changes of the line, as for example the conductor sag variations due to temperature shifts; measurements thus fail in finding them. Computer programs, on the other hand, because of the number of parameters involved in the propagation phenomenon, are not a practical alternative for locating poles.

In this chapter a graphical method for predicting delta line responses is

presented. This method -first proposed by Senn et. al. [12,13,14], in addition to frequency response predictions, provides accurate information concerning the location of cancellation poles. Although Senn's method is restricted to delta lines, its importance is justified as these lines are perhaps the most commonly used, as well as by the fact that they are the ones that present the most severe modal cancellation effects. Since the method does not require a digital computer for its application, it is recommended for engineering work.

4.1. REFLECTIONLESS WAVE PROPAGATION.

The input/output relationship of a transmission line involves the voltage vectors as well as the current vectors. As has been pointed out in chapter 3, either the currents or the voltages may be eliminated by considering the line terminations. Senn's method assumes reflection-free propagation, which is equivalent to assuming that the line is terminated at both ends in its characteristic impedance. For most practical cases it may be considered that the line terminations are fairly close to this perfect matching condition; thus, for an homogeneous line of length l, expression 3.20 becomes:

$$\mathbb{V}_\ell = \mathbb{M}\,\mathbb{L}\,\mathbb{M}^{-1}\,\mathbb{V}_0 \qquad \text{.....(4.1)}$$

were **L** stands for exp(- $\boldsymbol{\Gamma}$ l).

Except for perfectly symmetric lines, the transpositions always produce wave reflections; however, these may be neglected at carrier frequencies [13]. Therefore for a line divided by a transposition in two homogeneous sections of lengths

l_1 and l_2, the following expression may be applied:

$$\mathbb{V}_\ell = \mathbb{M}\,\mathbb{L}_1\mathbb{M}^{-1}\,\mathbb{T}\,\mathbb{M}\,\mathbb{L}_2\mathbb{M}^{-1}\mathbb{V}_0 \qquad \text{.....(4.2)}$$

where $\mathbf{L}_1 = \exp(-\Gamma l_1)$ $L_2 = \exp(-\Gamma l_2$. For a bigger number "**m**" of transpositions, expression 4.2 may be generalized as follows:

$$\mathbb{V}_\ell = \mathbb{M}\,\mathbb{L}_0\mathbb{M}^{-1}\prod_{i=1}^{m}\left\{\mathbb{T}_i\,\mathbb{M}\,\mathbb{L}_i\mathbb{M}^{-1}\right\}\cdot\mathbb{V}_0 \qquad \text{.....(4.3)}$$

When dealing with PLC systems, one is interested in the voltage v_r at the receiver's input as a function of the voltage v_t at the output of the transmitter. These scalar voltages $-v_r$ and v_t- may be related to $\mathbf{VL}=\mathbf{V}(l)$ and $\mathbf{V}_0=\mathbf{V}(0)$ respectively in the following form:

$$v_r = \left[\, C_{r1}\,,\ C_{r2}\,,\ \ldots\ C_{rn}\,\right]\begin{bmatrix} v_{\ell_1} \\ v_{\ell_2} \\ \vdots \\ v_{\ell_n}\end{bmatrix}$$

or

$$v_r = \mathbb{C}_r^T\,\mathbb{V}_\ell\,, \qquad \text{.....(4.4)}$$

and

$$\mathbb{V}_0 = \begin{bmatrix} C_{t1} \\ C_{t2} \\ \vdots \\ C_{tn}\end{bmatrix}\cdot v_t$$

or

$$\mathbb{V}_0 = \mathbb{C}_t \, v_t \qquad \text{.....(4.5)}$$

where $\mathbf{C}_r$ and $\mathbf{C}_t$ are vectors that describe the coupling connections at the receiving and transmitting ends respectively. From 4.4 and 4.5 expression 4.3 yields:

$$v_r = \mathbb{C}_r^T \, \mathbb{M} \, \mathbb{L}_0 \mathbb{M}^{-1} \prod_{i=1}^{m} \left\{ \mathbb{T}_i \, \mathbb{M} \, \mathbb{L}_i \, \mathbb{M}^{-1} \right\} \mathbb{C}_t \cdot v_t \qquad \text{.....(4.6)}$$

The line insertion loss may be already obtained from 4.6; however, before doing this, it is convenient to factorize the mode 1 loss term. This is acomplished by expressing each $\mathbf{L}_i$ in the following form:

$$\mathbb{L}_i = \exp(-\gamma_1 \ell_i) \begin{bmatrix} 1 & 0 & \cdots & 0 \\ \vdots & \exp[-(\gamma_2-\gamma_1)\ell_i] & & \vdots \\ & & \ddots & \\ 0 & 0 & \cdots & \exp[-(\gamma_2-\gamma_1)\ell_i] \end{bmatrix}$$

$$\mathbb{L} \triangleq \exp(-\gamma_1 \ell_1) \, \mathbb{L}' \qquad \text{.....(4.7)}$$

Recalling that "l" is the total length of the line:

$$\ell_0 + \ell_1 + \ldots + \ell_m = \ell ,$$

expression 4.6 becomes thus:

$$v_r = \exp(-\gamma_1 \ell) \, \mathbb{C}_r^T \, \mathbb{M} \, \mathbb{L}_0 \mathbb{M}^{-1} \prod_{i=1}^{m} \left\{ \mathbb{T} \, \mathbb{M} \, \mathbb{L}_i' \, \mathbb{M}^{-1} \right\} \cdot \mathbb{C}_t \, v_t \qquad \text{.....(4.8)}$$

Now, from the consideration that the receiving end coupling impedance is equal

to the one at the transmitting end, the line insertion loss is:

$$A = 20 \log_{10} \left| \frac{v_t}{v_r} \right|$$

$$A = (20 \log_{10} e) \alpha_1 \ell - 20 \log_{10} \left| \mathbb{C}_r^T \mathbb{M} \mathbb{L}_0 \mathbb{M}^{-1} \times \prod_{i=1}^{m} \left\{ \mathbb{T}_i \mathbb{M} \mathbb{L}_i \mathbb{M}^{-1} \right\} \mathbb{C}_t \right. \qquad \text{.....(4.9)}$$

The first term of 4.9 is indeed the attenuation of a pure mode 1 signal; it is therefore refered to as theoretical minimum attenuation or as mode 1 attenuation; it will be represented, henceforth, by "A_1".

The second term of expression 4.9, known as supplementary loss:

$$A_S = 20 \log_{10} \left| \mathbb{C}_r^T \mathbb{M} \mathbb{L}_0 \mathbb{M}^{-1} \prod_{i=1}^{m} \left\{ \mathbb{T}_i \mathbb{M} \mathbb{L}_i \mathbb{M}^{-1} \right\} \mathbb{C}_t \right| \qquad \text{.....(4.10)}$$

accounts for the coupling losses as well as for the modal interaction effects. As this is far more complicated than the mode 1 term, most of the attention is devoted to it.

4.2. SUPPLEMENTARY LOSSES IN DELTA TRANSMISSION LINES.

It was shown in section 3.4 that for delta transmission lines, the modal transformation matrices are the following:

$$\mathbb{M} = \begin{bmatrix} 1 & 1 & 1 \\ p & 0 & q \\ 1 & -1 & 1 \end{bmatrix} \qquad \mathbb{M}^{-1} = \frac{1}{2(q-p)} \begin{bmatrix} q & -2 & q \\ q-p & 0 & p-q \\ -p & 2 & -p \end{bmatrix}$$

where "p" and "q" are given by formulae 3.19 and 3.20. Within the PLC frequency range (from 30 to 500 kHz) and for horizontal lines:

. $p \cong -2.0$ and $q \cong 1.0$

If these approximations are applied to **M** and $\mathbf{M}^{-1}$ in 4.11, they become the Clarke transformation matrices.

Whereas it is possible to approximate the modal vectors, their propagation constants have to be as accurate as possible, since it is the slight difference between them that determines the cancellation poles location.

Since mode 3 attenuation is very high, it practically vanishes within the first few kilometers of line. Mode 3 may therefore be disregarded and **M** and $\mathbf{M}^{-1}$ become:

$$\mathbb{M} = \begin{bmatrix} 1 & 1 \\ -2 & 0 \\ 1 & -1 \end{bmatrix} \qquad \mathbb{M}^{-1} = \left(\frac{1}{6}\right) \begin{bmatrix} 1 & -2 & 1 \\ 3 & 0 & -3 \end{bmatrix} \qquad \text{.....(4.12)}$$

4.2.1. Homogeneous lines.

By applying the modal transformation matrices 4.12 to an homogeneous line, the supplementary loss term becomes:

$$A_s = -20 \log_{10} \left| \mathbb{C}_r^T \left(\frac{1}{6}\right) \begin{bmatrix} 1 & 1 \\ -2 & 0 \\ 1 & -1 \end{bmatrix} \begin{bmatrix} 1 & 0 \\ 0 & x \end{bmatrix} \begin{bmatrix} 1 & -2 & 1 \\ 3 & 0 & -3 \end{bmatrix} \mathbb{C}_t \right| .$$

Two things should be noted here; the first is that as the third row and column of L' are not needed anymore, they have been eliminated; the second one is that the following definition has been used:

$$x \triangleq \exp\left[-(\gamma_2 - \gamma_1)\ell\right] \qquad \text{.....(4.13)}$$

By performing the matrix products in 4.12, a first degree polynomial is obtained:

$$A_s = -20 \log_{10} \left| (p_0 + p_1 x)/K \right| \qquad \text{.....(4.14)}$$

As an example, consider the transmission system of figure 4.1. Here:

$$A_s = 20 \log_{10} \left| \frac{1}{6} \begin{bmatrix} 1 \\ 0 \\ 0 \end{bmatrix}^T \begin{bmatrix} 1 & 1 \\ -2 & 0 \\ 1 & -1 \end{bmatrix} \begin{bmatrix} 1 & 0 \\ 0 & x \end{bmatrix} \begin{bmatrix} 1 & -2 & 1 \\ 3 & 0 & -3 \end{bmatrix} \begin{bmatrix} 1 \\ 0 \\ 0 \end{bmatrix} \right|$$

The matrix products yield:

$$A_s = 20 \log_{10} \left| (1 + 3x)/6 \right|$$

It is clear that different couplings will produce different polynomials; table 4.1 provides their coefficients for the most common couplings -phase to ground and phase to phase in differential mode (push-pull).

4.2.2. Transposed lines.

Consider first the case of a transposed line where the two homogeneous sections have equal length; the following expression may be deduced from 4.10:

$$A_s = 20\log_{10} \left| \mathbb{C}^T \mathbb{M} \mathbb{L}_0' \mathbb{M}^{-1} \mathbb{T} \mathbb{M} \mathbb{L}_0' \mathbb{M}^{-1} \mathbb{C}_r \right| \qquad \text{.....(4.15)}$$

if the following definition is used:

$$X \triangleq \exp\left[-(\gamma_2 - \gamma_1)\right]$$

with l_0 the length of each homogeneous section. Expression 4.15 yields a second degree polynomial in X:

$$A_s = 20\log_{10} \left| (P_0 + P_1 X + P_2 X^2)/K \right| \qquad \text{.....(4.16)}$$

As an example, consider the system depicted in figure 4.2; here:

$$P_2(x) = \left(\frac{1}{36}\right) \begin{bmatrix} 1 \\ 0 \\ 0 \end{bmatrix}^T \begin{bmatrix} 1 & 1 \\ -2 & 0 \\ 1 & -1 \end{bmatrix} \begin{bmatrix} 1 & 0 \\ 0 & x \end{bmatrix} \begin{bmatrix} 1 & -2 & 1 \\ 3 & 0 & -3 \end{bmatrix} \times$$

$$\begin{bmatrix} 0 & 1 & 0 \\ 0 & 0 & 1 \\ 1 & 0 & 0 \end{bmatrix} \begin{bmatrix} 1 & 1 \\ -2 & 0 \\ 1 & -1 \end{bmatrix} \begin{bmatrix} 1 & 0 \\ 0 & x \end{bmatrix} \begin{bmatrix} 1 & -2 & 1 \\ 3 & 0 & -3 \end{bmatrix} \begin{bmatrix} 0 \\ 0 \\ 1 \end{bmatrix}$$

$$P_2(x) = (-1 - 6x + 3x^2)/12$$

It is possible to show that for a line divided in "**m**" homogeneous sections by "**m**-1" transpositions, the supplementary loss term involves an **m**-th degree polynomial:

$$A_s = -20 \log_{10} \left| \frac{1}{k} \sum p_i x^i \right| \qquad \text{.....(4.17)}$$

Very often in practice, transpositions are spaced at unequal distances; in these cases,a polynomial expression as 4.17 can also be obtained. This is shown next for a line consisting of two unequal sections; the generalization for a bigger number of sections is straightforward.

Suppose that a line of length "l_{tot}" is divided into two line sections of lengths l_1 and l_2. Let the ratio l_1/l_2 be approximated by means of two integers "n_1" and "n_2" in the following manner:

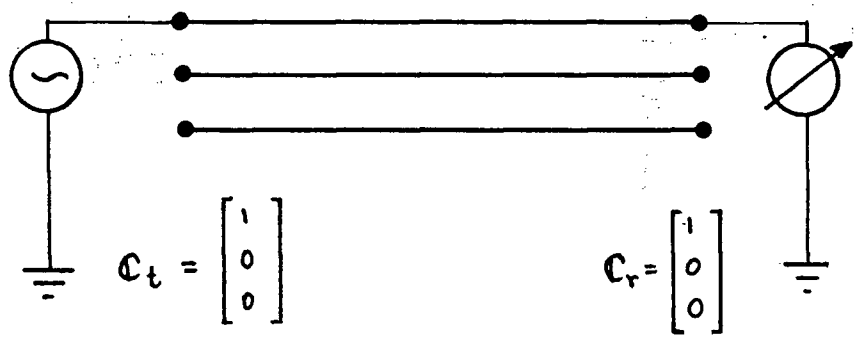

FIGURE 4.1) Example of carrier coupling on a nontransposed line.

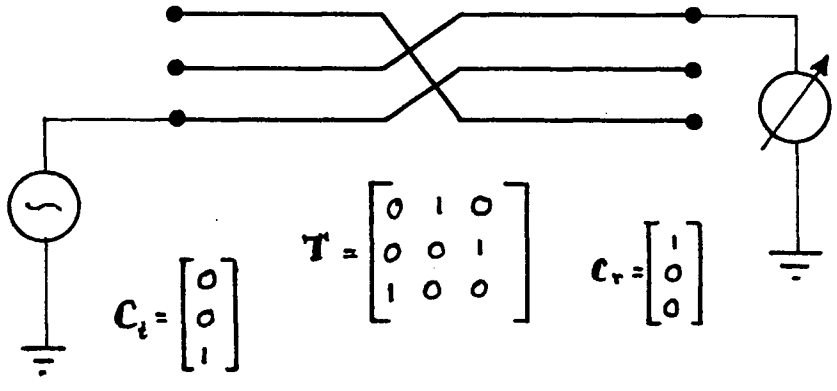

FIGURE 4.2) Example of coupling on a single transposed line.

$$\frac{\ell_1}{\ell_2} \cong \frac{n_1}{n_2} \quad , \qquad \text{.....(4.18)}$$

where the common factors between n_1 and n_2 have been already eliminated. Now, a section of length

$$\ell = \frac{\ell_{TOT}}{n_1 + n_2} \qquad \text{.....(4.19)}$$

is chosen as basis. In a similar way as in 4.13, "X" may be defined as:

$$X \triangleq \exp\left[-\ell_0(\gamma_2 - \gamma_1)\right]$$

For the first line section:

$$\mathbb{L}'_1 = \begin{bmatrix} 1 & 0 \\ 0 & X^{n_1} \end{bmatrix}$$

and, for the second one:

$$\mathbb{L}'_2 = \begin{bmatrix} 1 & 0 \\ 0 & X^{n_2} \end{bmatrix}$$

the supplementary loss term thus becomes:

$$A_s = 20 \log_{10} \left| \mathbb{C}_r^T \mathbb{M} \begin{bmatrix} 1 & 0 \\ 0 & X^{n_1} \end{bmatrix} \mathbb{M}^{-1} \mathbb{T} \mathbb{M} \begin{bmatrix} 1 & 0 \\ 0 & X^{n_2} \end{bmatrix} \mathbb{M}^{-1} \mathbb{C}_t \right|$$

It is clear that this expression yields a polynomial whose degree is at most "n_1+n_2".

From expression 4.18, it is obvious that -in general- a better approximation to the l_1/l_2 ratio is achieved by choosing bigger values for n_1 and n_2; this, however, is inconvenient from the numerical standpoint, for the degree of the polynomial will increase accordingly. It is clear then, that in these cases there has to be a trade off.

Perhaps the most common case of lines with unequal section lengths are those where the transpositions are located at 1/6-th 3/6-ths and 5/6-ths of the line length; this transposition scheme is depicted in figure 4.3d. Figures 4.3a, 4.3b and 4.3c show, respectively, the most common layouts of lines with zero, one and two transpositions. The polynomials associated to all these line schemes, for the most conventional coupling arrangements, are provided in tables 4.1, 4.2, 4.3 and 4.4

4.2.3. Insertion loss calculation.

Once the polynomial coefficients for a specific line layout are available, the line response to a frequency excitation can be obtained through the following steps:

1. Obtain the electrical parameters **Z** and **Y** of the line by means of the methods given in reference 2 as well as in chapter 2.
2. From the electrical parameters derive the modal propagation constants using the formulae given in section 3.4. Only

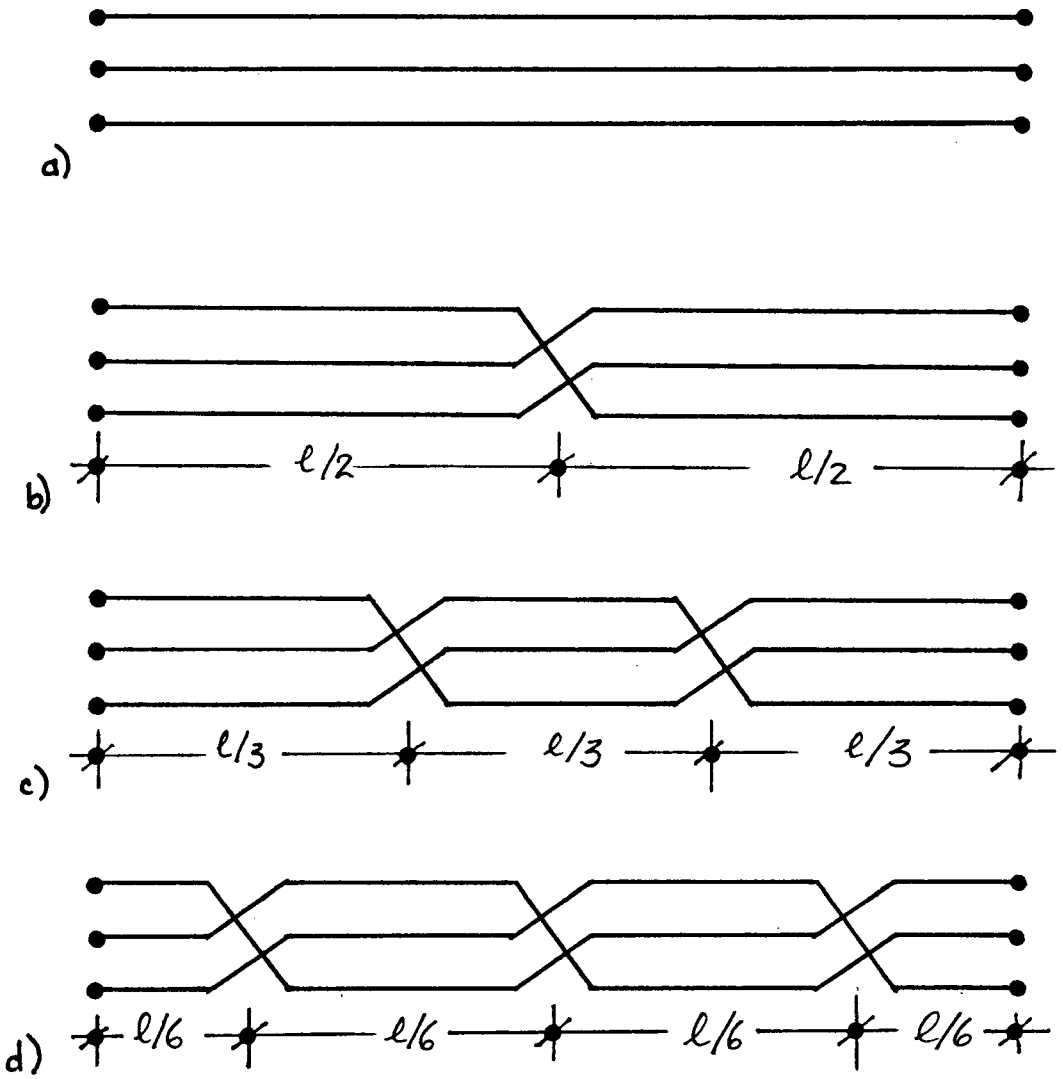

FIGURE 4.3) Transmission line transposition layouts most commonly found in practice.
a) Untransposed line. b) One transposition.
c) Two transpositions. d) Three transpositions unequal spacing.

$\gamma_1 = \alpha_1 + j\beta_1$ and $\gamma_2 = \alpha_2 + j\beta_2$ are required.

3. Given the basic homogeneous section length "l_0," obtain X:

$$X = \exp\left[-\ell_0(\gamma_2 - \gamma_1)\right]$$

4. Calculate the supplementary loss term as:

$$A_s = -20\log_{10}\left|\left(\sum_{i=0}^{m} p_i X^i\right)\right|$$

5. Calculate the mode 1 attenuation:

$$A_1 = (20\log_{10}e)\cdot(\alpha_1\cdot\ell)$$

where "l" is the total line length.

6. Obtain the total insertion loss:

$$A = A_1 + A_s \qquad \text{.....(4.20)}$$

4.2.4. Modal cancellation poles.

Since α_1 as well as "l" (the total length of the line) are always non-negative and finite, the mode 1 term:

$$A_1 = 20\log_{10}(e)\cdot\alpha_1\ell$$

can only take non-negative finite values.

The supplementary loss term -on the other hand- may become infinite. It is apparent from expression 4.17 that this can only happen at the root values of

$$P_m(X) = \sum_{i=0}^{m} p_i X^i \quad .$$

By recalling the definition of X:

$$X \triangleq \exp\left[-l_0(\gamma_2-\gamma_1)\right]$$

$$X = \exp\left[-l_0(\alpha_2-\alpha_1) - l_0(\beta_2-\beta_1)\right]$$

and the fact that:

$$\alpha_2 \geq \alpha_1 \geq 0$$

it becomes clear that not all the roots of $P_m(X)$ have physical meaning. Only those roots such that:

$$0 < |X| \leq 1$$

are related to poles; these will be henceforth referred to as poles.

Tables 4.1, 4.2, 4.3 and 4.4 include the poles corresponding to each polynomial. Their values are specified by means of two new variables: " $\Delta\alpha$ " and " $\Delta\theta$ ", that are related to "X" as indicated as follows:

$$X = \exp\left(-\Delta a + j\Delta\theta\right) \qquad \text{.....(4.21)}$$

therefore:

$$\Delta a \triangleq l_0(\alpha_2-\alpha_1) \qquad \text{.....(4.22)}$$

$$\Delta\beta \triangleq l_0 (\beta_1 - \beta_2) \qquad \text{.....(4.23)}$$

$\Delta\theta$ may be interpreted as the phase change suffered by mode 2 with respect to mode 1 as they travel through a basic line length "l_0". $\Delta\alpha$ thus represents the attenuation difference (in Nepers) between mode 2 and mode 1 for the basic line length.

4.3. SENN'S METHOD FOR EVALUATING INSERTION LOSSES.

The steps required for evaluating a line response to a carrier signal are given in sub-section 4.2.3; alternatively, Senn [12,13,14] proposed a graphical method that is to be presented next.

From the definitions 4.22 and 4.23 it follows that the supplementary loss may be regarded as a function of $\Delta\alpha$ and of $\Delta\theta$; it may thus be plotted for a range of values of these two variables as it is shown in figure 4.4a.

Since three-dimensional plots -as the one in figure 4.4a- are not very practical, Senn proposes the use of contour map representations instead. See for example the contour map in figure 4.4b which corresponds to figure 4.4a three dimensional graph.

Relation 4.17 can be expressed as follows:

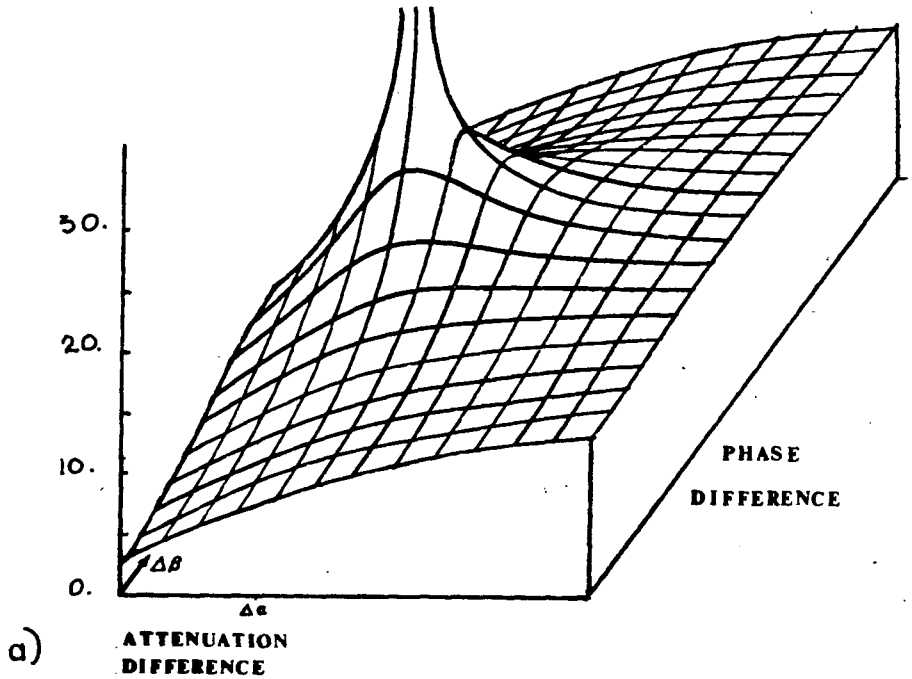

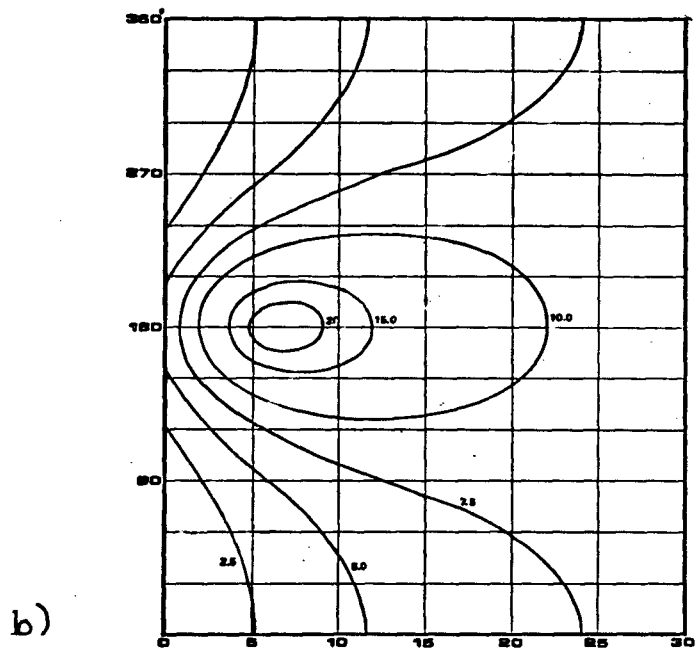

FIGURE 4.4) Plot of the function

$$A_S = 20\log_{10}|(X^2-6X-3)/8|$$

a) Three dimensional graph. b) Contour representation.

$$\left| \sum p_i X^i \right| = K \times 10^{(-A_s/20)} \qquad \text{.....(4.24)}$$

In order to generate the contours, a constant value (i. e., a level value) is asigned to A_S, then "X" has to be solved from 4.24; the absolute value bars there preclude its direct solution as a polynomial equation. The method here proposed makes use of the following definition:

$$|z^2| = z \cdot z^*$$

where z^* is the complex conjugate of z. Equation 4.24 thus yields:

$$\left(\sum_{i=0}^{m} p_i X^i \right) \left(\sum_{k=0}^{m} p_k X^{*k} \right) = K^2 \, 10^{(-A_s/10)}$$

By recalling 4.21,and after some algebraic manipulations:

$$\sum p_i^2 \left(e^{-2i\Delta a} \right) + \sum \sum 2 p_i p_k e^{-(i+k)\Delta a} \cos[(k-i)] \Delta\theta = K^2 \cdot 10^{(A_s/10)} \qquad \text{.....(4.25)}$$

Assuming that $\Delta\theta$ is given and, if " exp(- Δa)" is replaced by "Y", it becomes clear that 4.25 is a 2m degree polynomial A contour can thus be generated by assigning successive values to $\Delta\theta$ from 0^0 to 360^0,and solving this 2m degree polynomial each time.

In a similar way as with the poles, not all the roots of 4.25 have physical meaning; only those that are real and satisfy the inequality:

$$0 < Y \leq 1$$

belong to a contour segment.

Since the contour maps are obtained for general values of $\Delta\alpha$ and $\Delta\theta$, they do not depend on the specific dimensions or the electrical properties of the lines; therefore they are generic to delta lines with the same transposition scheme and coupling arrangements.

Once the contours are available, specific values for $\Delta\alpha$ and $\Delta\theta$ must be determined. In figure 4.5a $\Delta\theta$ is plotted against Aa for the line described in figure 4.5b; the frequency is varied continuously and the earth resistivity assumes 5 different values. The supplementary loss term may be obtained easily by superposing figure 4.5a curve -also known as modal curve- to the corresponding contour map.

Although the modal curve has to be elaborated usually for each particular case, the same curve may be used several times for evaluating different couplings by just superposing it with the contour maps corresponding to each coupling. An example is provided next.

4.3.1. Example.

For the line scheme of figure 4.6, it is desired to compare the following couplings providing metallic continuity:

C_1: $C_t=(1,0,0)/C_r=(0,0,1)$

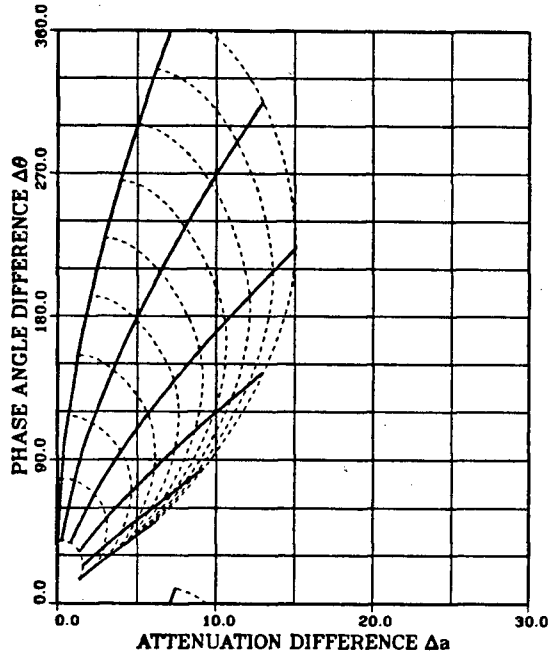

a)

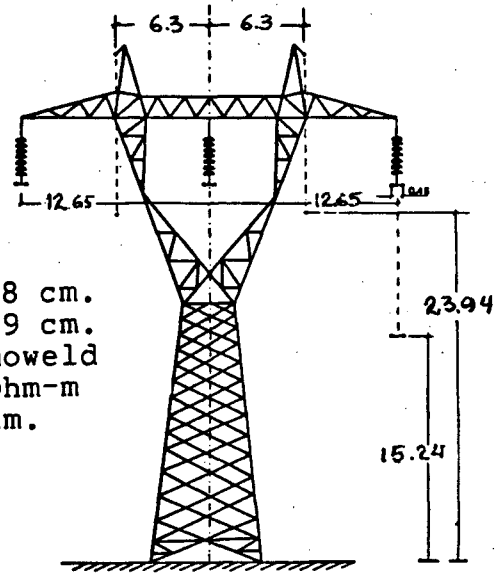

Conductor radius ..... 1.598 cm.
Gnd. wire radius ..... 0.489 cm.
Gnd. wire material..... Alumoweld
Earth resistivity ..... 300 Ohm-m
Line section length .... 30 km.

b)

FIGURE 4.5) a) Graph of Δa-$\Delta\theta$ for different frequencies and different earth resistivities.
b) line data for the graph 4.5a.

C_2: $C_t=(0,1,0)/C_r=(1,0,0)$

C_3: $C_t=(0,0,1)/C_r=(0,1,0)$,

against the discontinuous one:

C_4: $C_t=(0,1,0)/C_r=(0,1,0)$.

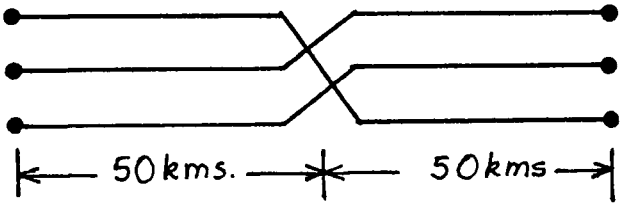

FIGURE 4.6) Example.

The line dimensions and conductors data are those of figure 4.5b; the earth resistivity is 300 Ohm-m.

The theoretical minimum attenuation, as well as the modal curve are readily obtained from the line data; they are plotted, respectively, in figures 4.7a and 4.7b.

The contour maps corresponding to couplings C_1 and C_2 are given in figures 4.8a and 4.8b, with the modal curve already superposed. The contour map of coupling C_3 is equal to that of C_2. For C_4 a contour map is not required -the supplementary loss is a constant equal to 9.5424 dB.

The total insertion loss for each coupling is obtained by adding the supplementary loss terms to the theoretical minimum attenuation; the results are plotted in figure 4.9. Note that -contrary to the common sense, the discontinuous metallic path is the best; it is, in fact, the only one free of poles.

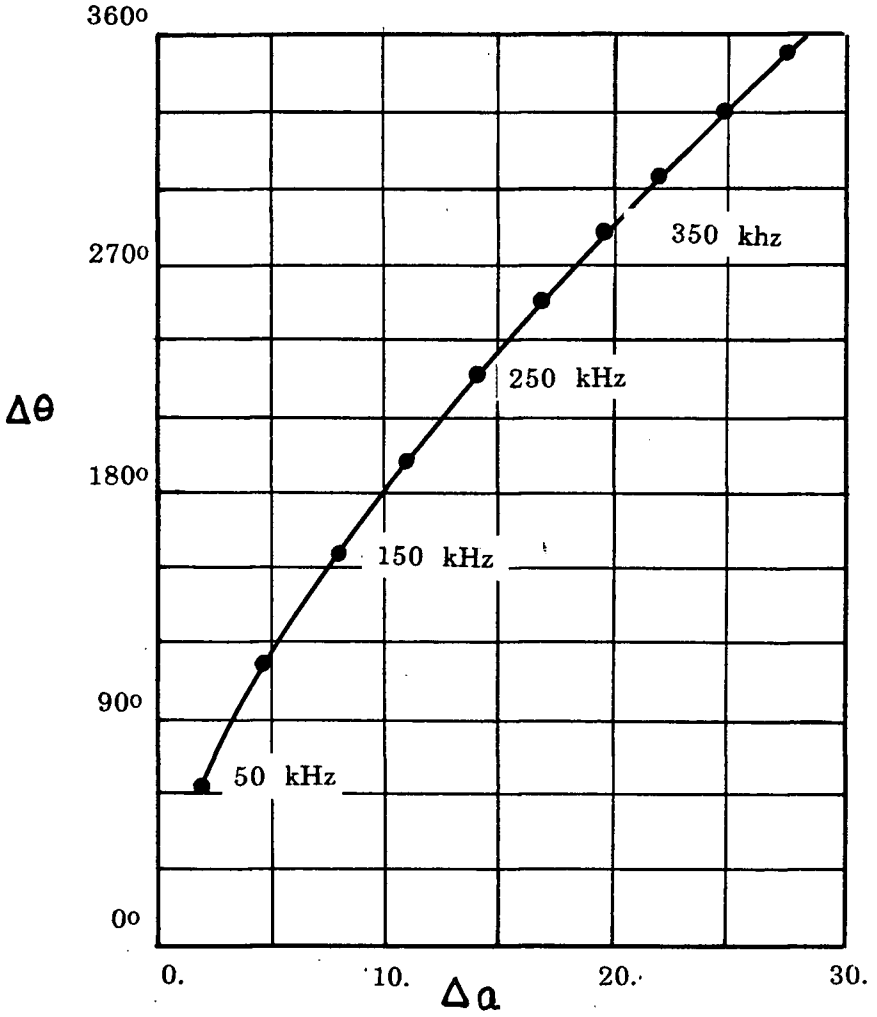

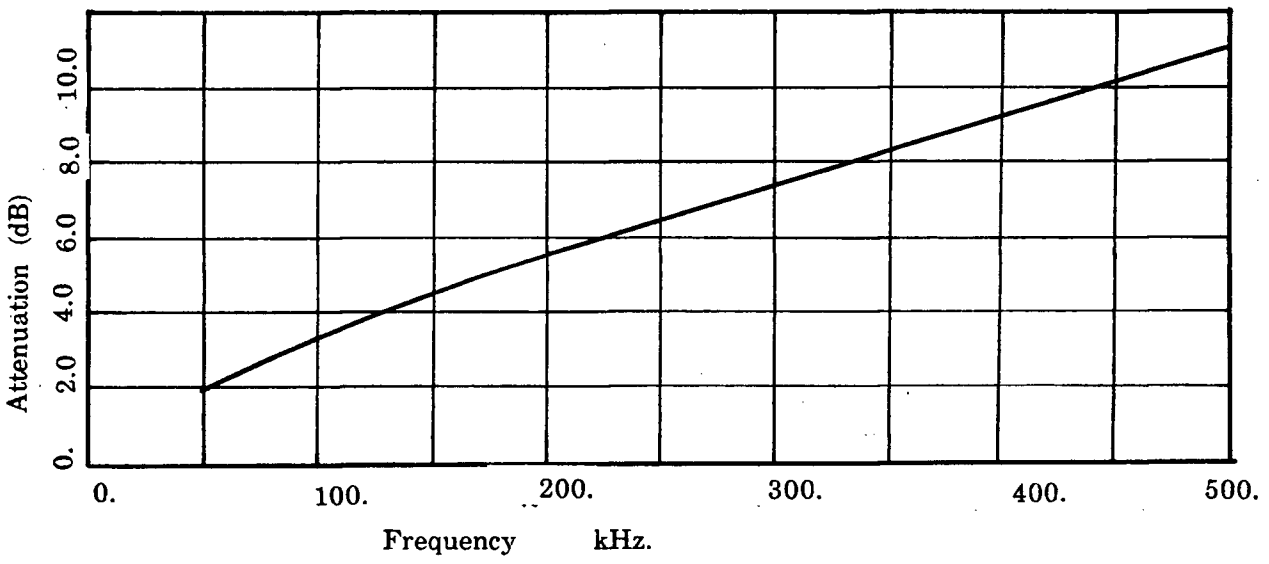

FIGURE 4.7) Example. a) Modal curve.
b) theoretical minimum attenuation.

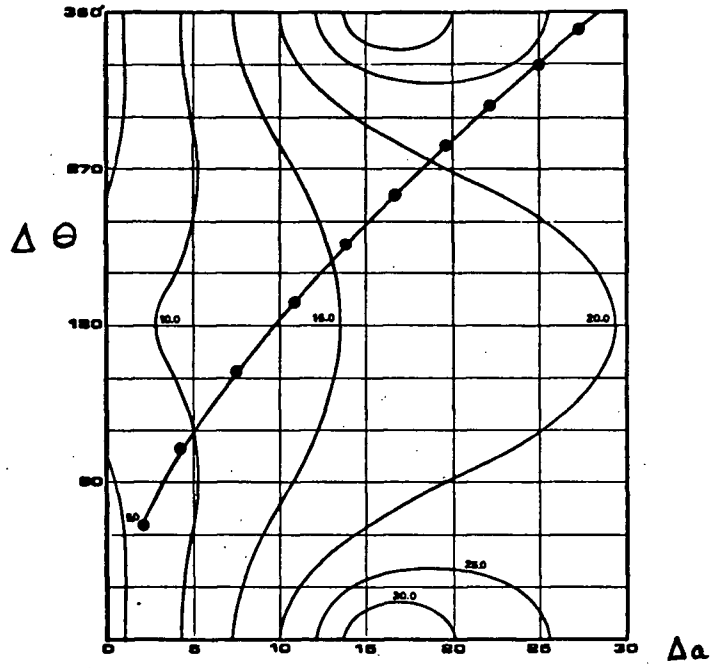

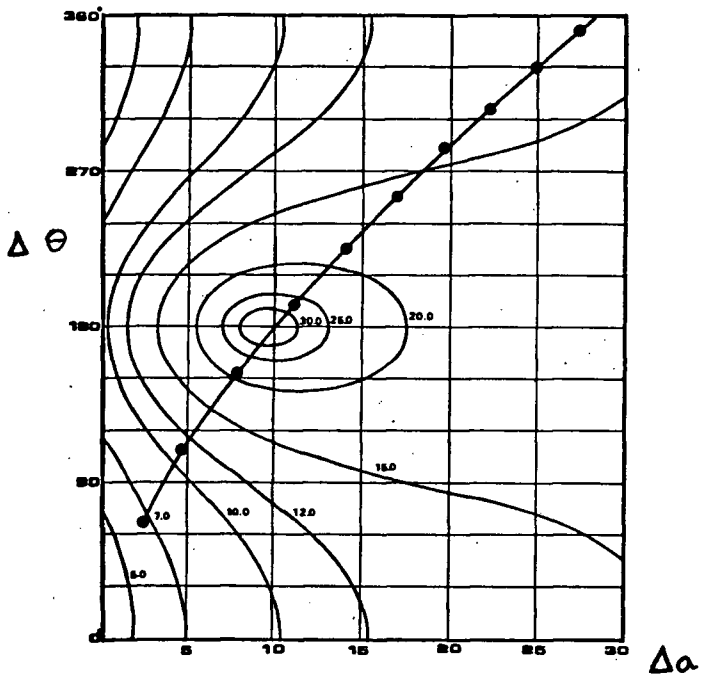

FIGURE 4.8) Contour maps with modal curve superposed.
a) Coupling $C_t=(1,0,0)/C_r=(0,0,1)$.
a) Couplings $C_t=(0,1,0)/C_r=(1,0,0)$ and $C_t=(0,0,1)/C_r=(0,1,0)$.

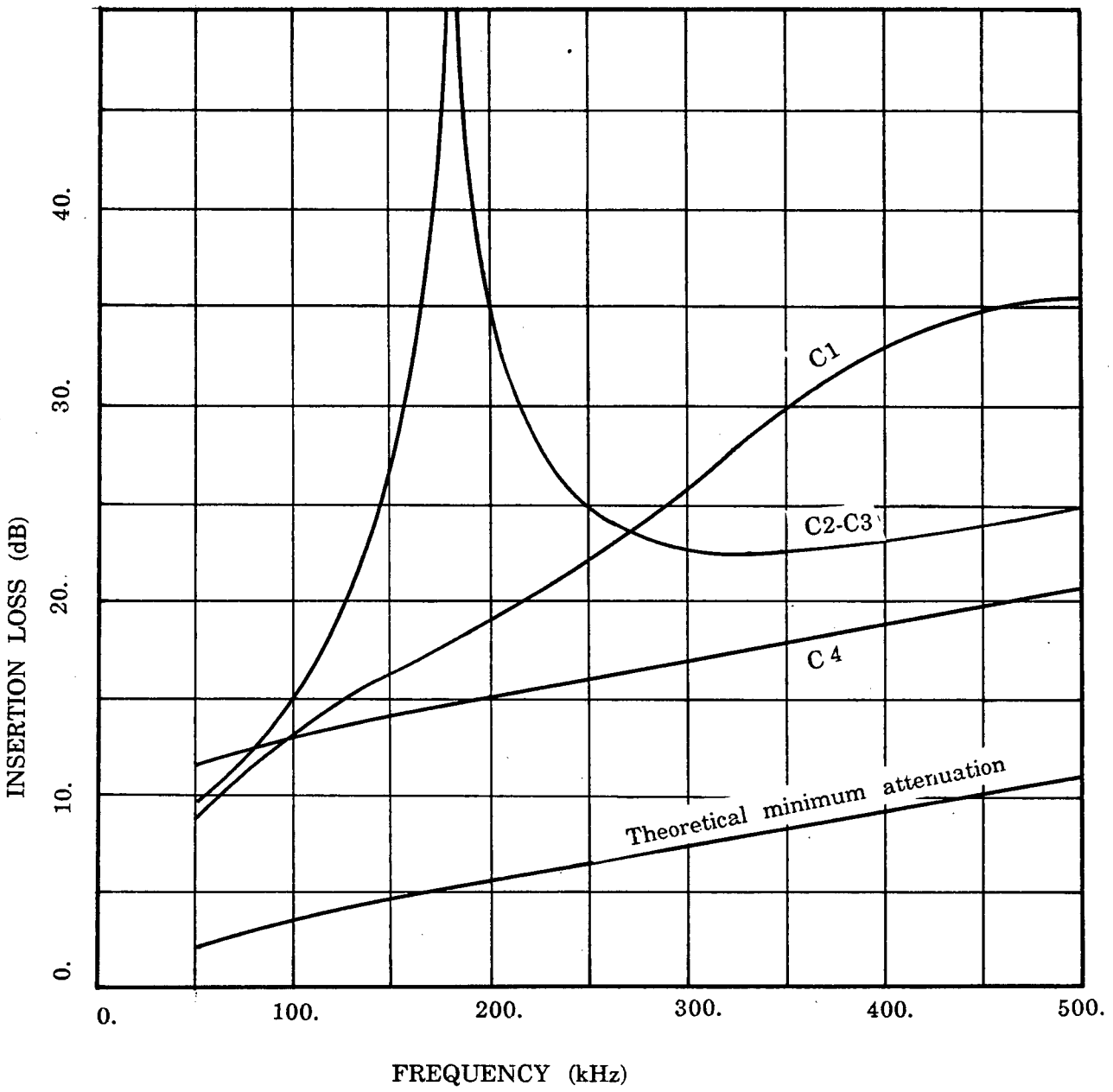

FIGURE 4.9) Line response for different couplings.

4.4. REMARKS.

A simplified method for PLC response prediction has been presented in this chapter.

By assuming reflectionless propagation, it was possible to express the insertion loss term as the sum of the theoretical minimum attenuation of the line and of a supplementary loss term. The further assumption of constant modal transformations led to expressing the supplementary loss in terms of a polynomial whose roots correspond to the modal cancellation poles of the line.

With the supplementary loss term in analytical form, a set of contour maps may be derived. The contours, together with another type of curves - the modal curves, facilitate the line response calculation.

The computer is required only to generate the contour maps. Afterwards it is not needed any longer; hence, the method is suitable for field applications. Two additional advantages of the graphical method are:

1. A single modal curve may be used to evaluate different couplings.
2. The proximity of poles, which may cause subsequent problems, is readily detected from the contour maps.

TABLE 4.1- POLYNOMIALS OF UNTRANSPOSED LINES.

COUPLING Trnsm./rceiv.	POLYNOMIAL	POLES
(1,0,0)/(1,0,0) (0,0,1)/(0,0,1)	(3X+1)/6	9.5424 <180°
(1,0,0)/(0,0,1) (0,0,1)/(1,0,0)	(3X-1)/6	9.5424 <0°,<360°
(1,0,0)/(0,1,0) (0,1,0)/(1,0,0) (0,1,0)/(0,0,1) (0,0,1)/(0,1,0)	(-2)/6	none
(0,1,0)/(0,1,0)	(4)/6	none
(1,-1,0)/(1,-1,0) (0,1,-1)/(0,1,-1)	(X+3)/4	none
(1,-1,0)/(1,0,-1) (1,0,-1)/(1,-1,0) (0,1,-1)/(1,0,-1) (1,0,-1)/(0,1,-1)	(X)/2	none
(1,-1,0)/(0,1,-1) (0,1,-1)/(1,-1,0)	(X-3)/4	none
(1,0,-1)/(1,0,-1)	X	none

TABLE 4.2- POLYNOMIALS OF SINGLE TRANSPOSED LINES

COUPLING Trnsm./rceiv.	POLYNOMIAL	POLES
(1,0,0)/(1,0,0) (0,0,1)/(0,0,1)	$(3X^2+1)/12$	4.77 $<90^o,270^o$
(1,0,0)/(0,1,0) (0,1,0)/(0,0,1)	$(3X-1)/6$	9.54 $<0^o,360^o$
(1,0,0)/(0,0,1)	$(3X^2+6X-1)/12$	16.21 $<0^o,360^o$
(0,1,0)/(1,0,0) (0,0,1)/(0,1,0)	$(3X+1)/6$	9.5424 $<180^o$
(0,1,0)/(0,1,0)	$(-1)/3$	none
(0,0,1)/(1,0,0)	$(3X^2-6X-1)/12$	16.2102 $<180^o$
(1,-1,0)/(1,-1,0) (0,1,-1)/(0,1,-1)	$(X^2+3)/8$	none
(1,-1,0)/(1,0,-1) (1,0,-1)/(0,1,-1)	$(X^2+3X)/4$	none
(1,-1,0)/(0,1,-1)	$(X^2+6X-3)/8$	6.67 $<0^o,360^o$
(1,0,-1)/(1,-1,0) (0,1,-1)/(1,0,-1)	$(X^2-3X)/4$	none
(1,0,-1)/(1,0,-1)	$(X^2)/2$	none
(0,1,-1)/(1,-1,0)	$(X^2-6X-3)/8$	6.6677 $<180^o$

TABLE 4.3-POLYNOMIALS OF DOUBLE TRANSPOSED LINES.

COUPLING Trnsm./rceiv.	POLYNOMIAL	POLES
(1,0,0)/(1,0,0) (0,0,1)/(0,0,1)	$(3X^3-9X^2-3X+1)/24$	6.29 <180° 13.55<0°,360°
(1,0,0)/(0,1,0) (0,1,0)/(0,0,1)	$(3X^2+6X-1)/12$	16.21 <0°,360°
(1,0,0)/(0,0,1)	$(3X^3-3X^2+9X-1)/24$	18.79 <0°,360°
(0,1,0)/(1,0,0) (0,0,1)/(0,1,0)	$(3X^2+1)/12$	4.77 <90°,270°
(0,1,0)/(0,1,0)	$(3X-1)/6$	9.54<0°,360°
(0,0,1)/(1,0,0)	$(3X^3-15X^2-3X-1)/24$	11.94 <180°+/-66.18°
(1,-1,0)/(1,-1,0) (0,1,-1)/(0,1,-1)	$(X^3-3X^2-9X+3)/16$	10.30<0°,360°
(1,-1,0)/(1,0,-1) (1,0,-1)/(0,1,-1)	$(X^3+3X)/8$	none
(1,-1,0)/(0,1,-1)	$(X^3+3X^2+15X-3)/16$	14.33<0°,360°
(1,0,-1)/(1,-1,0) (0,1,-1)/(1,0,-1)	$(X^3-6X^2-3X)/8$	6.67<180°
(1,0,-1)/(1,0,-1)	$(X^3-3X^2)/4$	none
(0,1,-1)/(1,-1,0)	$(X^3-9X^2+3X-3)/16$	4.62<180+/-105.07°

TABLE 4.4-POLYNOMIALS OF THREE TRANSPOSED LINES.

COUPLING Trnsm./rceiv.	POLYNOMIAL	POLES
(1,0,0)/(1,0,0) (0,0,1)/(0,0,1)	$(3X^6-21X^4-15X^2+1)/48$	1.49 <90°,270° 12.115<0°,180°,360°
(1,0,0)/(0,1,0) (0,1,0)/(0,0,1)	$(3X^5+3X^4-6X^3+6X^2+3X-1)/24$	5.7 <180° 12.36<0°,360°
(1,0,0)/(0,0,1)	$(3X^6+6X^5-15X^4-12X^3-3X^2+6X-1)/48$	1.40 <135.5°,224.5° 8.857<O°,360° 13.4<O°,360°
(0,1,0)/(1,0,0) (0,0,1)/(0,1,0)	$(3X^5-3X^4-6X^3-6X^2+3X+1)/24$	5.7 <0°,360° 12.36<180°
(0,1,0)/(0,1,0)	$(3X^4+6X^2-1)/12$	8.106<0°,180°,360°
(0,0,1)/(1,0,0)	$(3X^6-6X^5-15X^4+12X^3-3X^2-6X-1)/48$	1.4046 <44.509°,315.49° 8.857<180° 13.4<180°
(1,-1,0)/(1,-1,0) (0,1,-1)/(0,1,-1)	$(X^6-15^4-21X^2+3)/32$	8.835<0°,180°,360°
(1,-1,0)/(1,0,-1) (1,0,-1)/(0,1,-1)	$(X^6+3X^5-6X^4-6X^3-3X^2+3X>)/16$	0.8189<132.56°,227.44° 6.882<0°,360°
(1,-1,0)/(0,1,-1)	$(X^6+6X^5+3X^4-12X^3+5X^2+6X-3)/32$	1.2<35.4°,324.6° 2.5475<180° 6.46<0°,360°
(1,0,-1)/(1,-1,0) (0,1,-1)/(1,0,-1)	$(X^6-3X^5-6X^4+6X^3-3X^2-3X)/16$	0.8189<47.44°,312.56° 6.88<180°
(1,0,-1)/(1,0,-1)	$(X^6-6X^4-3X^2)/8$	3.333<90°,270°
(0,1,-1)/(1,-1,0)	$(X^6-6X^5+3X^4+12X^3-15X^2-6X-3)/32$	5.375<0°,360° 10.15<180°

CHAPTER 5. COUPLING RECOMMENDATIONS.

Although the modal theory or - in the case of delta lines Senn's graphical method may be used for comparing coupling alternatives, it is desirable to have a set of general recommendations or guidelines for selecting adequate line couplings.

Prior to the development of the modal theory, coupling recommendations were based on simplistic line concepts. It was found, afterwards, that most of them were incorrect; however, the recommendations are still widespread. One of these rules, for instance, advises the use of the couplings that provide a continuous metallic path between the transmitter and the receiver; a counter-example to this rule was presented in section 4.3.1.

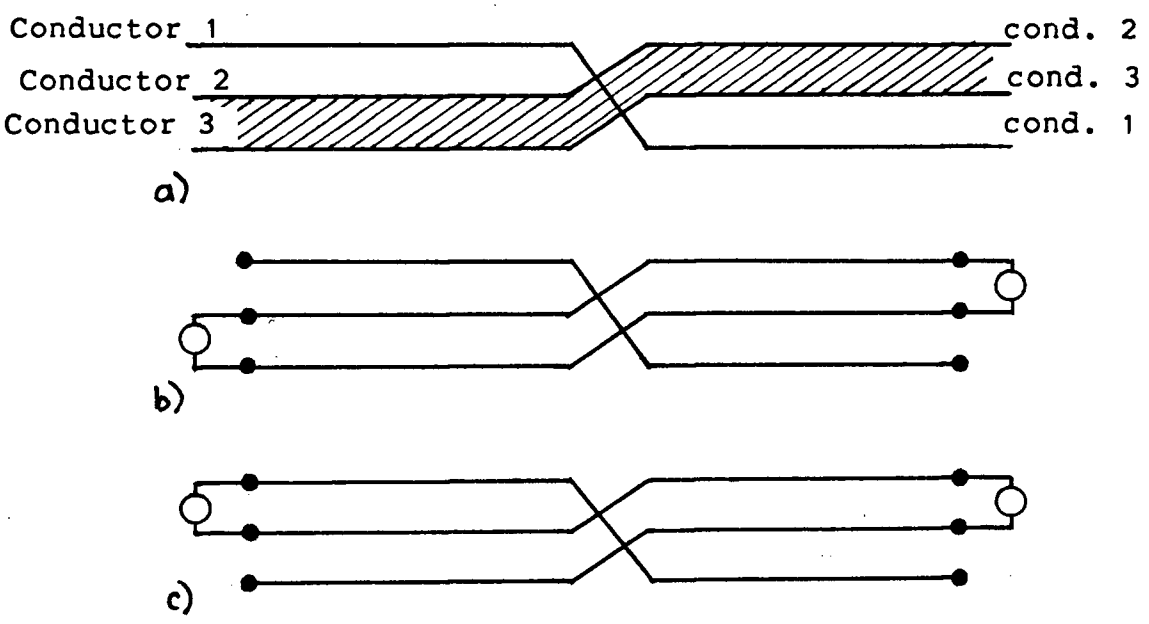

FIGURE 5.1) a) Transmission line layout example.
b) Coupling alternative 1. c) Alternative 2.

Another rule recommends that, for phase to phase couplings, the two conductors which stay closest to each other for most of the distance along the line be chosen; for example, according to this rule, in figure 5.1a conductors 2 and 3 must be selected. This coupling, represented in figure 5.2b, hereafter referred to as coupling 1, is to be compared against coupling 2 on figure 5.2c.

By assuming the line data provided in figure 4.5b, a modal plot is obtained. In figures 5.2a and 5.2b, this plot is superposed to the contour maps corresponding to coupling 1 and coupling 2. The resulting line responses are plotted in figure 5.2c; it is clear there that coupling 2 is much better than coupling 1. It may be concluded, thus, that the abovementioned rule is unfounded.

Some more recent studies [20,21] introduce the concept of optimum coupling; however, in a strict sense, optimum couplings very seldom exist. In reference 21, coupling 2 of the previous example is presented as the optimum phase to phase arrangement for single transposed lines. This coupling is indeed the most recommendable in that case for, among other things it is free of poles; however, it cannot be said that it is optimum. For instance, in figure 5.2c, coupling 1 performance is much better at frequencies below 120 kHz and slightly better above 320 kHz.

The purpose of the first section is to introduce the concept of recommended couplings along with a technique for generating the recommendations; this technique is based on Senn's graphical method. In section 5.2 coupling recommendations are produced for the transposition schemes that are supposed to

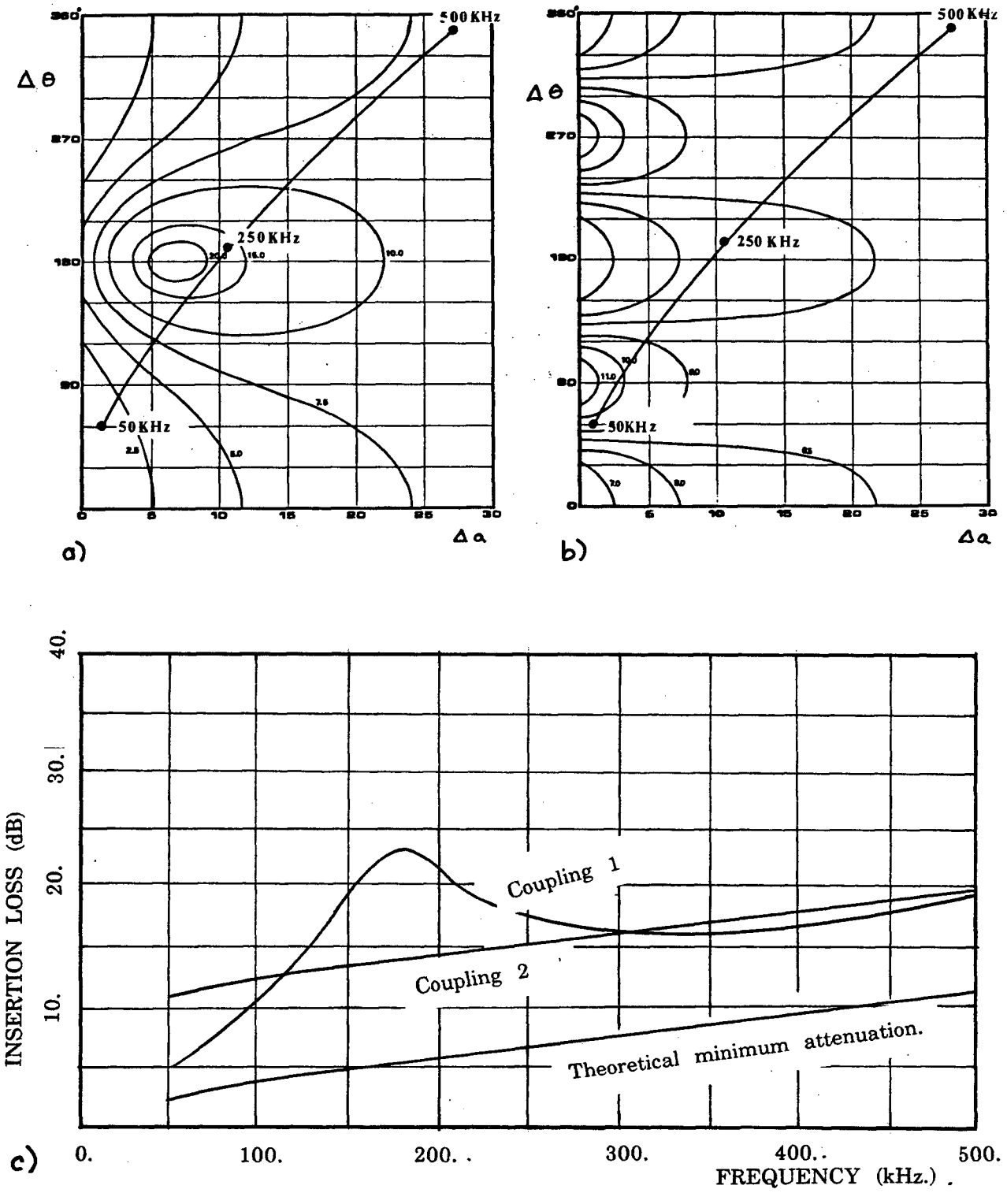

FIGURE 5.2) a) Coupling 1 contour. b) Coupling 2 contour. c) Frequency responses.

be the most commonly found in practice. Finally, in section 5.3 the performance of non-conventional couplings is analyzed.

5.1. PROPOSED METHOD FOR ASSESSING COUPLING ALTERNATIVES.

The type of recommended couplings of concern here is the one that, in addition to providing low losses, minimizes the risk of modal cancellation.

It was shown in chapter 4 that the line insertion loss is composed by two terms:

$$A = A_1 + A_s$$

Whereas the supplementary loss term changes from one coupling to the other, the mode 1 term remains equal; thus, coupling comparisons can be based on their supplementary loss terms solely. Here, it is proposed that, in order to compare two couplings, their corresponding supplementary loss terms be subtracted:

$$A_{s(\text{coupling } 1)} - A_{s(\text{coupling } 2)}$$

The difference may be represented in the $\Delta\alpha$-$\Delta\Theta$ plane by means of two colors; one color indicating that the difference is positive, i. e., coupling 2 is better than coupling 1, and the other color indicating the opposite. As an example, for the two color plot of figure 5.3a, the coupling of figure 5.1b has been chosen as coupling 1 and that on figure 5.1c as coupling 2.

The two color plot provides a quick overview of the comparative performance between two couplings; however, it may be misleading. In figure 5.3, for

a)

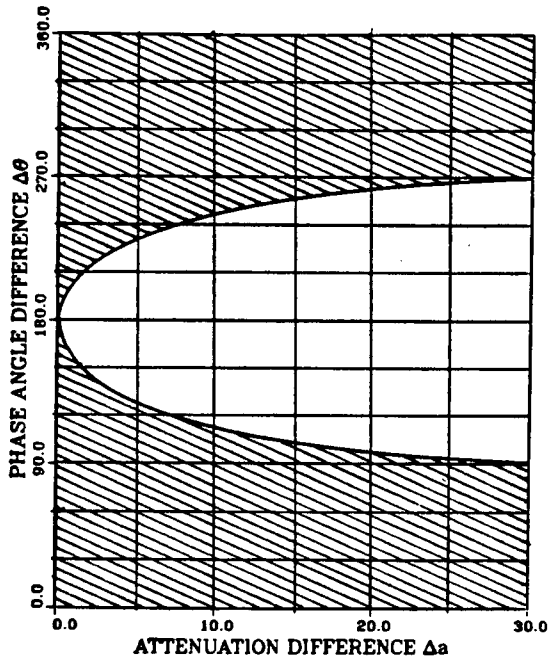

b)

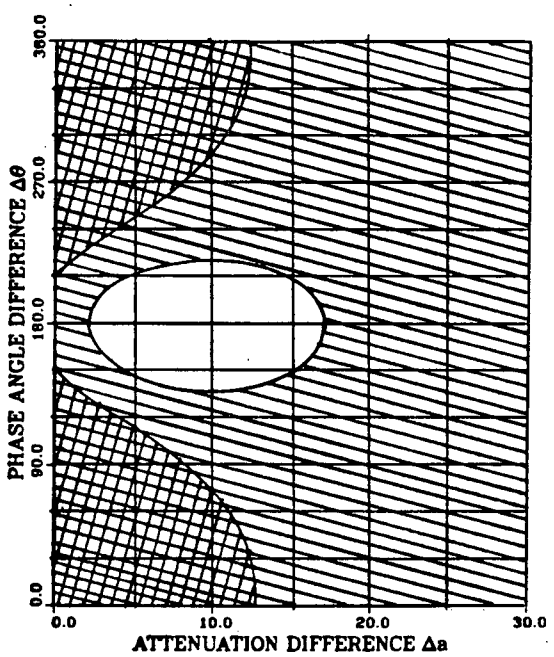

FIGURE 5.3) a) Example of a two color plot.
b) Example of a three color plot.

instance,the black region covers more than half of the $\Delta\alpha$-$\Delta\theta$ plane; it may seem then, that coupling 1 is better than coupling 2. A look at their frequency responses in figure 5.2c shows that this appreciation is incorrect. The first point to notice is that some of the differences between the two couplings may be irrelevant; it can be seen at figure 5.2c that above 300 kHz both responses are very similar. Another point to consider is that not all regions of the $\Delta\alpha$-$\Delta\theta$ plane are equally important; in the current example, the central region containing the pole of coupling 1 seems to have a high probability of occurrence in the practice.

As in PLC communications a difference of 3 dB is considered as unimportant, a three color plot -as the one in figure 5.3b, is introduced in order to remove the irrelevant differences. There, the third region in gray color may be considered as a neutral zone where the response differences are comprised in the +/- 3 dB range. The black and white regions designate thus only meaningful differences.

In order to establish the regions of the $\Delta\alpha$-$\Delta\theta$ plane that are relevant for the coupling comparisons, a second type of plot, which henceforth will be referred to as "feasible regions map", is introduced. An example is provided in figure 5.4.

The shaded region of figure 5.4 was produced by varying three of the line physical parameters -frequency, earth resistivity and conductors medium height.

It is important in practice to consider the variations of the earth resistivity and of the conductor height for two reasons. Firstly, these two parameters are

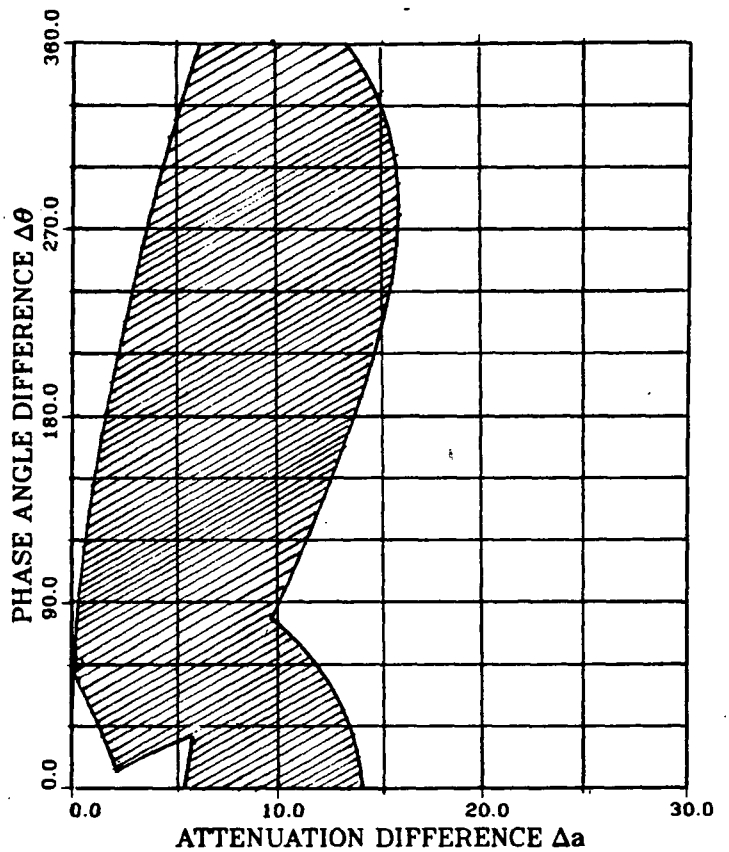

LINE DATA:

- -Medium heights of phase conductors 12-18m
- -Horizontal distance
- -between conductors ..... 9.0 m
- -Conductor radius ..... 4x1.05 cm.
- -Gnd. wires ..... None
- -Earth resistivities ... 30-3000 Ohm-m
- -Frequencies ..... 50-450 kHz
- -Line section length .... 30 km.

FIGURE 5.4) a) Example of a feasible regions map.

affected by the climate -the conductor sag depends on the temperature and the earth resistivity on the humidity. Secondly, the earth resistivity parameter, due to its nature, involves a considerable uncertainty. Figure 5.5a shows the influence of the earth resistivity on the modal curves of the line specified by table 5.1, and figure 5.5b shows the effects of varying the conductors medium height.

The feasible regions maps, in addition to establishing the $\Delta\alpha$-$\Delta\theta$ meaningful regions for the coupling comparisons, help to detect the possibility of falling into a cancellation pole; this this is very important since, as it will become apparent in the next section, it is not always possible to find pole-free couplings.

5.2. COUPLING CONSIDERATIONS FOR COMMON LINE CASES.

The method described in the previous section is applied here to the selection of couplings for the most common transposition schemes; i. e., those depicted in figure 4.3.

It is found here that only in the most simple case -untransposed line phase to ground coupling, the recommended arrangement is optimum. It is also found that, for lines with two or more transpositions it may not be possible to find pole-free couplings; for these cases, obviously, the recommendations cannot be considered of general validity, and the use of feasible region maps is strongly recommended.

The contour maps for all the couplings mentioned along this section are provided in the appendix.

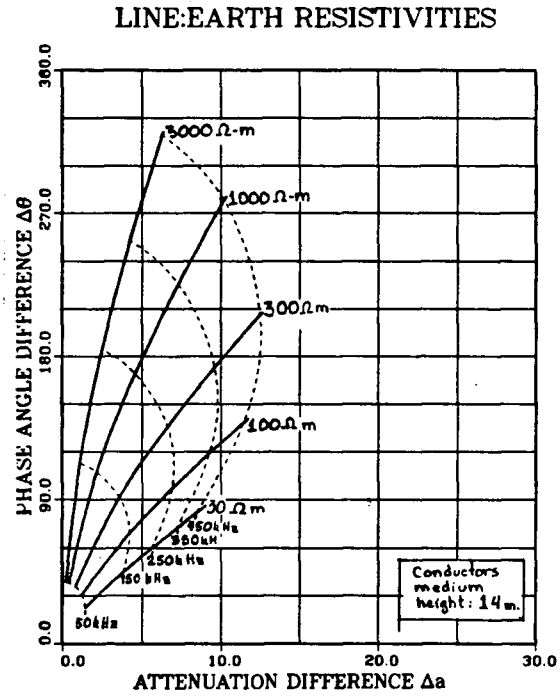

FIGURE 5.5) a) Effect of the earth resistivity on the modal plots.

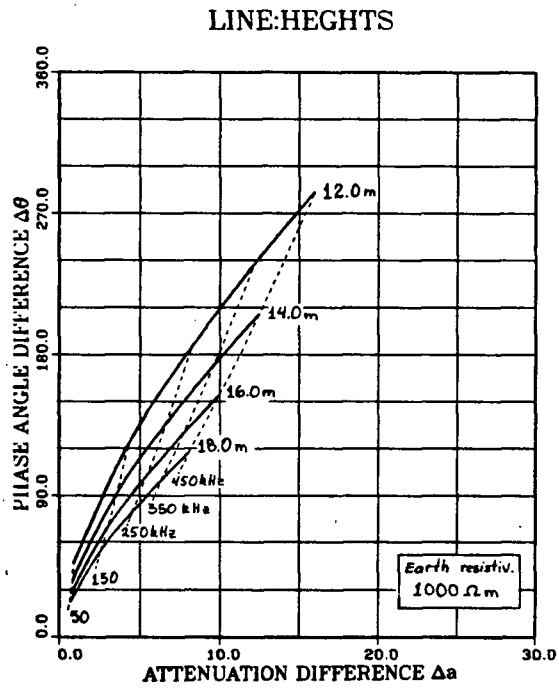

FIGURE 5.5)b) Effect of the conductors medium height . on the modal plots.

5.2.1. Untransposed lines.

5.2.1.1. Phase to ground coupling.

As it was mentioned before, this is the most simple case found in practice. The following coupling arrangement:

(0 , 1 , 0) / (0 , 1 , 0)

depicted in figure 5.6, is the recommended one. This coupling is optimum; its supplementary losses -according to Senn's simplified method- are constant and equal to:

As = 3.5218.

These losses are due only to mode conversion at both end of the line.

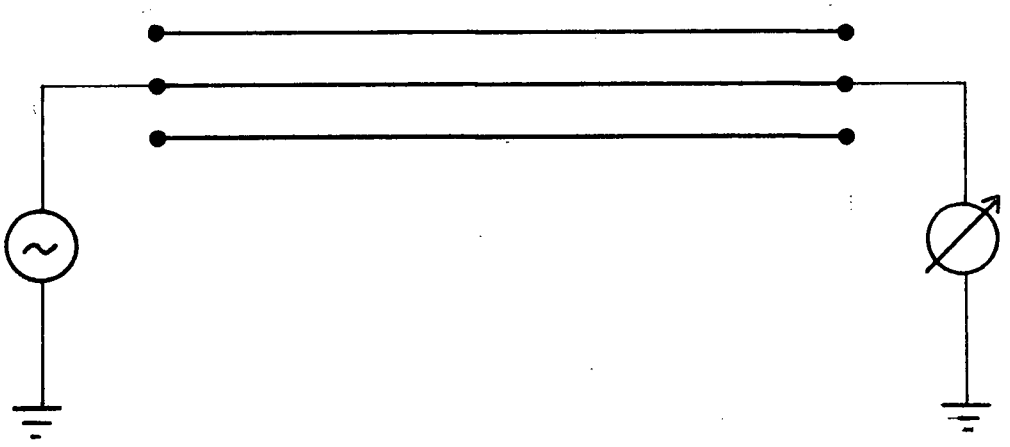

FIGURE 5.6) Recommended phase to ground coupling for untransposed lines.

5.2.1.2. Phase to phase coupling.

For phase to phase differential mode coupling (push-pull), the arrangement:

(1 , -1 , 0) / (1 , -1 , 0),

represented in figure 5.7a, is the recommended one. This coupling cannot be considered optimum. It may be seen from the two and three color plots in figures 5.8a and 5.8b, that the coupling:

(1 , -1 , 0) / (0 , 1 , -1),

represented in figure 5.7b, has a very similar performance and in some regions, small though, it is better.

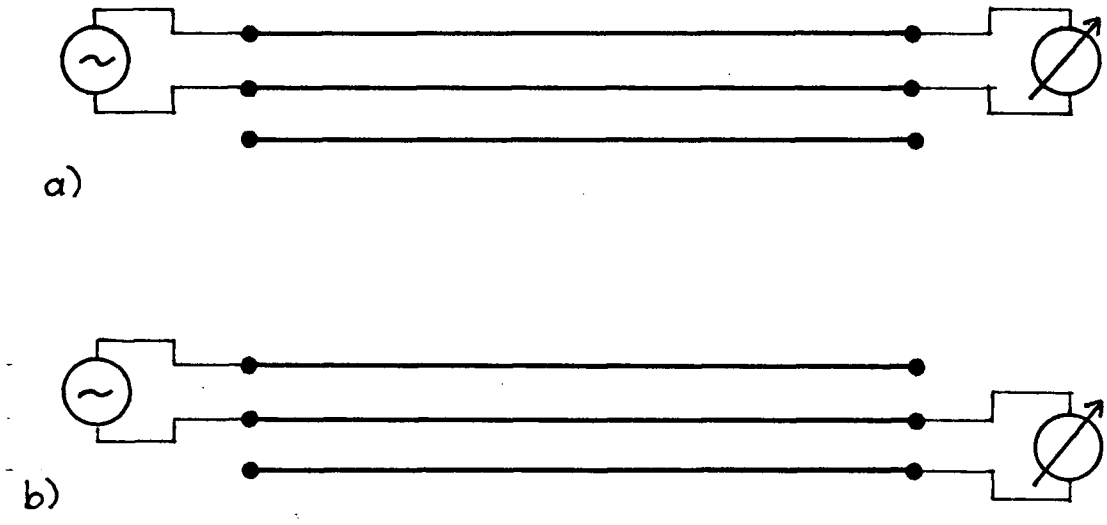

FIGURE 5.7) a) Recommended phase to phase coupling on untransposed lines. b) Second best coupling.

a)

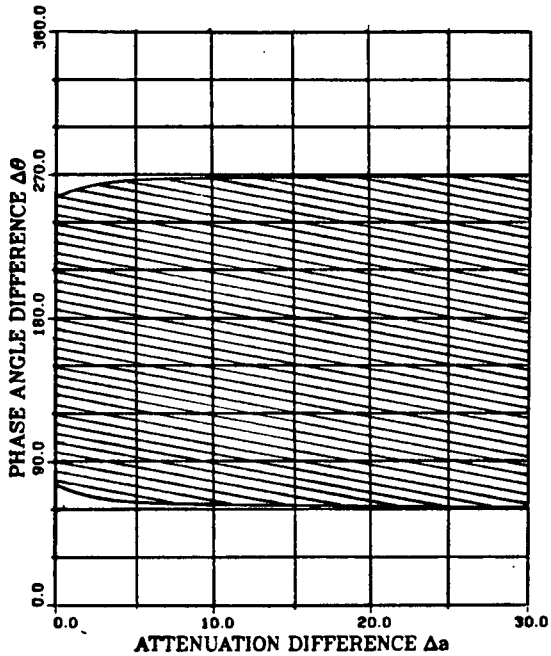

b)

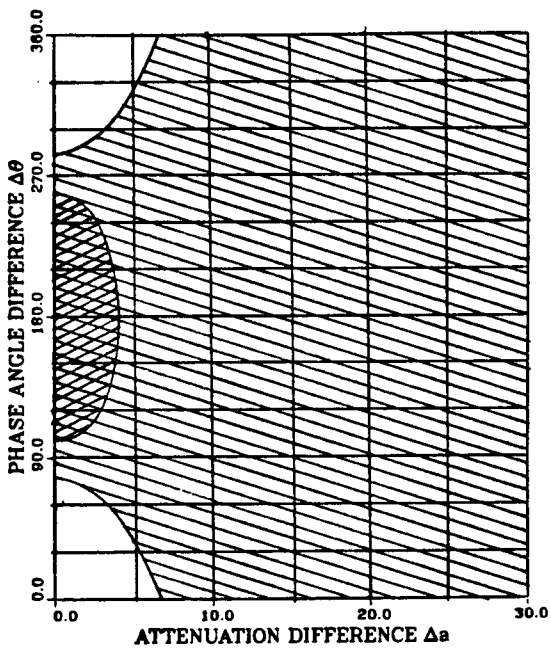

FIGURE 5.8) Comparison of the couplings depicted in figures 5.7a and 5.7b. a) Two color plot. b) Three color plot.

5.2.2. Single transposed lines.

5.2.2.1. Phase to ground coupling.

The coupling of figure 5.9 is the best recommended, mainly because it is pole-free. The other alternatives may have better performance in small regions of the $\Delta\alpha$-$\Delta\theta$ plane which correspond to low frequencies and/or very high earth resistivities; additionally alll them present cancellation poles.

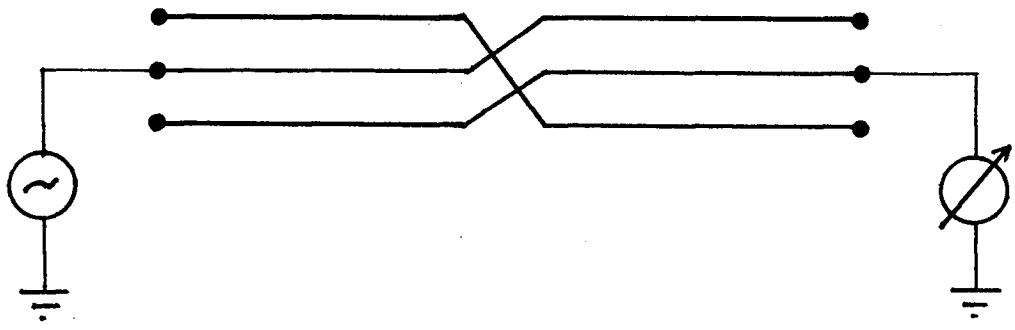

FIGURE 5.9) Recommended phase to ground coupling for single transposed lines.

Note that section 4.3 provides a specific example of this coupling.

5.2.2.2. Phase to phase cooupling.

The arrangement depicted in figure 5.10 is the recommended differential mode coupling for single transposed lines. There are some other alternatives that are also free of poles; however, the two color plots indicate that figure 5.10 coupling has a better performance in most of the Δa-$\Delta\theta$ plane; moreover, the small regions where the other alternatives are better, correspond to low frequencies and/or to very high earth resistivities. The two couplings depicted in figure 5.11 should be avoided. The coupling on figure 5.11a has been already analyzed in the example at the beginning of the chapter.

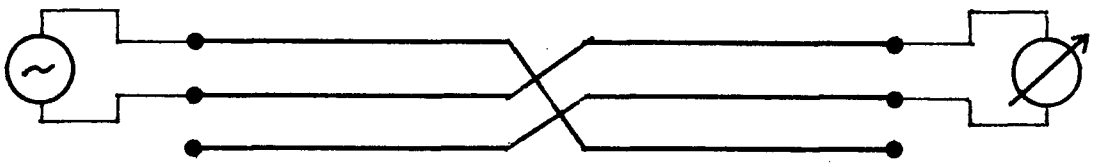

FIGURE 5.10) Phase to phase recommended coupling for single transposed lines.

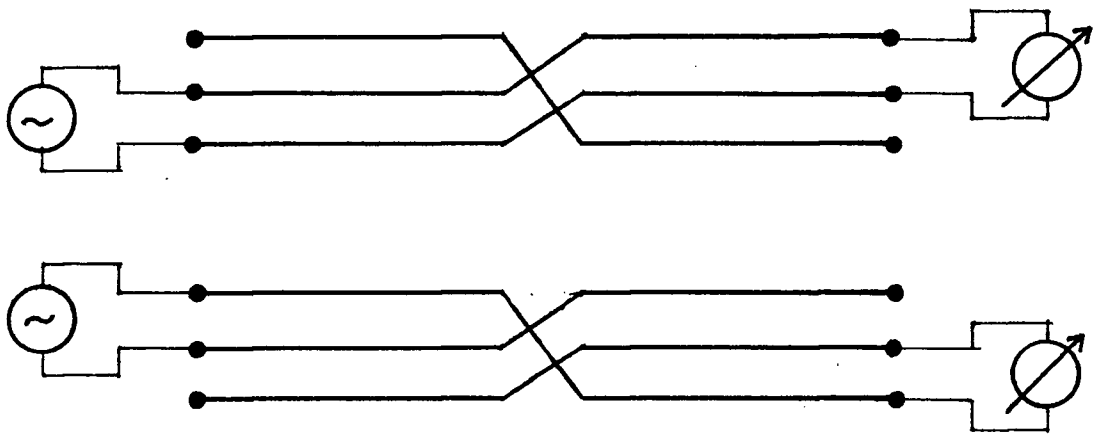

FIGURE 5.11) Couplings that should be avoided.

5.2.3. Lines with two transpositions.

5.2.3.1. Phase to ground coupling.

As it may be seen from table 4.3, in this case none of the couplings is free of poles; for this reason, the coupling recommended here (figure 5.12) cannot be considered as generally valid.† Before choosing a carrier frequency, it is thus convenient to check, by means of a feasible regions map, that there is no danger of modal cancellation.

As an example, the coupling of figure 5.13 is the one whose performance is the closest to that of the recommended one.The two color plot comparing these two couplings is shown in figure 5.14. Apart from the fact that the white area where the recommended coupling performs better is bigger, its poles are slightly closer to the rigth hand side of the $\Delta\alpha$-$\Delta\theta$ plane; this means that they are less likely to happen.

5.2.4. Phase to phase coupling.

Here the selection of a coupling is much more difficoult than in the previous cases. There are actually two pole-free couplings:

$$(1 , -1 , 0) / (1 , 0 , -1)$$

which is equivalent to:

$$(1 , 0 , -1) / (0 , 1 , -1),$$

†Note: Reference [21] refers to this coupling as optimum.

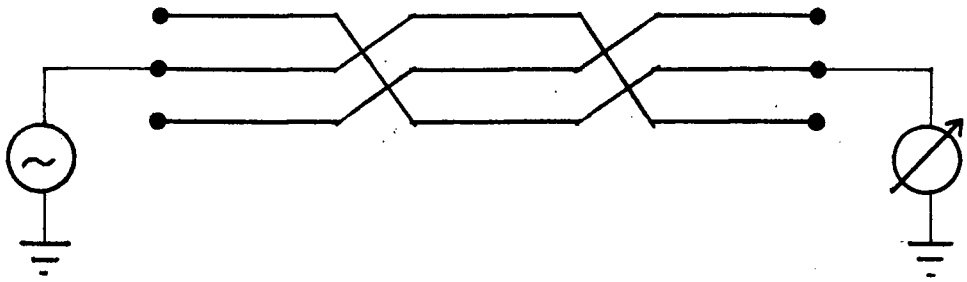

FIGURE 5.12) Recommended phase to ground coupling in a double transposed line.

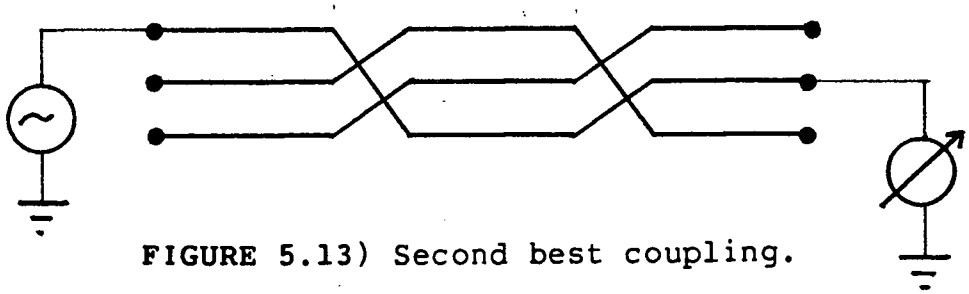

FIGURE 5.13) Second best coupling.

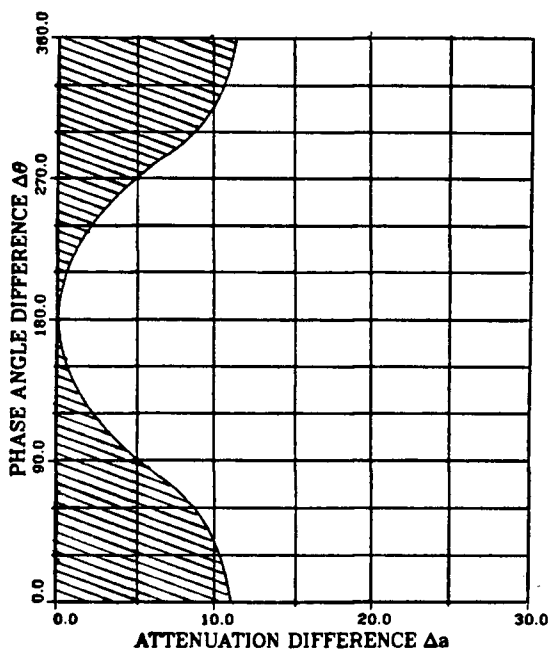

FIGURE 5.14) Two color plot comparing couplings depicted in figures 5.12 and 5.13.

and

$$(1 , 0 , -1) / (1 , 0 , -1);$$

Unfortunatelly, their losses grow very quickly as $\Delta\alpha$ increases. The first coupling, depicted in figure 5.15, is better than the second one.

The coupling of figure 5.16 has the smallest losses for most of the $\Delta\alpha$-$\Delta\Theta$ plane; however, it is not pole-free. † The coupling of figure 5.17 is similar in performance to that of 5.16. With these two couplings the possibility of modal cancellation exists for high earth resistivities and for long lines with medium earth resistivities. For figure 5.17 coupling, this danger also exists at low frequencies. As the supplementary losses of figure 5.15 coupling are small at the region on the left hand side of the $\Delta\alpha$-$\Delta\Theta$ plane -which is precisely where couplings 5.16 and 5.17 have their poles, it is possible to consider the former as the complement of the latter ones; however, it is strongly recommended that every application be supported by means of its corresponding feasible regions map.

5.2.5. Lines with three transpositions.

It may be seen from table 4.5 that all the three-transposed line couplings present cancellation poles; thus, the selection of frequencies should be aided by a feasible regions map.

For phase to ground coupling, the recommended arrangement is represented in

†NOTE: At reference 21 this coupling is refered to as *optimum coupling* without warning about the possibility of modal cancellation.

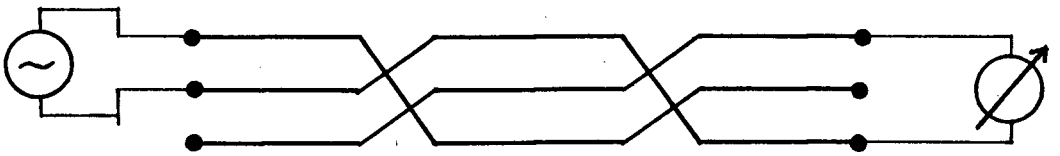

FIGURE 5.15) Complementary phase to phase coupling on a double transposed line.

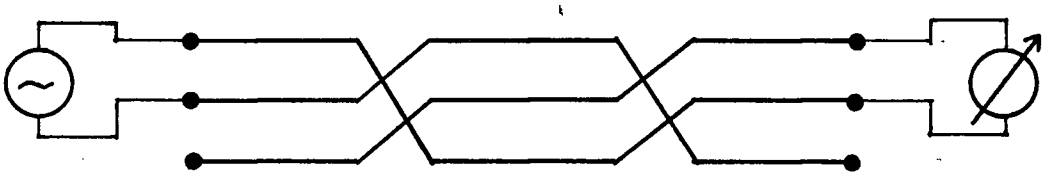

FIGURE 5.16) Recommended phase to phase coupling for a double transposed line.

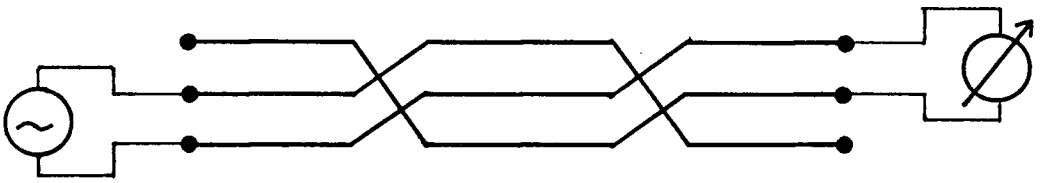

FIGURE 5.17) Second best phase to phase coupling for a double transposed line.

figure 5.18; the recommended one for phase to phase coupling is the one given in figure 5.19a; although, the coupling of figure 5.19b is as nearly as good as that in figure 5.19a.

The three suggested couplings have the common characteristic that their poles lie close to the left hand side of the $\Delta\alpha$-$\Delta\theta$ plane, which means that the possibility of modal cancellation exists for lines with high earth resistivity or for very long lines with medium earth resistivity.

5.3. NONCONVENTIONAL COUPLINGS.

The coupling arrangements analyzed in the previous section are the ones traditionally used in the power sector. However, other arrangements are possible -they are referred to here as nonconventional couplings.

In order to find better couplings (i. e., pole-free) in lines with two and three transpositions, two nonconventional phase to phase alternatives were analyzed:

1. Common mode (push-push) transmission with differential mode (push-pull) reception
2. Differential mode transmission with common mode reception.

Tables 5.1 and 5.2 provide the polynomials of the analyzed couplings together with their cancellation poles. None of the analyzed alternatives resulted as attractive as to justify the departure from the conventional practices.

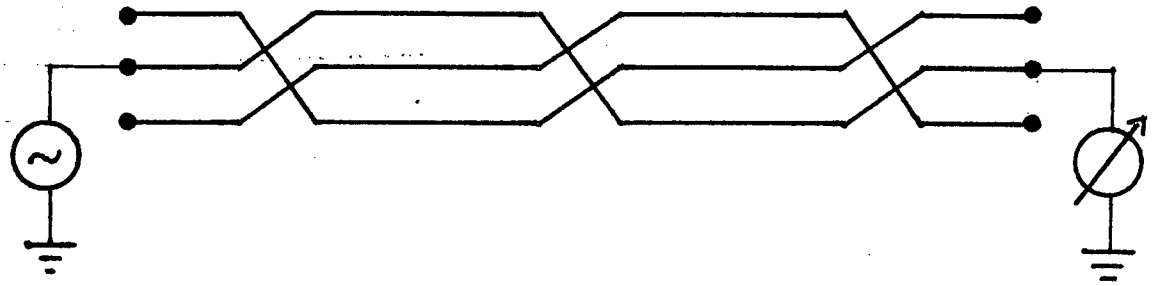

FIGURE 5.18) Phase to ground recommended coupling for a three transposed line.

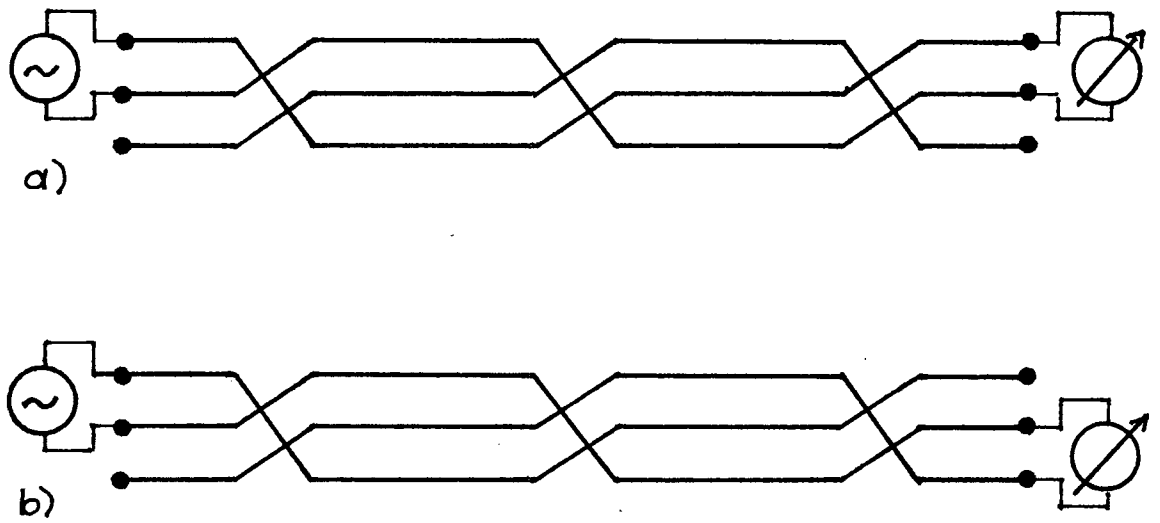

FIGURE 5.19) Phase to phase recommended couplings for a three transposed line. a) Best coupling. b) Second best coupling.

Another nonconventional coupling arrangement that was analyzed is the so called mode 1 coupling. This is an alternative several carrier equipment manufacturers advocate for. In mode 1 coupling the carrier signal is injected to the three phase conductors of the line with the following current (or voltage) distribution:

$$(1 , -2 , 1).$$

The intention with this coupling is to put as much energy as possible into mode 1 form, which is usually the mode with the least losses.

Figure 5.20 shows the contour map of mode 1 coupling on a double-transposed line. Note that it has cancellation poles. This map can be compared with the one of the recommended phase to ground coupling given in the appendix; the difference between them is a constant value of 3.52 dB. The insertion loss difference between mode 1 coupling and the recommended phase to phase coupling -although it is not constant- may be approximated to the figure of 2.5 dB, which is very accurate for most of the $\Delta\alpha$-$\Delta\Theta$ plane.

It may be concluded from the above results that, since mode 1 coupling does not eliminate the possibility of modal cancellation, an improvement of 2.5 dB would hardly justify the additional expense of the three-phase coupling.

Figure 5.21 shows the contour map for the mode 1 coupling on a three-transposed line; note that this coupling presents more poles than the recommended phase to ground coupling of figure 5.18, or than the phase to phase coupling of figure 5.19. As $\Delta\alpha$ increases the supplementary loss difference between mode 1 coupling and the recommended phase to ground one tends to

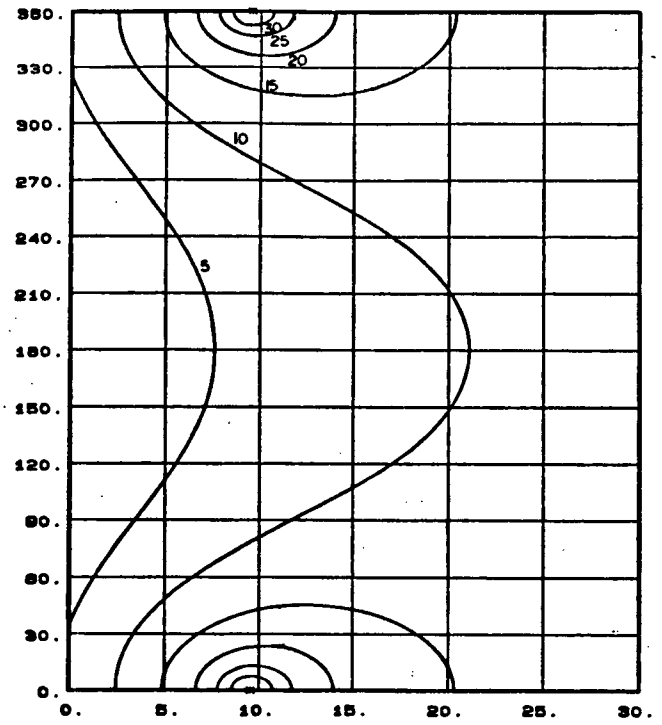

FIGURE 5.20) Contour map of mode 1 coupling on a double transposed line.

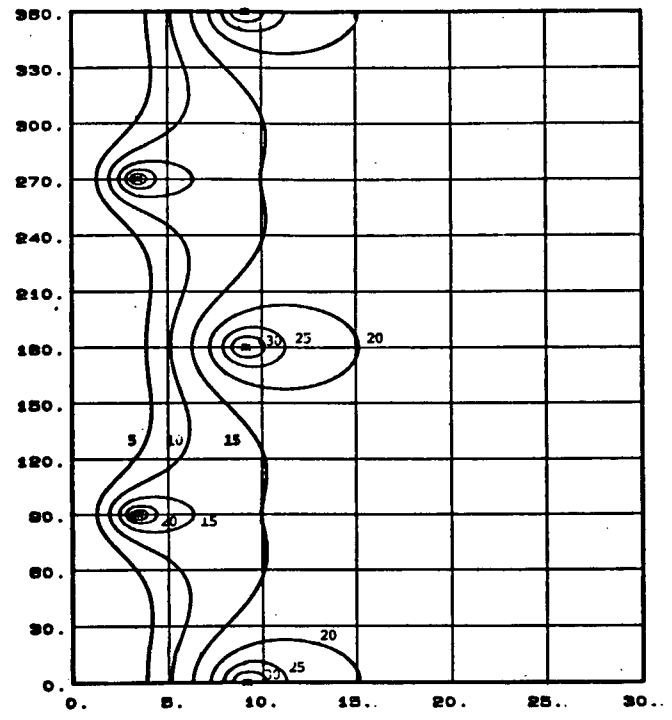

FIGURE 5.21 Contour map of mode 1 coupling on a three transposed line.

3.5; whereas its difference with respect to figure 5.19a coupling tends to 2.5 dB. By the same token as with double-transposed lines, mode 1 coupling does not seem that atractive for three-transposed lines.

TABLE 5.1-POLYNOMIALS OF DOUBLE TRANSPOSED LINES. NONCONVENTIONAL COUPLINGS.

COUPLING Trnsm./rceiv.	POLYNOMIAL	POLES
(1,1,0)/(1,1,0) (0,1,1)/(0,1,1)	$(3X^3-9X^2-3X+1)/48$	6.29 <180° 13.55<0°,360°
(1,1,0)/(1,0,1) (1,0,1)/(0,1,1)	$(3X^2+1)/24$	4.77 <90°,270°
(1,1,0)/(0,1,1)	$(3X^3-15X^2-3X-1)/48$	11.93 <113.82°,246.18°
(1,0,1)/(1,1,0) (0,1,1)/(1,0,1)	$(3X^2+6X-1)/24$	16.21 <0°,360°
(1,0,1)/(1,0,1)	$(3X-1)/12$	9.54<0°,360°
(0,1,1)/(1,1,0)	$(3X^3-3X^2+9X-1)/48$	18.78 <0°,360°
(1,-1,0)/(1,1,0)	$(X^3+X^2+7X-1)/16$	8.46<100.9°,259.1°
(0,1,-1)/(0,1,1)	$(X^3-7X^2-X-1)/16$	17.1<0°,360°
(1,-1,0)/(1,0,1)	$(X^2+4X-1)/8$	12.54<180°
(1,0,-1)/(0,1,1)	$(X^3-4X^2-X)/8$	12.54<0°,360°
(1,-1,0)/(0,1,1)	$(X^3-X^2-X+1)/16$	0<0°,180°,360°
(1,0,-1)/(1,1,0)	$(X^3-2X^2+X)/8$	0<0°,360°
(0,1,-1)/(1,0,1)	$(X^2-2X+1)/8$	0<0°,360°
(1,0,-1)/(1,0,1)	$(X^2+X)/4$	0<180°
(0,1,-1)/(1,1,0)	$(X^3-5X^2-5X-1)/16$	0<180° 15.3<0°,360°

TABLE 5.2-POLYNOMIALS OF THREE TRANSPOSED LINES. NONCONVENTIONAL COUPLINGS.

COUPLING Trnsm./rceiv.	POLYNOMIAL	POLES
(1,1,0)/(1,1,0) (1,0,1)/(0,1,1)	$(3X^6-21X^4-15X^2+1)/96$	1.49 <90°,270° 12.116<0°,180°,360°
(1,1,0)/(1,0,1) (1,0,1)/(0,1,1)	$(3X^5-3X^4-6X^3-6X^2+3X+1)/48$	5.7 <0°,360° 12.36<180°
(1,1,0)/(0,1,1)	$(3X^6-6X^5-15X^4+12X^3-3X^2-6X-1)/96$	1.40 <44.48°,315.52° 8.857<180° 13.4<180°
(1,0,1)/(1,1,0) (0,1,1)/(1,0,1)	$(3X^5+3X^4-6X^3+6X^2+3X-1)/48$	5.7 <180° 12.36<0°,360°
(1,0,1)/(1,0,1)	$(3X^4+6X^2-1)/24$	8.106<0°,180°,360°
(0,1,1)/(1,1,0)	$(3X^6+6X^5-15X^4-12X^3-3X^2+6X-1)/96$	1.4046 <135.5°,224.5° 8.857<0°,360° 13.4<0°,360°
(1,-1,0)/(1,1,0)	$(X^6-4X^5-3X^4+8X^3+3X^2-4X-1)/32$	0<0°,180°,360° 12.54<180°
(0,1,-1)/(0,1,1)	$(X^6+4X^5-3X^4-8X^3+3X^2+4X-1)/32$	0<0°,180°,360° 12.54<0°,360°
(1,-1,0)/(1,0,1)	$(X^6-X^5-6X^4+2X^3-3X^2-X>)/16$	2.33<67.73°,292.27° 11.8<180°
(1,0,-1)/(0,1,1)	$(X^5+3X^4-2X^3+6X^2+X-1>)/16$	7.1<180° 9.37<0°,360°
(1,-1,0)/(0,1,1)	$(X^6+2X^5-9X^4-4X^3-9X^2+2X+1)/32$	0<108.1°,251.2° 8.21<0°,360° 12.24<180°
(1,0,-1)/(1,1,0)	$(X^5-3X^4-2X^3-6X^2+X+1)/16$	5.7<180° 12.36<0°,360°
(0,1,-1)/(1,0,1)	$(X^6+X^5-6X^4-2X^3-3X^2+X)/16$	2.33<112.27°,247.73 11.8<0°,360°
(1,0,-1)/(1,1,0)	$(X^5-2X^3+X)/8$	0<0°,180°,360°
(0,1,-1)/(1,-1,0)	$(X^6-2X^5-9X^4+4X^3-9X^2-2X+1)/32$	12.25<0°,360° 8.21<180°

CHAPTER 6. CONCLUSIONS

A new method for comparing coupling alternatives in power line carrier communication systems has been proposed.

The method has been applied to practical cases, and a new set of coupling recommendations has been generated. In general, the coupling recommendations coincide with those proposed by the IEC in reference [21]; however, the IEC guide does not mention that some of these couplings are not 100% safe, nor does it provide alternatives; furthermore it is suggested there that these couplings are optimum.

To the best of the author's knowledge, coupling recommendations for three transposed lines have not been produced before.

The method has been applied also to the study of non-conventional couplings. As it is mentioned in chapter 5, none of the considered couplings resulted as attractive as to justify its adoption. This conclusion applies also to the so called mode 1 coupling, which is in its way of becoming a standard practice in North America [22]. Mode 1 is considerably more expensive than the conventional phase to ground or phase to phase couplings.

The method for comparing coupling alternatives is based on a graphical technique for evaluating power line frequency responses proposed by Senn [12]. Senn's technique has been wholy developedin chapter 4. Several gaps that were left out

in the related publications [12,13,14,20] are presented in detail in chapter 4. The results obtained with the method therein described coincide with those published by Senn.

In chapters 2 and 3, a series of procedures for calculating phase and modal parameters are presented. These procedures simplify the computations so much that it seems that it is possible now to perform line analysis by means of programmable calculators. It should be mentioned that this type of analysis usually requires a mainframe.

6.1. FUTURE RESEARCH

Along the research reported in this thesis, several topics that require further work became apparent. Three of them are mentioned next; one deals with constant modal transformation matrices, the other two with improvements to Senn's method.

6.1.0.1. Constant modal transformation matrices

The possibility of using frequency invariant transformation matrices has been always attractive, specially for transient studies of transmission lines. This has drawn some attention recently [23].

From the studies done for this thesis, it became evident that, whereas the

transformation matrices of aerial lines are fairly independent of frequency, they depend heavily on the line geometry.† The methods proposed in references 2 and 3, and in section 3.2 of the thesis, may be applied to substantiate the use of constant transformations as well as to generate them.

6.1.0.2. Coupling vectors in Senn's method

The way in which the coupling vectors C_r and C_t have been implemented -up to now- in Senn's method, assumes implicitly that the unused phases are grounded (at carrier frequencies); accurate modeling of line terminating impedances at high frequencies -on the other hand- is out of question in most practical cases. As an alternative, it is suggested here that the coupling vectors and their associated polynomials be obtained under the assumptions that the unused phases are, first, terminated in the line characteristic impedance and, second, in open circuit; the contour maps can then be elaborated from the three resulting polynomials on a worst case basis.

6.1.0.3. Pole trajectories in the $\Delta\alpha \cdot \Delta\theta$ plane.

In delta lines, the bigger the height of the central conductor is with respect to the external conductors, the less accurately the line modes resemble the Clarke components. In the example given in sections 2.3 and 3.4, for instance, p becomes closer to -3.5 instead of -2.0 and q becomes 0.8 instead of 1.0. Since the value of p affects the line polynomials, it is suggested here that the range

† NOTE: Recalling that the studies here deal with carrier frequencies

of feasible values for p be determined and, from it, pole trajectories in the $\Delta\alpha$-$\Delta\theta$ plane be plotted.

PAGE 88 OMITTED
IN PAGE NUMBERING

PAGE 88 OMISE
DANS LA PAGINATION

REFERENCES.

[1] Wedepohl,L. M.,"Application of Matrix Methods to the Solution of Travelling-wave Phenomena in Polyphase Systems", Proc. IEE, vol. 110, Dec. 1963, pp. 2200 2212.

[2] Galloway R.H., Shorrocks W.B., Wedepohl L.M.,"Calculation of Electrical Parameters for Short and Long Polyphase Transmission Lines". Proc. IEE, vol. 111 Dec 1964 pp. 2051-2059.

[3] Wedepohl L.M., "Electrical Characteristics of Polyphase Transmission Systems with Special Reference to Boundary Value Calculations at Power-line Carrier Frequencies." Proc. IEE, Vol. 112, No. 11, November 1965.

[4] Wedepohl L.M. "Wave Propagation in Nonhomogeneous Multiconductor Systems Using the Concept of Natural Modes." Proc. IEE, Vol. 113, No. 4, April 1966

[5] Wedepohl L.M., Wasley R.G., "Propagation of Carrier Signals in Homogeneous , Nonhomogeneous and Mixed Multiconductor Systems." Proc. IEE., Vol. 115, No. 1 January 1968

[6] Dubanton C., "Calcul Approche des parametres Primaires et Secondaries d' une Ligne de Transport. Valeurs Homopolaires.", Bulletin de la Direct. des Et. et Rech. E. D. F., No. 1, 1969, pp. 53-62.

[7] Gary C. "Approche Complete de la Propagation Multifilaire en Haute Frequence par Utilisation des Matrices Complexes" E.D.F. Bull. de la Direction des Etudes et Recherches serie B, No. 3/4 1976 pp 5-20.

[8] L. M. Wedepohl, Personal communication., 1981

[9] Frausto J., Naredo J. L., De La Rosa R., "Introduction to the Modern

Techniques of Power System Transient Calculation." 26-th Midwest Symposium on Circuits and Systems, Aug. 1983.

[10] Naredo J. L., Silva J. L., Romero R.,Moreno P., "Application of Approximated Modal Methods for PLC System Design". IEEE Transactions on Power Delivery, Vol. PWRD-2 No.1, Jan. 1987, pp. 57-63.

[11] Moreno P., De La Rosa R., Naredo J. L.," Computation of Transmission Line Transients in the Frequency Domain and its Comparison with the Method of the Characteristics.", Proceedings of the IASTED, International Symposium High Technology in the Power Industry., Aug 20-22 1986, pp. 234-237.

[12] Senn W. H., "A New Approach to Determine the Carrier Signal Attenuation on Horizontal HV Lines Both under Normal and Abnormal Conditions." International Conference on Large High Voltage Electric Systems, CIGRE 35-03, 1976 Session, Aug.-25/Sept.-2,

[13] Eggimann F.,Senn W.,Morf K.,"The Transmission Characteristics of High-Voltage Lines at Carrier Frequencies" Brown Boveri Rev. 8 1977

[14] Senn W. H.,"Power Line Carrier Signal Propagation Under Abnormal Conditions." IEE Conference on Developements in Power System Protection., Conference Publication No. 125, March 1975, pp. 168-174.

[15] Carson J. R., "Wave Propagation in Overhead Wires with Earth Return." Bell Syst. Tech. J. 1926, pp. 539-554.

[16] A. Deri, G. Tevan, A. Semlyen, A. Castanheira, "The Complex Ground Return Plane, a Simplified Model for Homogeneous and Multi-layer Earth Return.", IEEE Transactions on PAS, Vol. PAS-100, Aug. 1981, pp.3686-3693.

[17] Wedepohl L. M., Wasley R. G., "Wave Propagation in Multiconductor Overhead Lines - Calculation of Series Impedance for Multilayer Earth.", Proc. IEE, Vol. 113, No. 4, Apr. 1966, pp. 627 - 632.

[18] Wedepohl L. M., "Theory of Natural Modes in Multiconductor Transmission Lines.", Notes of the Course ELEC 552, The University of British Columbia.

[19] Pipes L. A.,"Matrix Methods for Engineering.", Prentice-Hall, 1963.

[20] Senn W. H., Morf K. P.,"Optimum Power Line Carrier Coupling Coupling Arrangement on Transposed Single Circuit Power Lines.", International Conference on Large High Voltage Electric Systems.(35-02), 21-29 August 1974.

[21] IEC.,"Planning of (Single-sideband) Power Line Carrier Systems.", International Electrotechnical Commission IEC Report. Publication 663/1980.

[22] "Notes of Northwest Power Pool Relay and Communication Engineers Meeting.", Vancouver, B. C., Canada, September 23, 1986.

[23] Marti J. R., Dommel H. W., Marti L., Brandwajn V., "Approximate Transformation Matrices for Unbalanced Transmission Lines.", Submitted to the 9-th Power Systems Computation Conference-PSCC, Aug. 30 - Sept. 4 1987, Lisbon, Portugal.

APPENDIX

Contour maps of the couplings considered in chapters 4 and 5

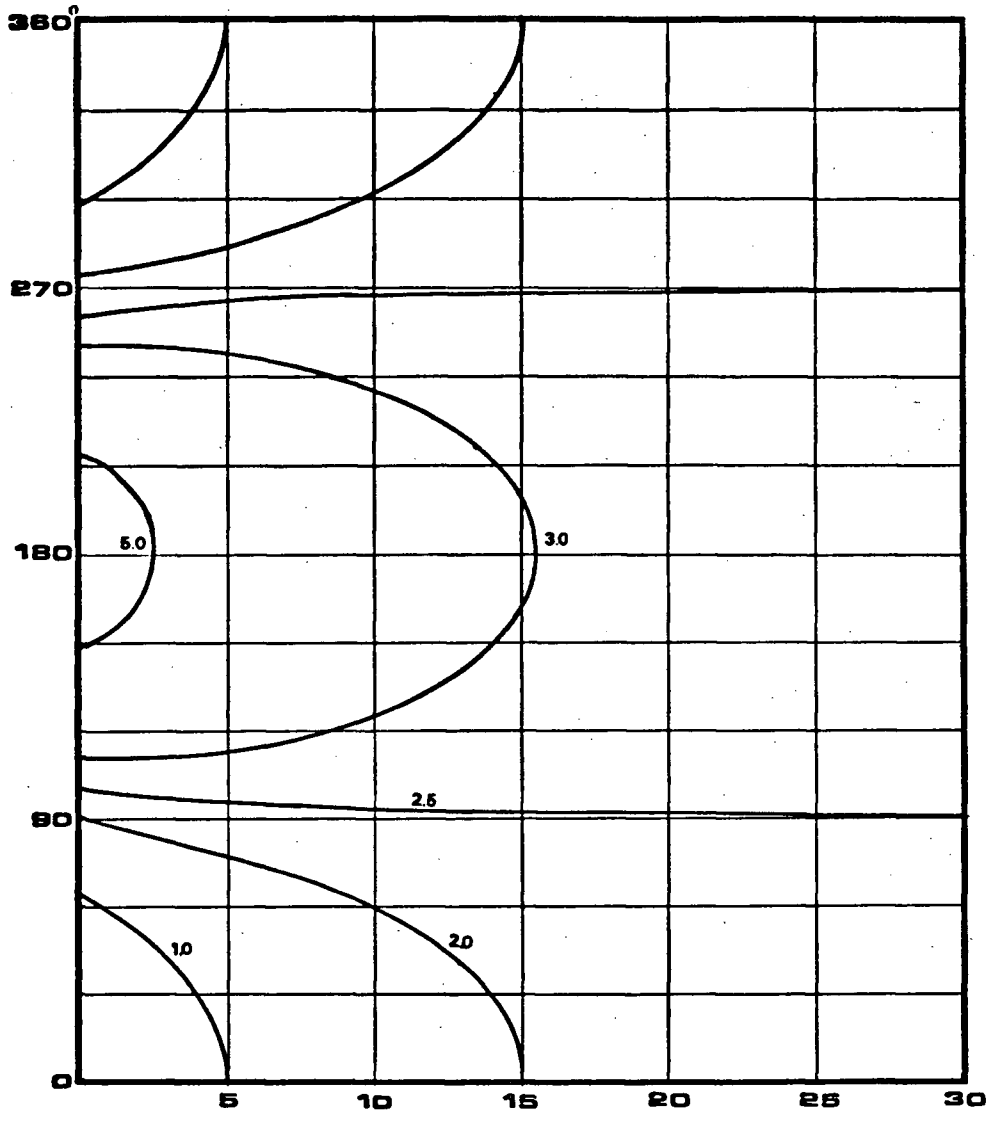
360°
270
180
90
0
5
10
15
20
25
30
5.0
3.0
2.5
1.0
2.0

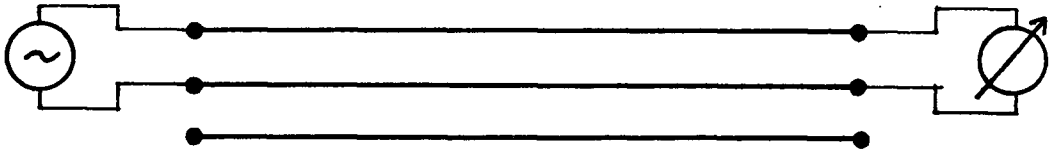

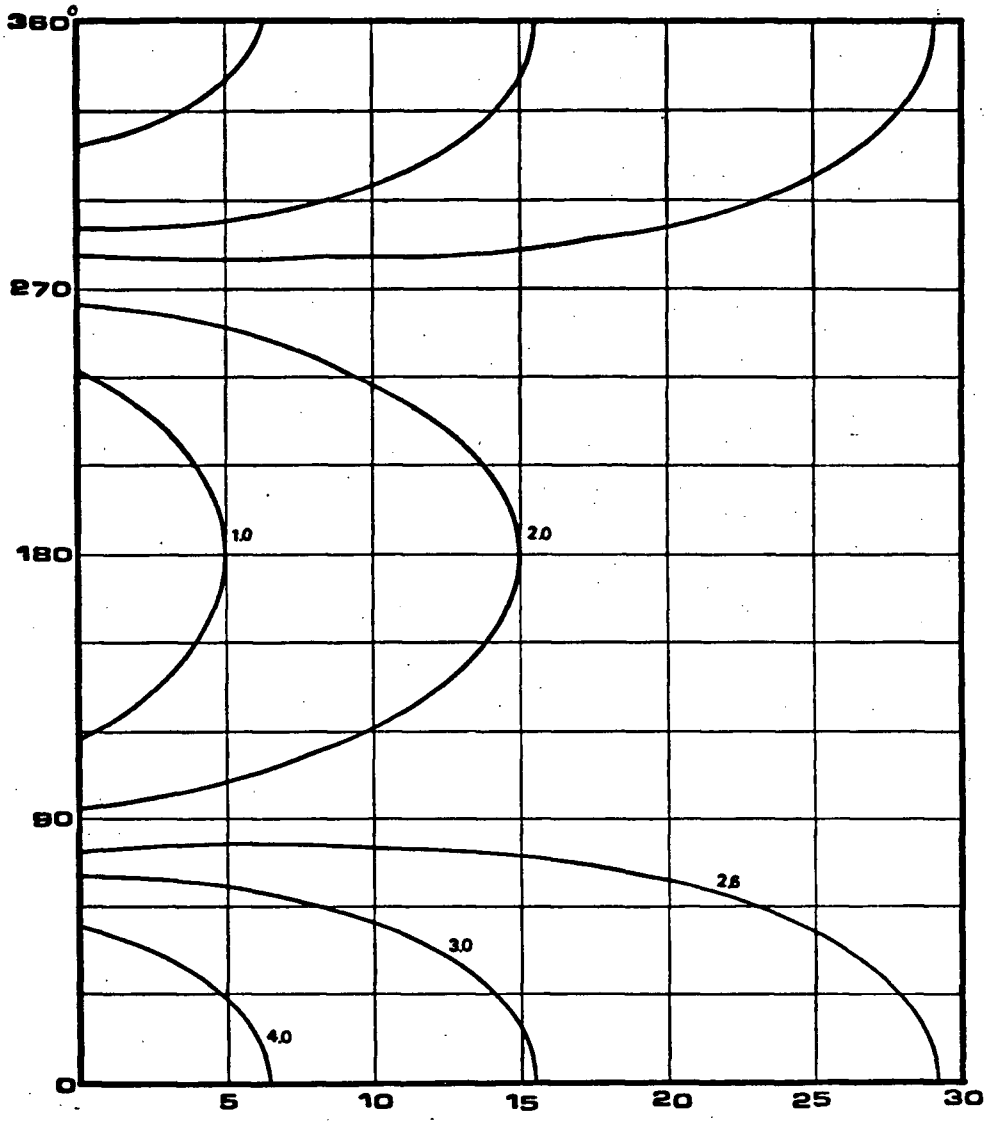

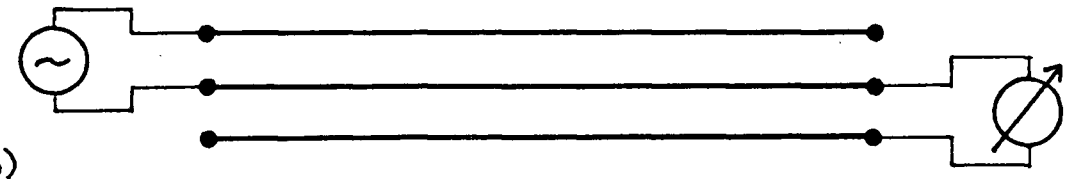

b)

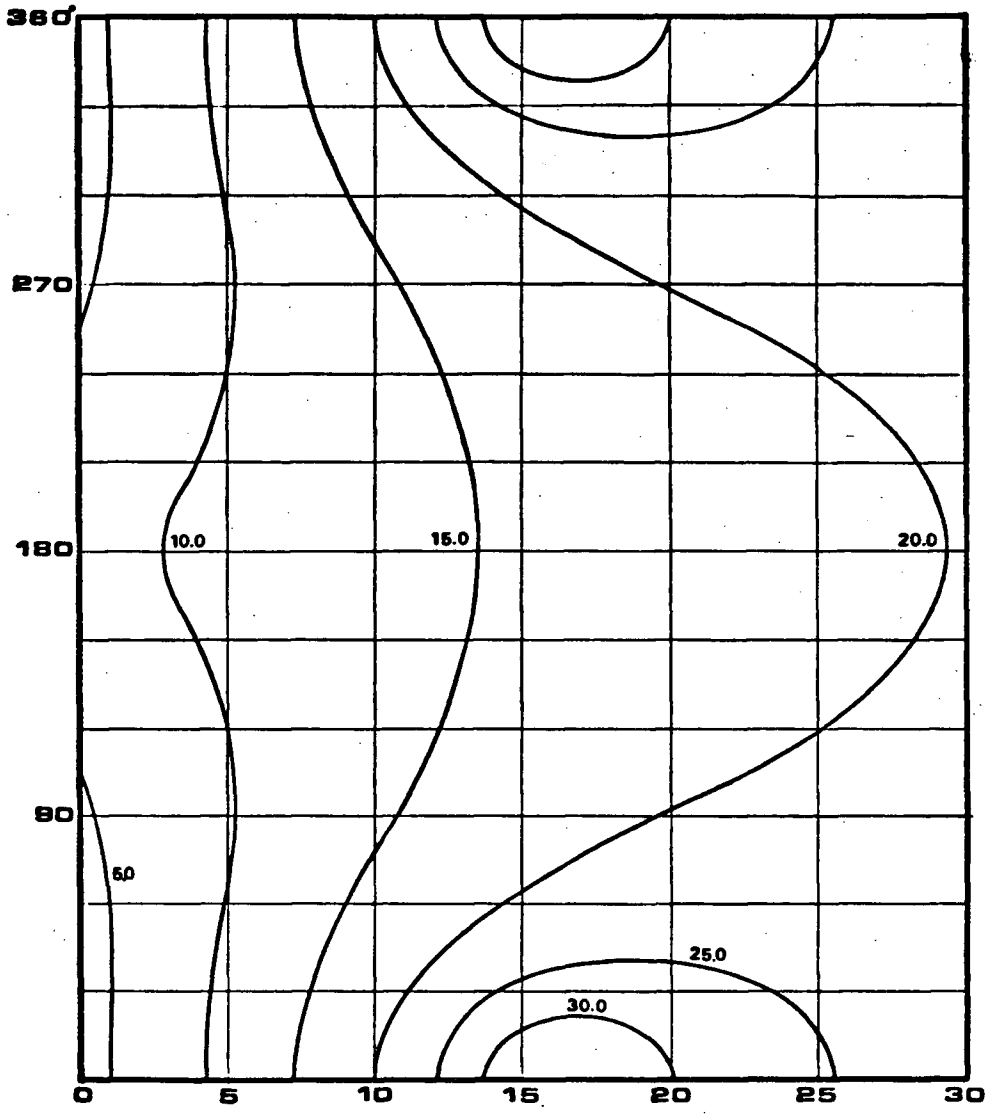
360
270
180
90
0
5
10
15
20
25
30
5.0
10.0
15.0
20.0
25.0
30.0

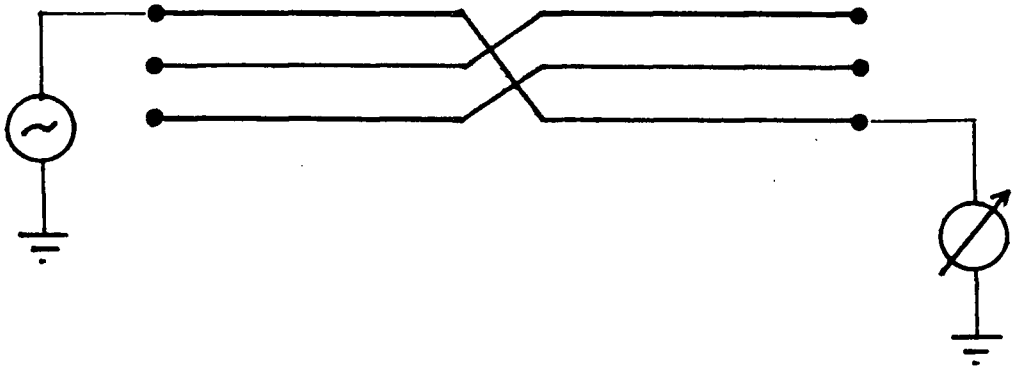

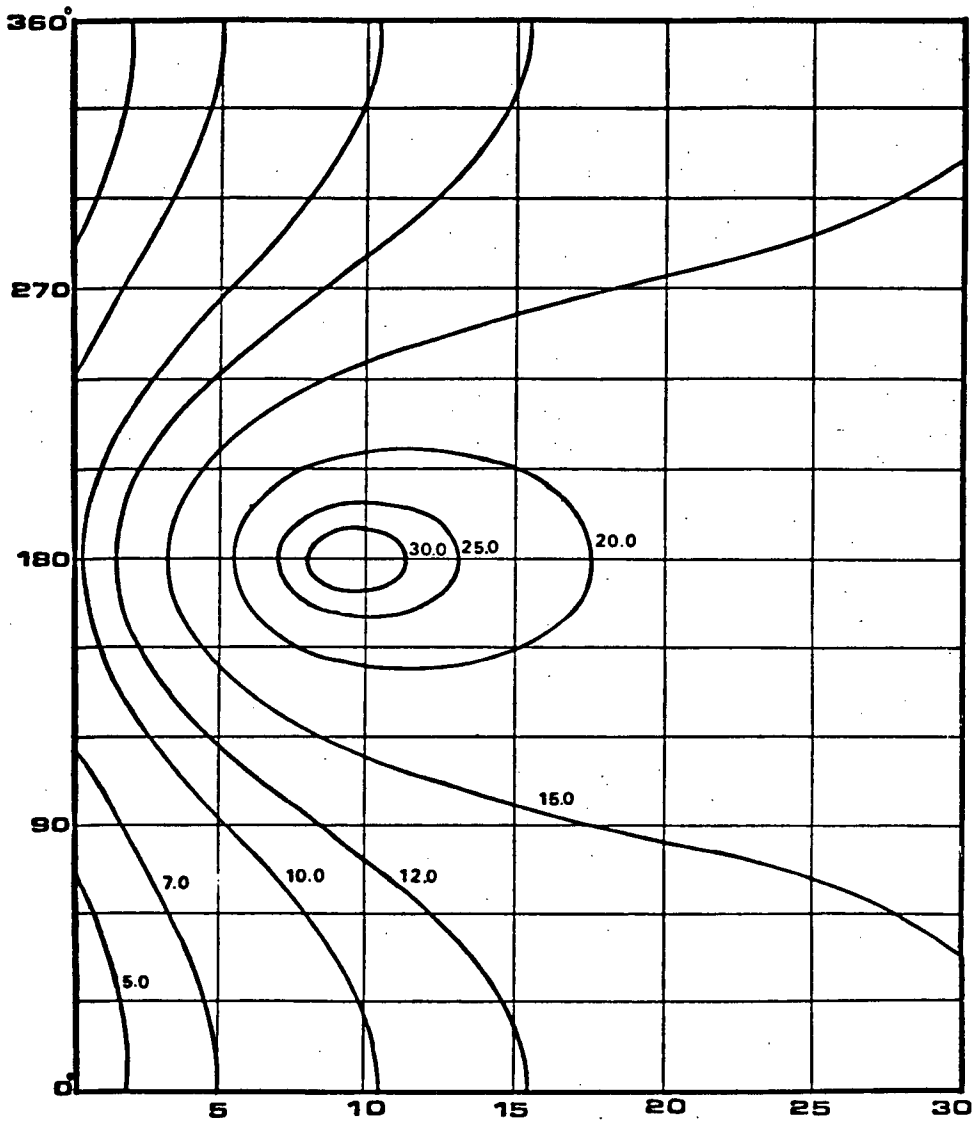
360°
270
180
90
0°
5
10
15
20
25
30
30.0
25.0
20.0
15.0
12.0
10.0
7.0
5.0

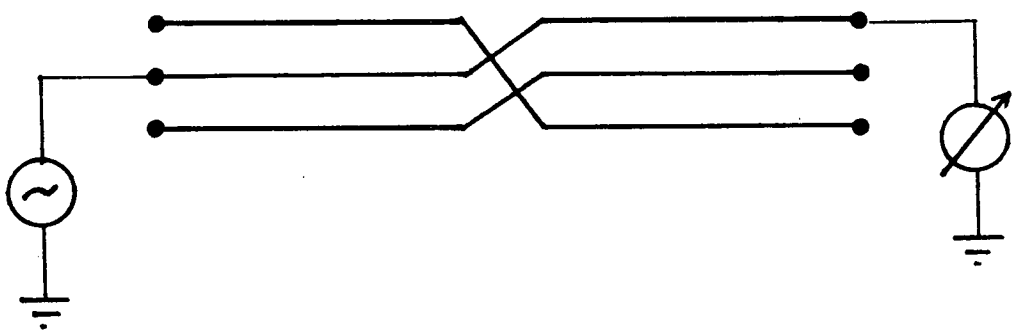

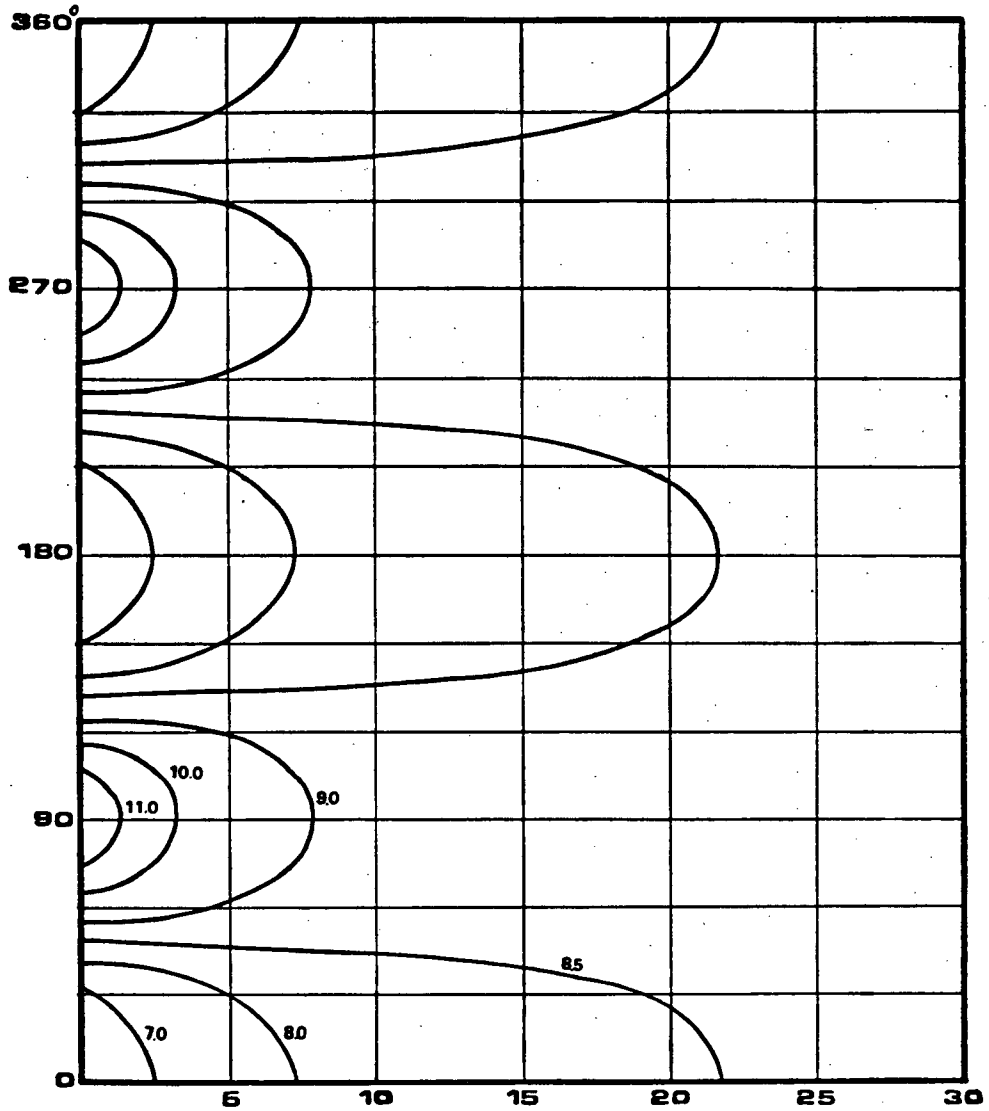
360°
270
180
90
0
5
10
15
20
25
30
10.0
11.0
9.0
8.5
7.0
8.0

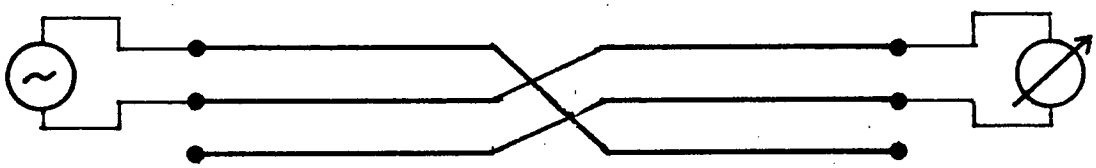

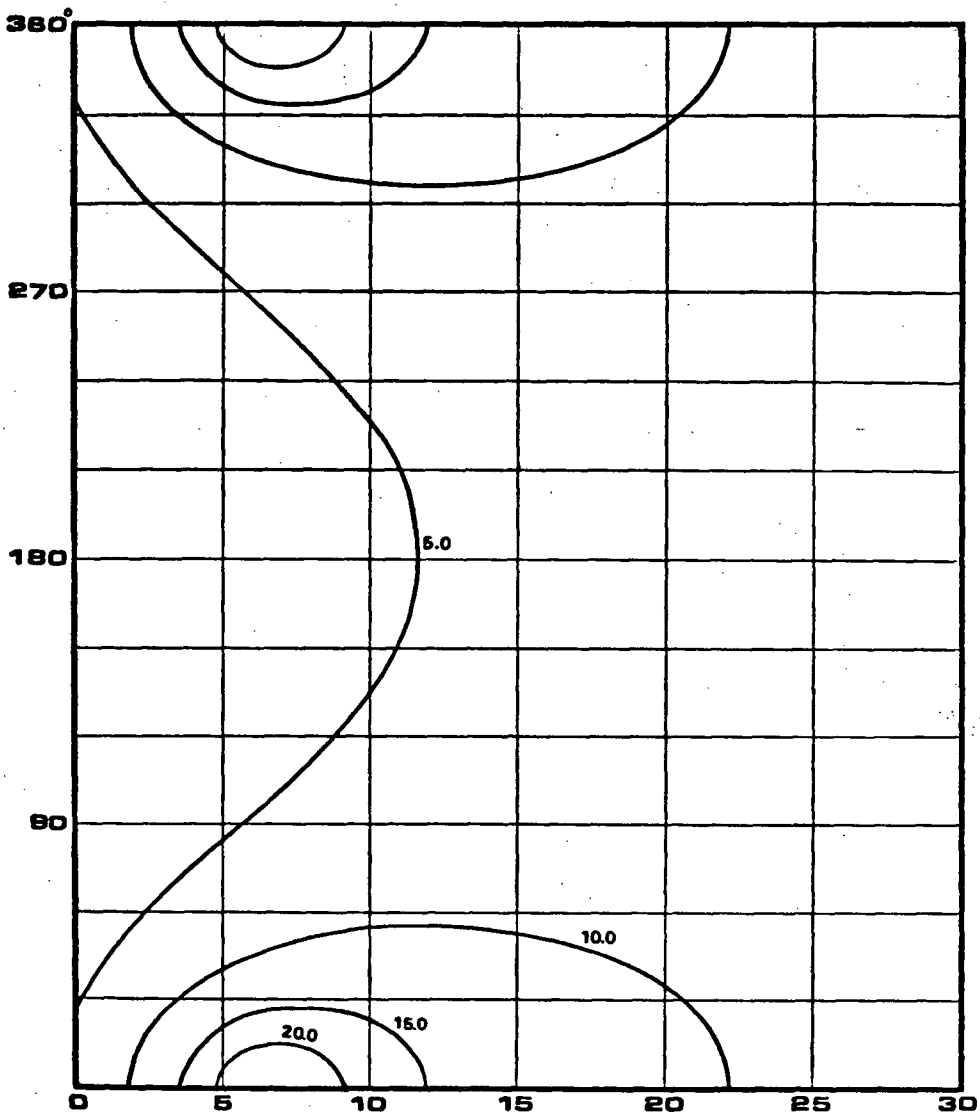
360°
270
180
90
0
5
10
15
20
25
30
5.0
10.0
15.0
20.0

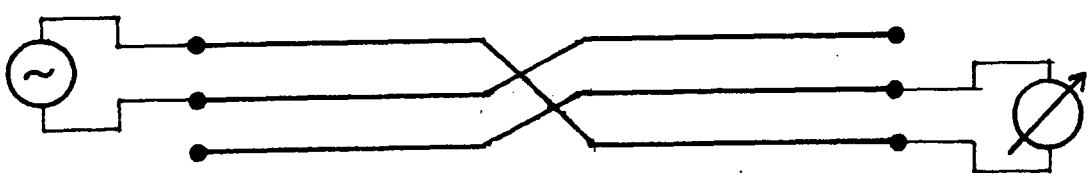

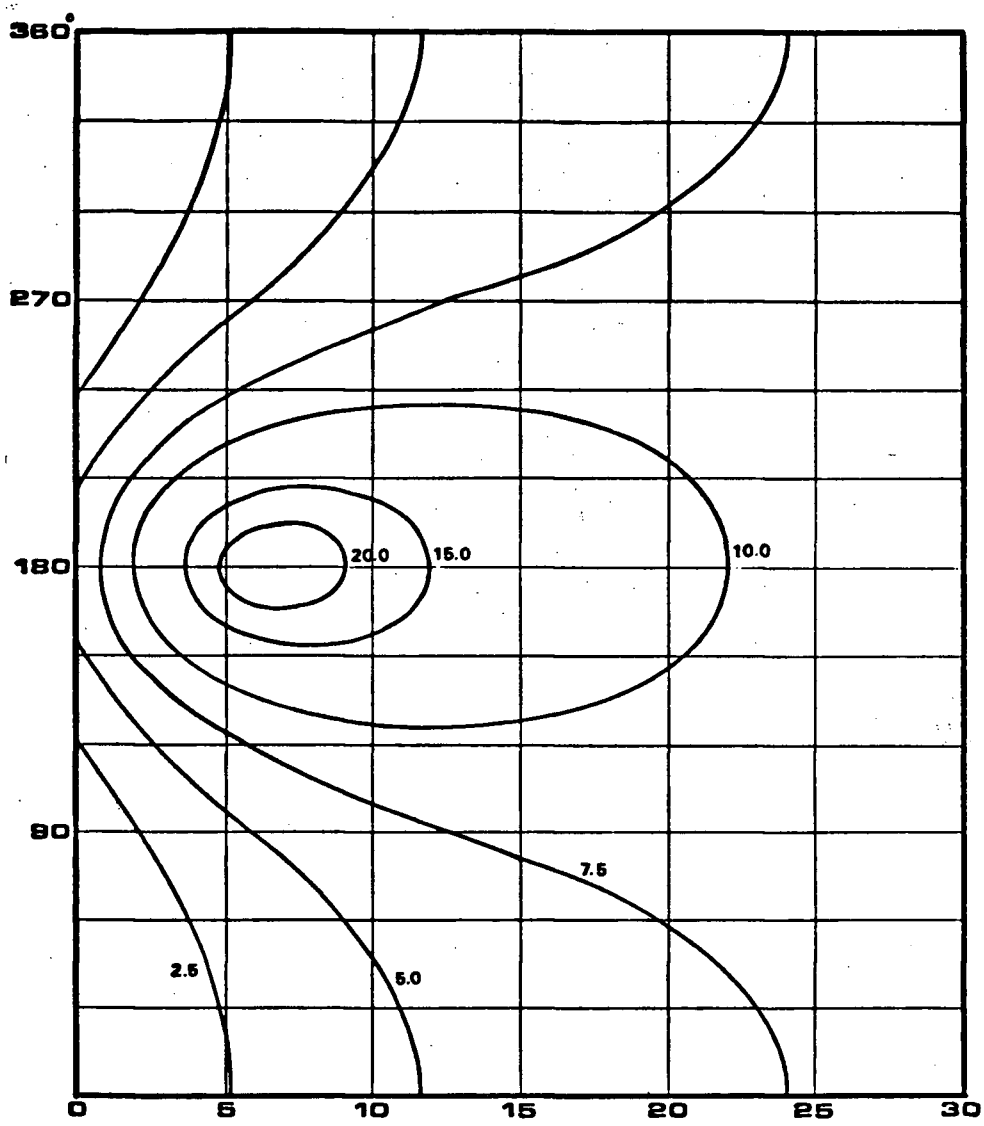
360°
270
180
90
0
5
10
15
20
25
30
20.0
15.0
10.0
7.5
5.0
2.5

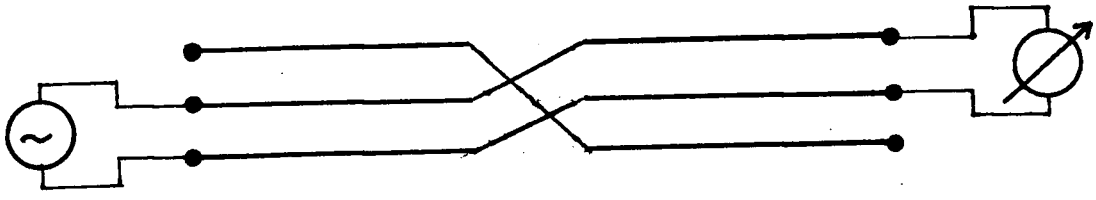

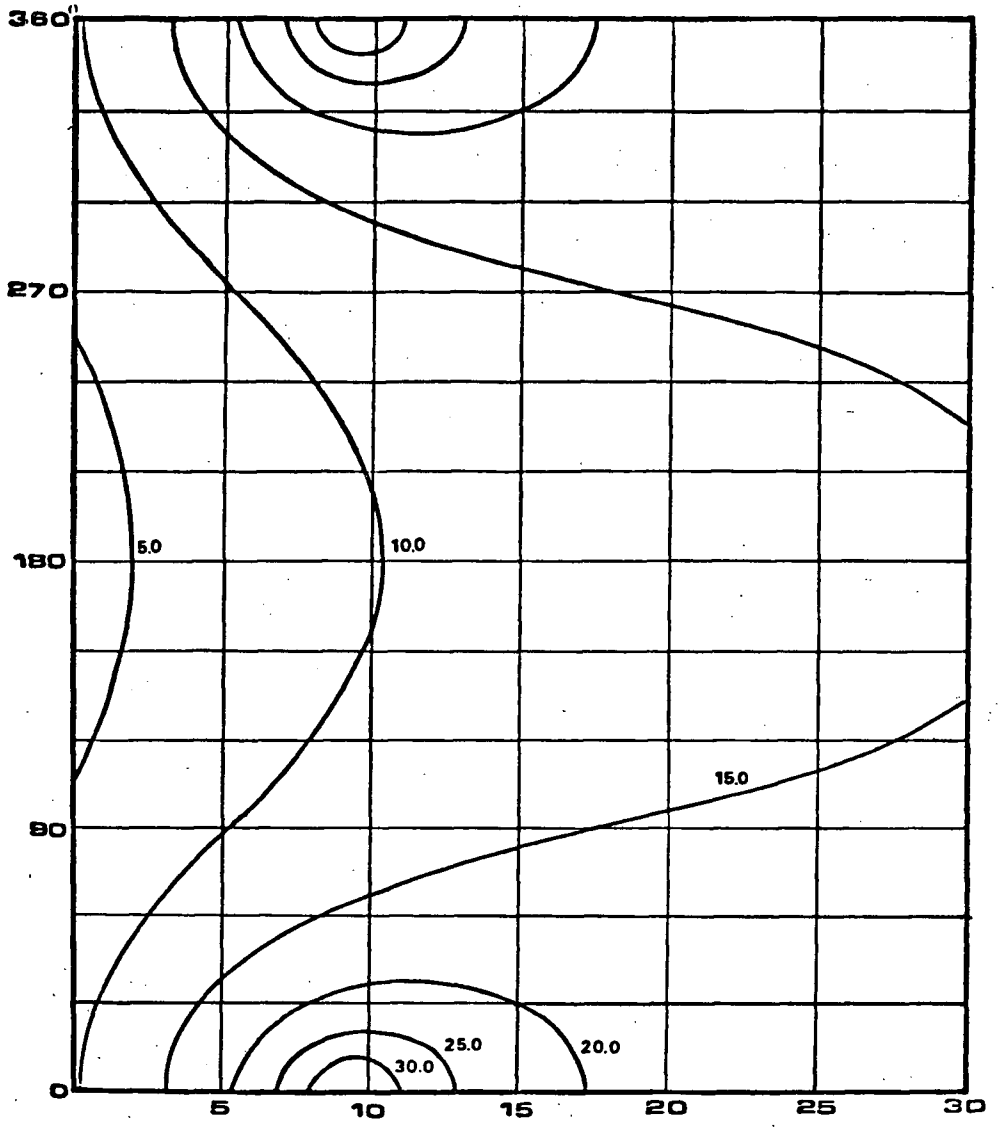
360
270
180
90
0
5
10
15
20
25
30
5.0
10.0
15.0
20.0
25.0
30.0

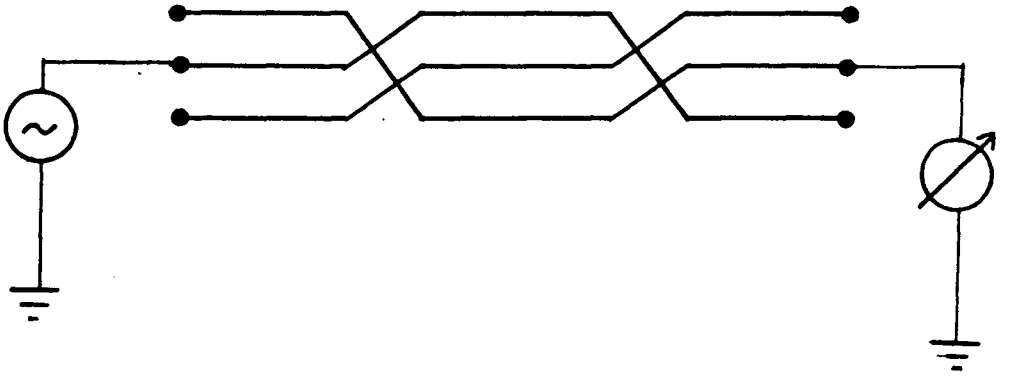

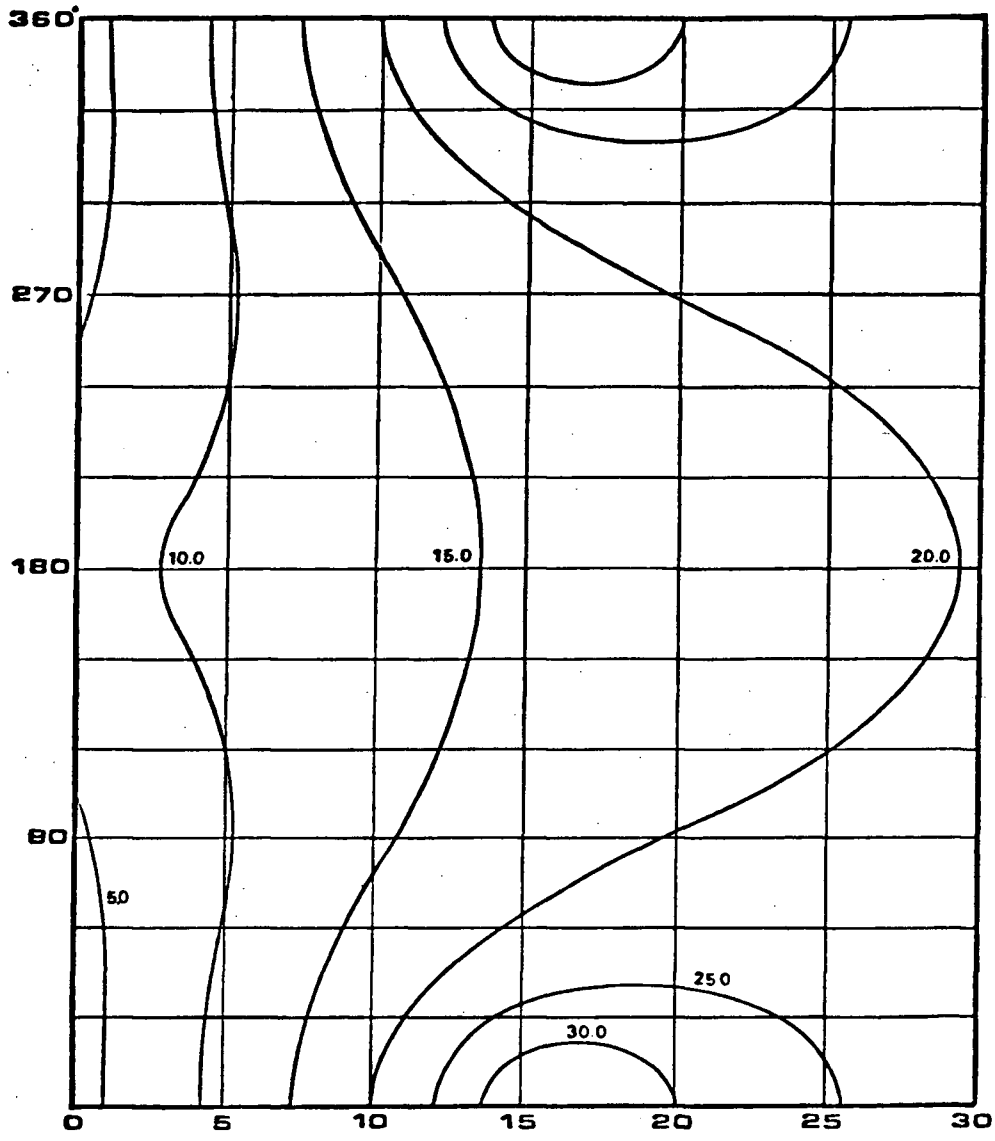
360°
270
180
90
0
5
10
15
20
25
30
10.0
15.0
20.0
5.0
25.0
30.0

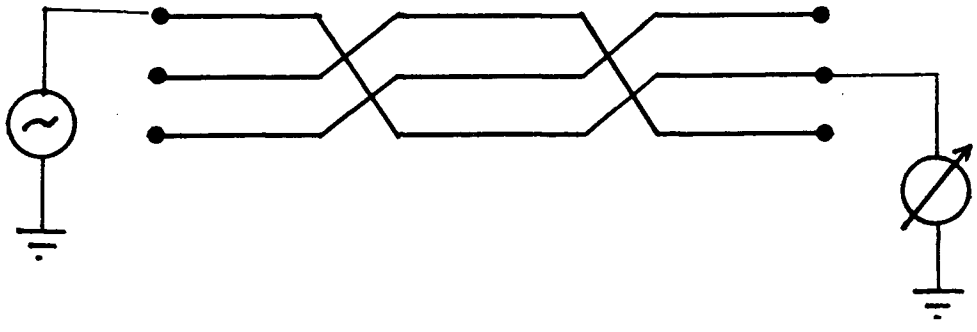

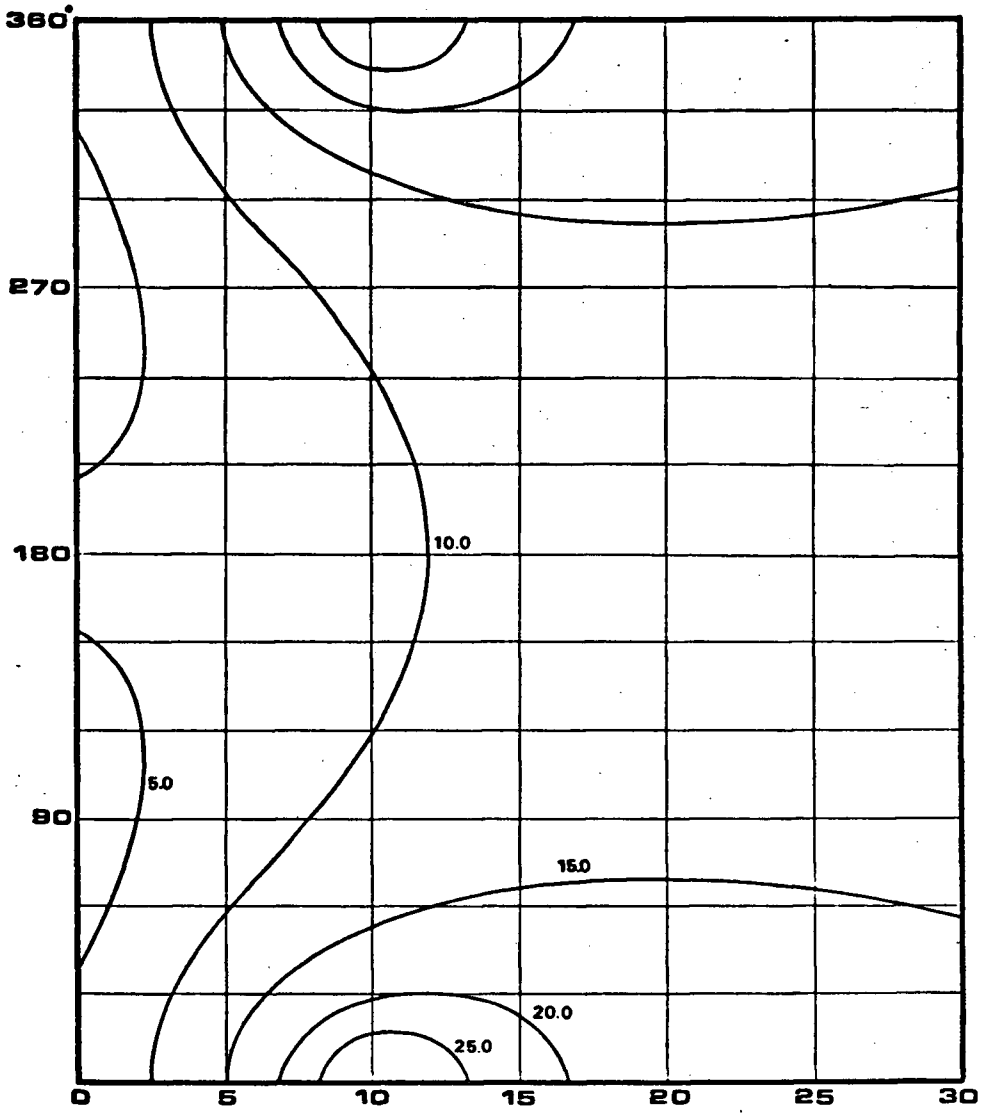
360°
270
180
90
0
5
10
15
20
25
30
5.0
10.0
15.0
20.0
25.0

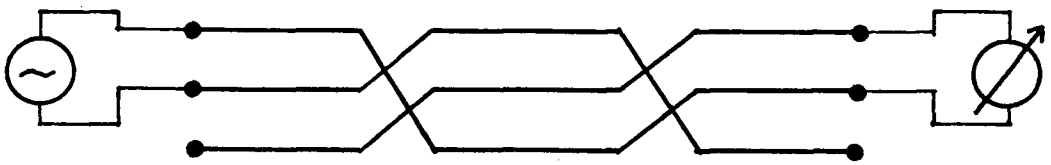

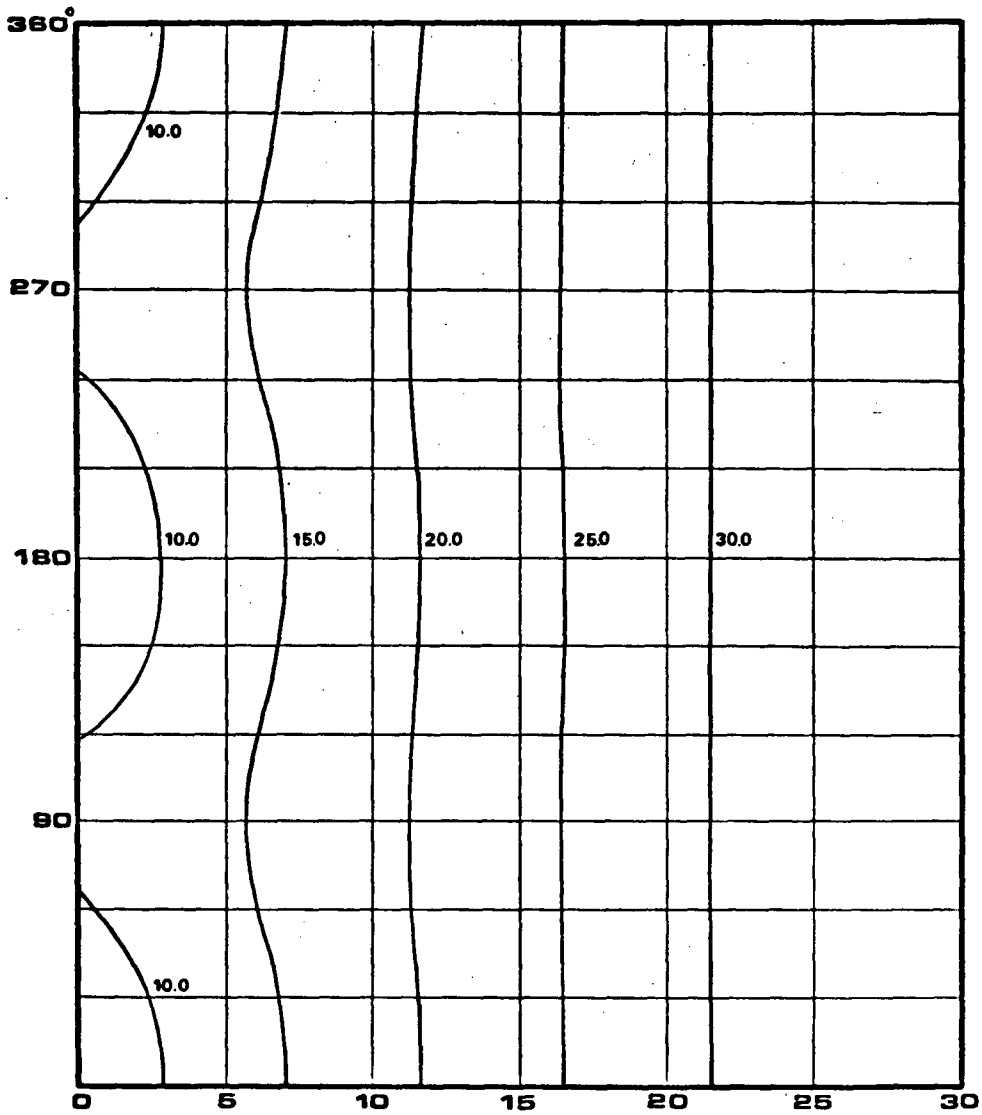
360°
270
180
90
0
5
10
15
20
25
30
10.0
10.0
15.0
20.0
25.0
30.0
10.0

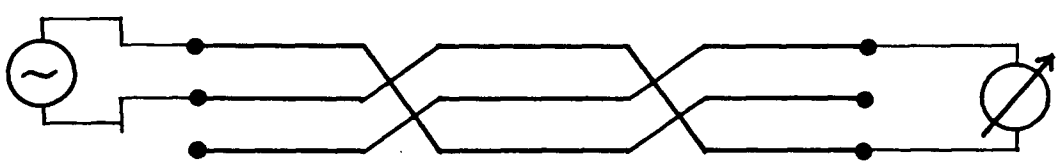

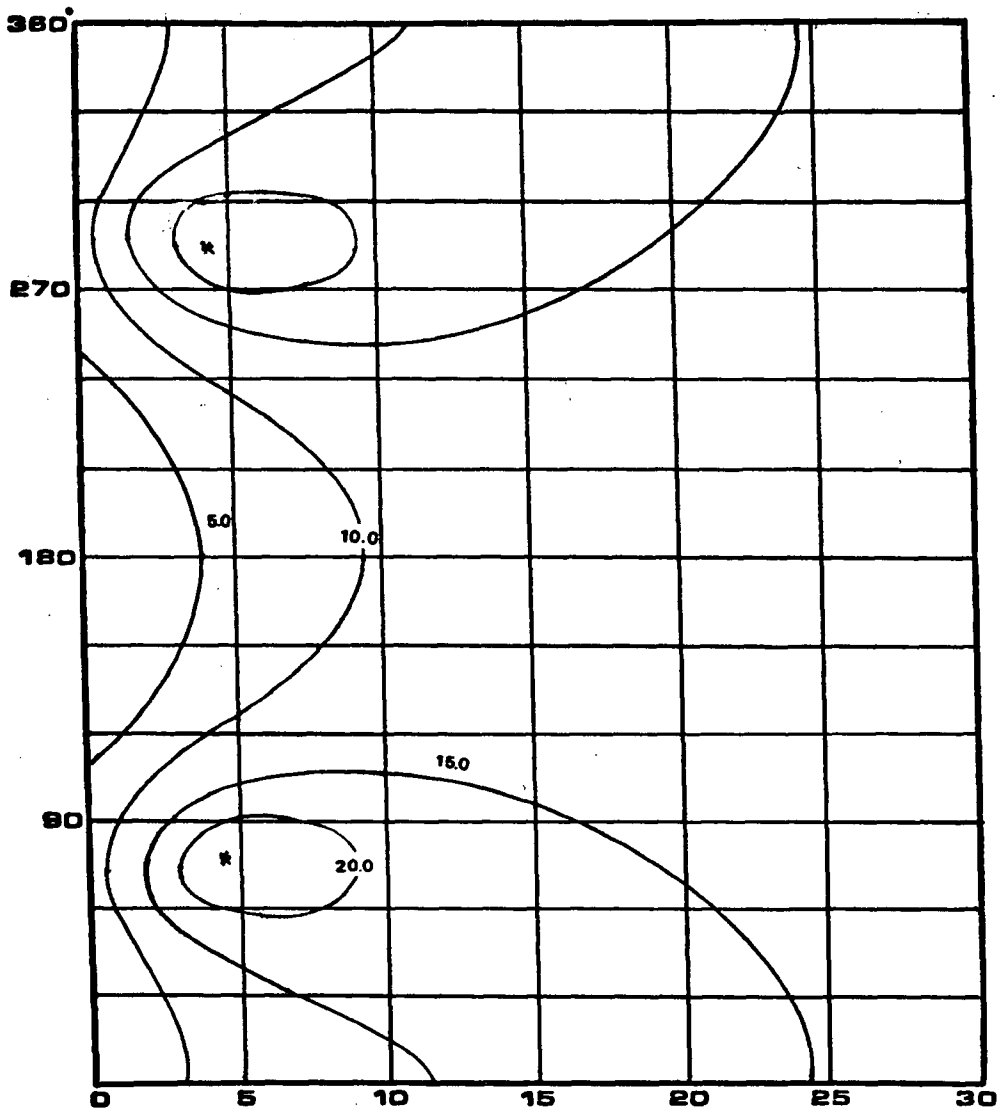
360°
270
180
90
0
5
10
15
20
25
30
5.0
10.0
15.0
20.0

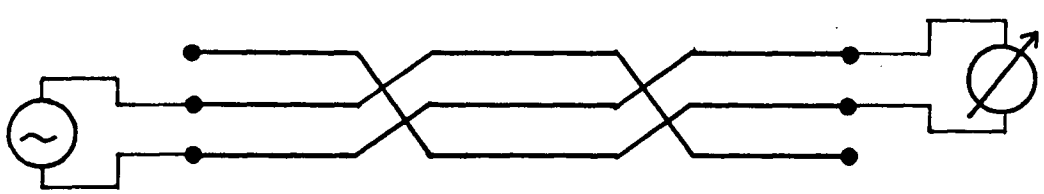

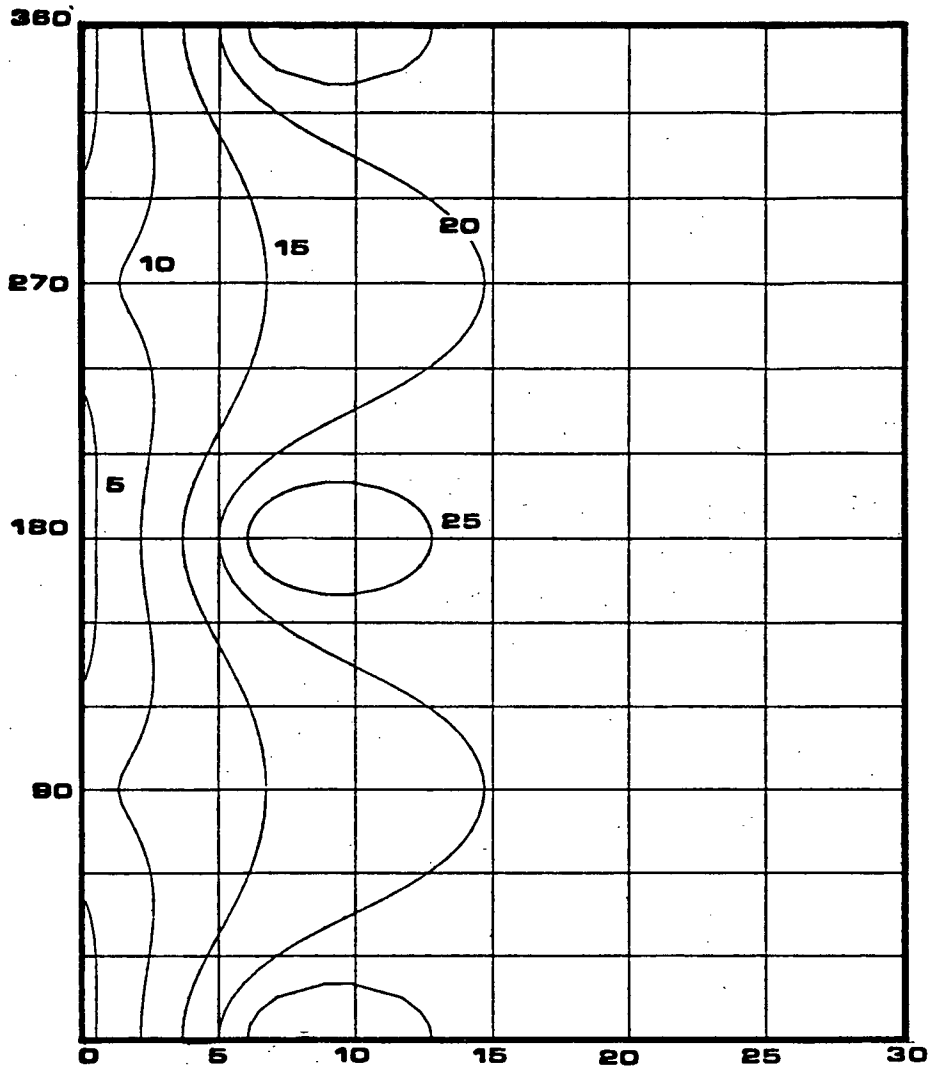
360
270
180
90
0
5
10
15
20
25
30
5
10
15
20
25

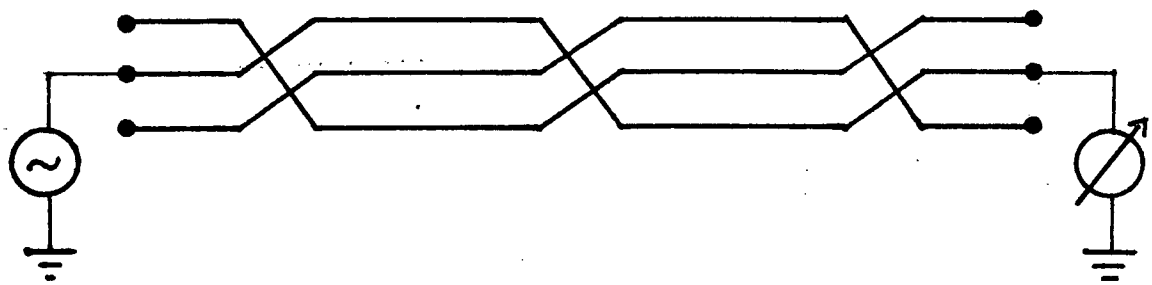

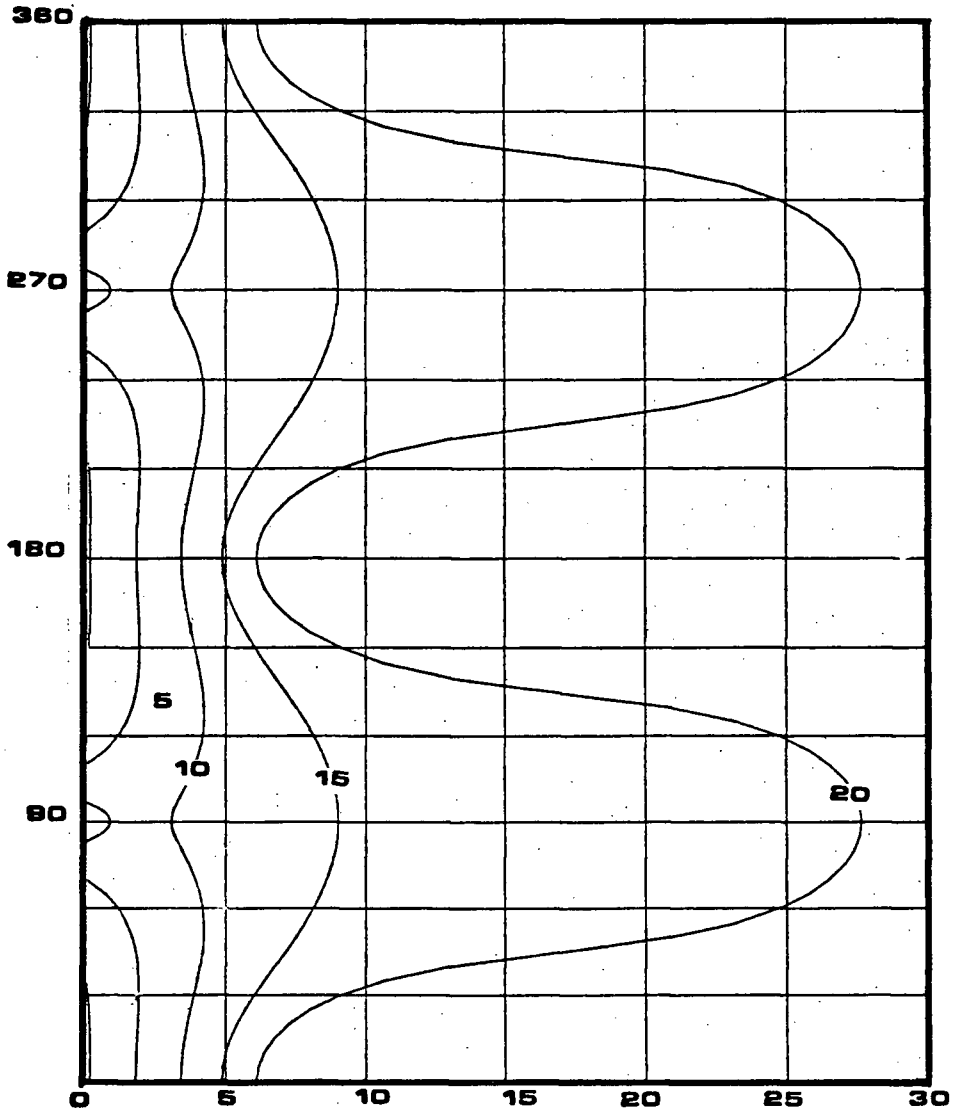
360
270
180
90
0
5
10
15
20
25
30
5
10
15
20

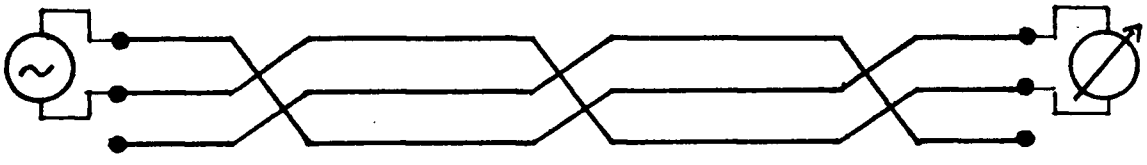

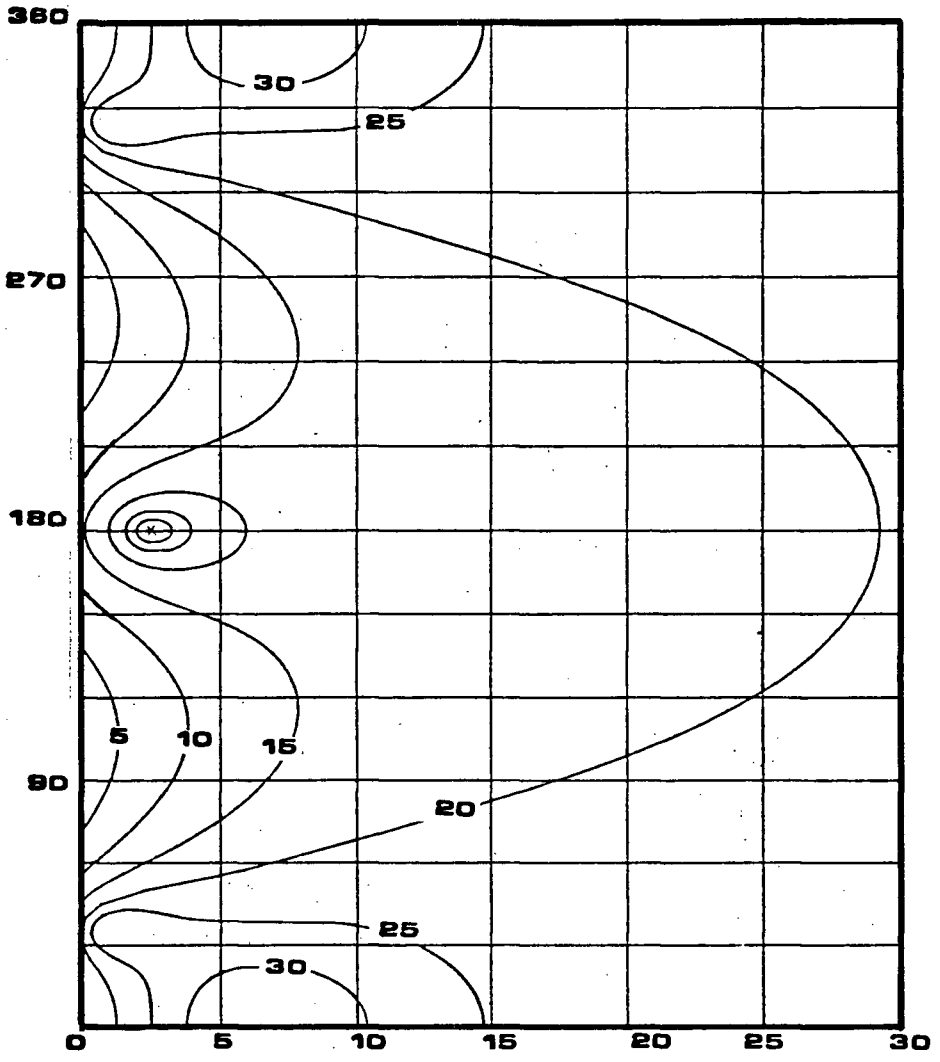
360
270
180
90
0
5
10
15
20
25
30
30
25
5
10
15
20
25
30